AFRL-OSR-VA-TR-2015-0044

Review of Zinc Oxide Thin Films

Tom Otiti
COLLEGE OF COMPUTING AND INFORMATION SCIENCE MAKERERE U

12/23/2014
Final Report

Air Force Research Laboratory
AF Office Of Scientific Research (AFOSR)/ ION
Arlington, Virginia 22203
Air Force Materiel Command

REPORT DOCUMENTATION PAGE

Form Approved
OMB No. 0704-0188

1. REPORT DATE *(DD-MM-YYYY)*	2. REPORT TYPE	3. DATES COVERED *(From - To)*
18-12-2014	Final Performance	01-07-2011 to 30-06-2014

4. TITLE AND SUBTITLE
ZINC OXIDE MATERIALS FOR PHOTOVOLTAIC APPLICATIONS

5a. CONTRACT NUMBER

5b. GRANT NUMBER
FA9550-11-1-0074

5c. PROGRAM ELEMENT NUMBER

6. AUTHOR(S)
Tom Otiti

5d. PROJECT NUMBER

5e. TASK NUMBER

5f. WORK UNIT NUMBER

7. PERFORMING ORGANIZATION NAME(S) AND ADDRESS(ES)
COLLEGE OF COMPUTING AND INFORMATION SCIENCE MAKERERE U
PLOT 56 UNIVERSITY ROAD
KAMPALA, 256 UG

8. PERFORMING ORGANIZATION REPORT NUMBER

9. SPONSORING/MONITORING AGENCY NAME(S) AND ADDRESS(ES)
AF Office of Scientific Research
875 N. Randolph St. Room 3112
Arlington, VA 22203

10. SPONSOR/MONITOR'S ACRONYM(S)
AFOSR

11. SPONSOR/MONITOR'S REPORT NUMBER(S)

12. DISTRIBUTION/AVAILABILITY STATEMENT
A DISTRIBUTION UNLIMITED: PB Public Release

13. SUPPLEMENTARY NOTES

14. ABSTRACT
The present review paper reports on the optimization attempts, so far, on two simultaneously occurring properties of zinc oxide (ZnO) thin films (electrical conductivity and optical transparency). These two properties are discussed in the context of zinc oxide material thin films as transparent conducting oxides (TCOs) for photovoltaic (PV) applications. They are very critical and so is their optimization for the realization of superior zinc oxide based TCOs for superior performance in photovoltaic devices. According to theory, the electrical resistivity (ρ)of the novel TCO material should be ~10-5Ωcm while the optical transparency should be over 80% in the visible radiation range as well as in the near infrared region [3, 4, 5, 99, 11]. This remarkable combination of conductivity and transparency is usually impossible in intrinsic stoichiometric TCOs; usually only partial transparency and fairly good conductivity may be obtained in the thin films. However, it is achieved by producing them with a non-stoichiometric composition or by introducing appropriate dopants which decrease the resistivity while retaining a good transparency [3, 4].

15. SUBJECT TERMS
ZINC OXIDE, PHOTOVOLTAIC

16. SECURITY CLASSIFICATION OF:			17. LIMITATION OF ABSTRACT	18. NUMBER OF PAGES	19a. NAME OF RESPONSIBLE PERSON
a. REPORT	b. ABSTRACT	c. THIS PAGE			Tom Otiti
U	U	U	UU		19b. TELEPHONE NUMBER *(Include area code)* 256 414 531498

Review of Zinc Oxide Thin Films

Abstract

The present review paper reports on the optimization attempts, so far, on two simultaneously occurring properties of zinc oxide (ZnO) thin films (electrical conductivity and optical transparency). These two properties are discussed in the context of zinc oxide material thin films as transparent conducting oxides (TCOs) for photovoltaic (PV) applications. They are very critical and so is their optimization for the realization of superior zinc oxide based TCOs for superior performance in photovoltaic devices. According to theory, the electrical resistivity (ρ)of the novel TCO material should be ~10^{-5}Ωcm while the optical transparency should be over 80% in the visible radiation range as well as in the near infrared region [3, 4, 5, 99, 11]. This remarkable combination of conductivity and transparency is usually impossible in intrinsic stoichiometric TCOs; usually only partial transparency and fairly good conductivity may be obtained in the thin films. However, it is achieved by producing them with a non-stoichiometric composition or by introducing appropriate dopants which decrease the resistivity while retaining a good transparency [3, 4].

Whereas high quality pure ZnO thin films have been fabricated before by a number of standard techniques [83-86], however, they are limited in their properties and stability for PV applications and require further development. The stability temperature for ZnO is ~ 250 [78, 95], above which the film quality starts to degrade by thermal decomposition [78, 80, 95]. Intrinisic thin film resistivities as low as 10^{-2} to 10^{-3} Ωcm and transmission coefficients (T) as high as 80%-90% have been achieved [3, 4, 76].

Past studies [15-18, 20, 58, 79, 65, 99-109, 128-131, 66, 67, 137, 138, 142] have recommended extrinsic doping of ZnO with a range of elements to produce more stable ZnO TCOs with better properties (especially electrical, optical). These doping elements are categorized into two: n-type and p-type conductivity dopants; the most commonly researched dopants include group III and VII elements for n-type and group I or VI for p-type conductivity. While impurity doping is

preferred to improve the standard of the simultaneous co-existence of both electrical and optical properties, more careful attention is needed to overcome the tradeoff between these two properties (where an increase in conductivity level leads to reduced optical transparency level). According to [11], a reduction in resistivity will require either an increase in the carrier concentration or mobility; and an increase in the former leads to an increase in the visible absorption. While mobility has no deleterious effect and is probably the best direction to follow; he suggested improvement in electrical properties could be achieved without degrading the optical properties but rather while improving on them by achievement of high-carrier mobility.

This review gives an in-depth discussion of the properties of ZnO (including, structural, mechanical, chemical, electrical, and optical) and issues of doping (n-type and *p*-type) up to date.

I. Introduction

Zinc Oxide (ZnO) is a multifunctional material with a wide range of applications [1]. It is preferred as a low cost alternative transparent conductive oxide (TCO) material in thin-film photovoltaic solar cells owing to its attractive electrical and optical properties [2]. Despite bearing satisfactory material properties for a number of applications during the past decades, today its preferred application in PV solar cells requires further development in its properties (especially electrical and optical properties) to meet the required theoretical novel TCO standard (ρ~10^{-5}Ωcm and T>80%)[3, 4, 5]. The thin film photovoltaic solar cells offer the opportunity to dramatically lower the price of solar energy devices by using small amounts of materials and low cost manufacturing technology[1, 6]. The performance of these solar energy devices is directly related to the properties of the TCO material Used. In particular electrical conductivity and optical transmittance are the most critical of all properties. Consequently, development of ZnO based TCOs with superior electrical and optical properties is imperative. Currently the superiority of these two critical properties in the various past and present

attempts of fabrication of ZnO based TCO materials is still limited and has not surpassed the required standard for commercialization [7]. The transmittance standard for various engineered ZnO TCOs has often been met but not simultaneously with the electrical resistivity standard as required. The lowest value of resistivity, so far, is of the order 10^{-4} Ω-cm [8, 9, 10]. There is a tradeoff between these two properties of the ZnO material; increase in conductivity levels leads to reduced optical transparency level. A novel ZnO TCO should essentially strike compromise between them [11]. The co-existence of electrical conductivity and optical transparency in the ZnO materials depends on a couple of factors: nature, number, and atomic arrangements of metal cations in crystalline or amorphous oxide structures, on the resident morphology, and on the presence of intrinsic or intentionally introduced defects.

Controlling and optimizing both electrical and optical properties in the ZnO material thin film is essentially through extrinsic doping with appropriate impurity elements (dopants). These doping elements are categorized into two: n-type and p-type conductivity dopants; the most commonly researched dopants include group III and VII elements for n-type and group I or VI for p-type conductivity. ZnO is asymmetrically doped, that is, it can be doped easily either *n*-type or *p*-type but not both. The *n*-type conductivity can be readily obtained via either native or extrinsic donor defects whereas the *p*-type doping can also be obtain in a similar way but remains more difficult [12, 13].

Recent research on n-type extrinsic doping with group III elements revealed that Aluminium (Al), Boron (B) and Gallium (Ga) doped ZnO films show low resistivity and high transmittance as well as better stability; and the highest conductivity was reported with Al and Ga doping [14, 15-18]. However, the resistivity is not low enough for commercial use in photovoltaics. Exploration of more doping options such as co-doping for much superior and high quality n-type ZnO thin films is imperative. Recently, Dutta *et al.*[19] regarded metal-co-doped ZnO films to be promising candidates for much better properties when he reported co-doped ZnO films with higher visible transmittances than those of single-doped ZnO films. Metal co-doping of ZnO was done by Hyun-il [20] with B and Al and the lowest electrical resistivity was 5.16×10^{-4}

Ωcm and optical transmittance was above 85%. The study also recommended co-doping ZnO with Al and Ga for even better results since both metals are the superior dopants for better optical and electrical properties for ZnO and combining them would most likely yield even superior properties.

On the other hand, the window for obtaining the p-type behavior seems to be very small and sensitive to experimental parameters, largely because of lack of suitable *p*-dopants to make it reliable and reproducible. The candidates are mainly group V elements [21-32] (nitrogen (N), Phosphorus (P), Arsenic (As)), with N as the most promising dopant; however, the resulting films have not been particularly stable and the mechanism by which N is incorporated is not clear. Theoretically, co-doping group V and III elements at a 2:1 ratio in ZnO can increase acceptor solubility and make acceptor levels shallower by reducing Madelung energy, solving the problems of p-type doping in ZnO. The theoretical feasibility of co-doping has been demonstrated by experiments. It's recommended to explore co-doping (with Ga, Al, Si, In and N) in ZnO for very low resistive films similar to the n-type ZnO. Co-doping studies have been done for Ga and Al, each co-doped with N but hardly any for Si and In [33-39]. However, instability, non reproducibility and high resistivity were the setbacks in the thin films. More attempts for different pairs of doping elements are essential and co-doping with In and N is considered [40].

This study is dedicated to explore doping of ZnO for superior properties in two folds: Mono-doping (using Al, Ga for n-type and N, In for p-type) and co-doping (using Al with Ga for n-type and N with In for p-type).

II. PROPERTIES OF ZINC OXIDE

This semiconductor has several favorable properties: good transparency, high electron mobility, wide bandgap, strong room-temperature luminescence, among others. Those properties are

already used in a wide range of emerging applications including in photovoltaics (solar cells) used for harnessing solar energy [41].

A. Chemical Properties

ZnO occurs as white powder known as zinc white or as the mineral zincite. Zinc oxide is an amphoteric oxide. It is nearly insoluble in water and alcohol, but it is soluble in (degraded by) most acids, such as hydrochloric acid. Bases also degrade the solid to give soluble zincate. ZnO decomposes into zinc vapor and oxygen only at around 1975 °C, reflecting its considerable stability. Heating with carbon converts the oxide into the metal, which is more volatile than the oxide [42, 43, 44, 45].

B. Physical Properties

A summary of the physical properties of wurtzite ZnO is displayed in Table 1.0

Table 1.0: Physical properties of wurtzite ZnO [46-57].

space group	$P6_3mc$
lattice parameter *a*	0.32475 – 0.32501 nm
lattice parameter *c*	0.52042 – 0.52075 nm
density	5.606 g cm^{-3}
sublimation point	2248 K
bulk modulus	183 GPa
Young's modulus	111.2 ± 4.7 GPa
hardness	5.0 ± 0.1 GPa
effective electron mass	$0.28m_e$
electron carrier concentration	6.0 10^{16} cm^{-3}
electron mobility	205 $cm^2 V^{-1} s^{-1}$
band gap	3.37 eV
exciton binding energy	60 eV

(i) Structure

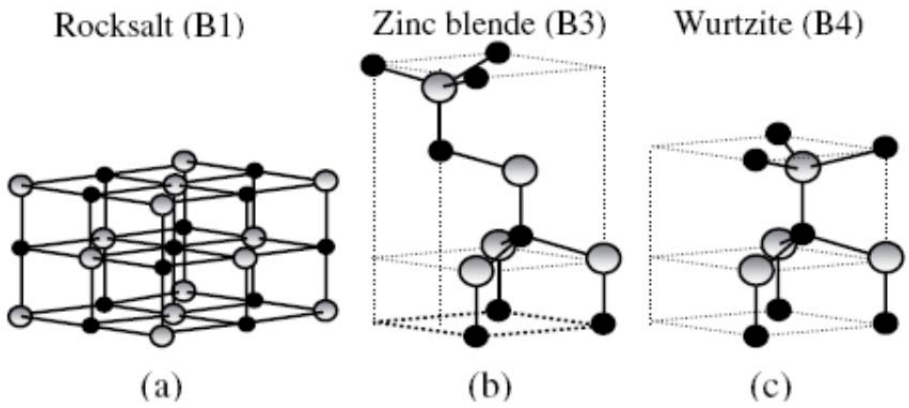

Fig 1.0. Stick and ball representation of ZnO crystal structures: (a) cubic rock salt (B1), (b) cubic zinc blende (B3), and (c) hexagonal wurtzite (B4). Shaded gray and black spheres denote Zn and O atoms, respectively [58].

The crystal structures shared by ZnO are wurtzite *B*4, zinc blende *B*3, and rock salt *B*1, as schematically shown in Fig. 1.0. At ambient conditions, the thermodynamically stable phase is wurtzite. The zinc blende ZnO structure can be stabilized only by growth on cubic substrates, and the rock salt NaCl structure may be obtained at relatively high pressures about 10 GPa. In contrast to other II–VI semiconductors, which exist both in the cubic zinc blende and the hexagonal wurtzite-type structures (like ZnS, which gave the name to both structures) ZnO crystallizes with great preference in the wurtzite-type structure [58].

Hexagonal and zincblende polymorphs have no inversion symmetry (reflection of a crystal relatively any given point does not transform it into itself). This and other lattice symmetry properties result in piezoelectricity of the hexagonal and zincblende ZnO, and in pyroelectricity of hexagonal ZnO.

The hexagonal structure has a point group 6 mm (Hermann-Mauguin notation) or C_{6v} (Schoenflies notation), and the space group is $P6_3mc$ or C_{6v}. The lattice constants are a = 3.25 Å and c = 5.2 Å; their ratio c/a ~ 1.60 is close to the ideal value for hexagonal cell c/a = 1.633. As in most group II-VI materials, the bonding in ZnO is largely ionic, which explains its strong

piezoelectricity. Due to the polar Zn-O bonds, zinc and oxygen planes bear electric charge (positive and negative, respectively). Therefore, to maintain electrical neutrality, those planes reconstruct at atomic level in most relative materials, but not in ZnO – its surfaces are atomically flat, stable and exhibit no reconstruction. This anomaly of ZnO is not fully explained yet [59, 60].

A research study by Gumu [61] on the crystal structure of ZnO presented the following findings: The Polycrystalline ZnO thin films were deposited on a glass substrate by a spray pyrolysis technique using solution of zinc acetate and air as the carrier gas at 400 °C temperature. The X-ray diffraction analysis (XRD) was used for the analysis of crystal structure (see fig. 1.1).

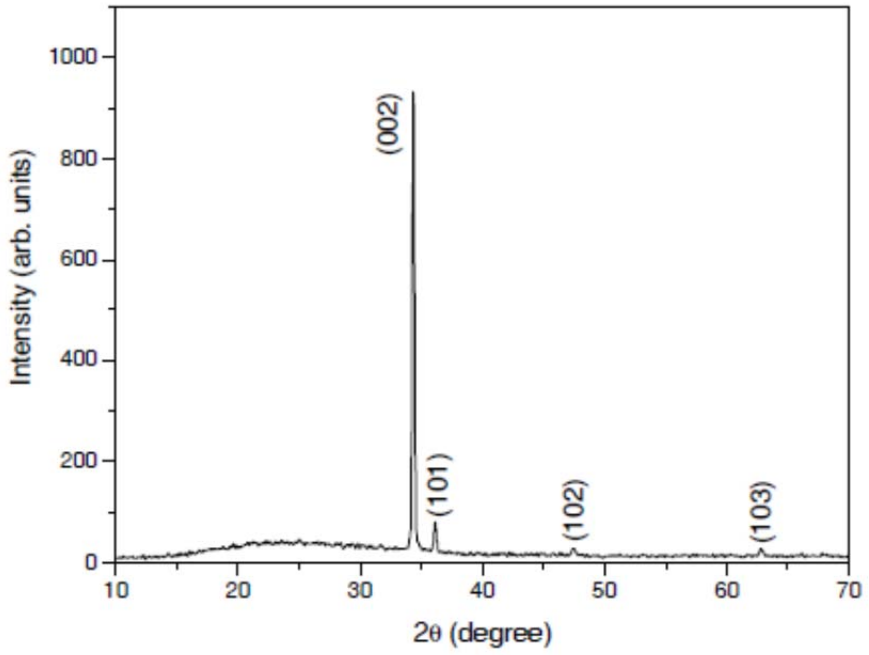

Fig. 1.1 shows the X-ray diffraction pattern of ZnO thin film deposited at 400 ^{0}C[61].

Fig. 1.1 shows the X-ray diffraction pattern of ZnO only with one sharp and three small peaks present. Diffraction pattern was obtained with 2θ from 10^{0} to 70^{0} at 60^{0} glancing angle. The XRD pattern of the film shows that the film is crystallized in the wurtzite phase and presents a

preferential orientation along the c-axis. The result is in agreement with the literature. The strongest peak observed at $2\theta = 34.39^0$ (d = 0.260 nm) can be attributed to the (002) plane of the hexagonal ZnO. The (101), (102) and (103) peaks were also observed at $2\theta = 36.17^0$, 47.47^0 and 62.78^0, respectively but these peaks are of much lower intensity than the (002) peak. The *c*-axis lattice constant of the ZnO thin film was calculated from XRD data as 5.21Å. The crystallite size was estimated at about 40 nm [61].

In another study, Kai wang [62] deposited ZnO thin films by Ion Beam Assisted Evaporation (IBAE). figure 1.2 reflects the XRD patterns with 2θ, ranging from 20^0 to 60^0 of the semiconducting ZnO film, fabricated at a discharge current of 2.25 A, discharge voltage of 120 V, and deposition rate of 1.5 Å/s. Only the (002) peak at $2\theta \approx 34^0$ is observed, identifying the formation of the ZnO film with a hexagonal structure and a preferred orientation with the *c*-axis perpendicular to the substrate.

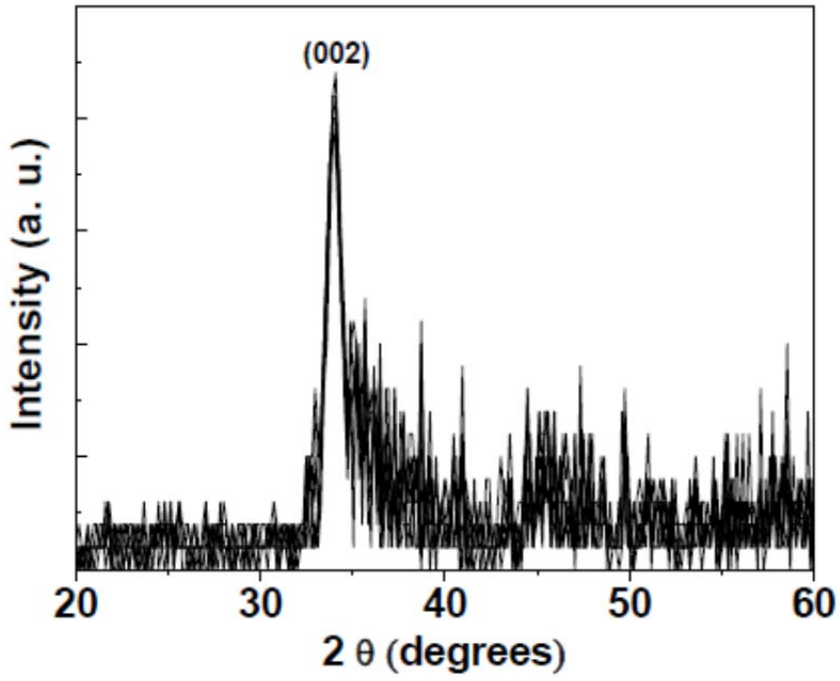

Figure 1.2: XRD patterns of the semiconducting ZnO film [62].

Similar results were also obtained by [63, 64, 65, 66, 67].

(ii) Mechanical properties

ZnO is a relatively soft material with approximate hardness of 4.5 on the Mohs scale [24]. Its elastic constants are smaller than those of relevant III-V semiconductors, such as gallium nitride (GaN). It has got high heat capacity and heat conductivity, low thermal expansion and high melting temperature which are beneficial for ceramics [68].

(iii) Electrical properties

ZnO has a relatively large direct band gap of ~3.3 eV at room temperature which has advantages such as higher breakdown voltages, ability to sustain large electric fields, lower electronic noise, and high-temperature and high-power operation. The bandgap of ZnO can further be tuned by alloying with magnesium oxide or cadmium oxide from 7.9 eV to 2.3 eV, spanning from deep ultraviolet (UV) to visible regions of the spectrum. It has a higher exciton binding energy (E_b of ~60 meV) than other wide band gap semiconductors like GaN and silicon carbide (SiC), leading to the efficient excitonic transitions at room temperature [24, 69].

The electrical properties of undoped ZnO film have been found to be of n-type, with a high conductivity due to the formation of native defects. These native (intrinsic) defects are: interstitial zinc, oxygen vacancies or hydrogen [70-75]. Generally, ZnO exhibits a wide range of conductivity from metallic to insulating. Typically, intrinisic thin film resistivities as low as 10^{-2} to 10^{-3} Ωcm could be achieved [76].

Generally, by Boltzmann's conductivity equation, ZnO conductivity is given by

$$\sigma = n\mu e$$

where σ, n, μ and e are electrical conductivity, carrier concentration, carrier mobility and electronic charge, respectively. Therefore, electrical conductivity of ZnO is directly related to the density (concentration) and mobility of charge carriers. Whereas the mobility mainly depends on the mechanism by which the carriers are scattered by lattice imperfections, such as ionized impurity scattering and grain boundary scattering [77], the density is determined by intrinsic (defects) or extrinsic (dopants) charge carriers present.

(iV) Optical Properties

Figure 1.3 shows the optical reflection, transmission and absorption spectra for ZnO transparent conducting oxide (TCO) on glass. First, the material is quite transparent, ~ 80%, in the visible portion of the spectrum, 400 – 700 nm. Suchea *et al* [78] and Lin. B [79] also concur that it's transparent to visible light (with a typical transmittance of 85-95%) and near-ultraviolet spectral regions, but strongly absorbs ultraviolet light below 3655Å (this threshold corresponds to the energy of 3655Å photons).

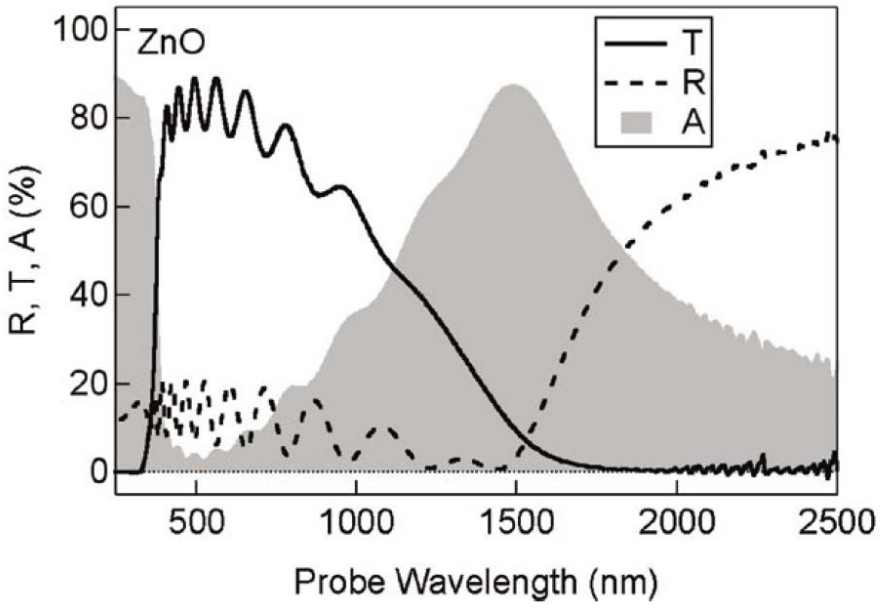

Figure 1.3 Optical Spectra of ZnO Transparent Conductor (Note, R-,T-,A- Reflection, Transmition and absorption, respectively) [80].

Across this spectral region where the sample is transparent, oscillations due to thin-film interference effects can be seen in both the transmission and reflection spectra. The short wavelength cut off in the transmission at ~300nm is due to the fundamental band gap excitation from the valence band to the conduction band of the ZnO semiconductor. The gradual long wavelength decrease in the transmission starting at ~ 1000nm and the corresponding increase in the reflection starting at ~ 1500nm are due to oscillations of the conduction band electrons known as plasma oscillations, or plasmons for short [80].

In a research study by Gumu [61], Highly transparent polycrystalline ZnO thin films were successfully prepared by the spray pyrolysis technique on glass substrate at 400 ^{o}C using solution of zinc acetate and air as a carrier gas. The films were found to exhibit high transmittance (>90 %), low absorbance and low reflectance in the visible regions. Fig. 1.4 shows the optical transmittance spectrum of ZnO thin film in the wavelength range from 300 to 1100 nm. The films are highly transparent in the visible range of the electromagnetic spectrum with an average transmittance values up to 95 %, and present a sharp ultraviolet cut-off at approximately 380 nm.

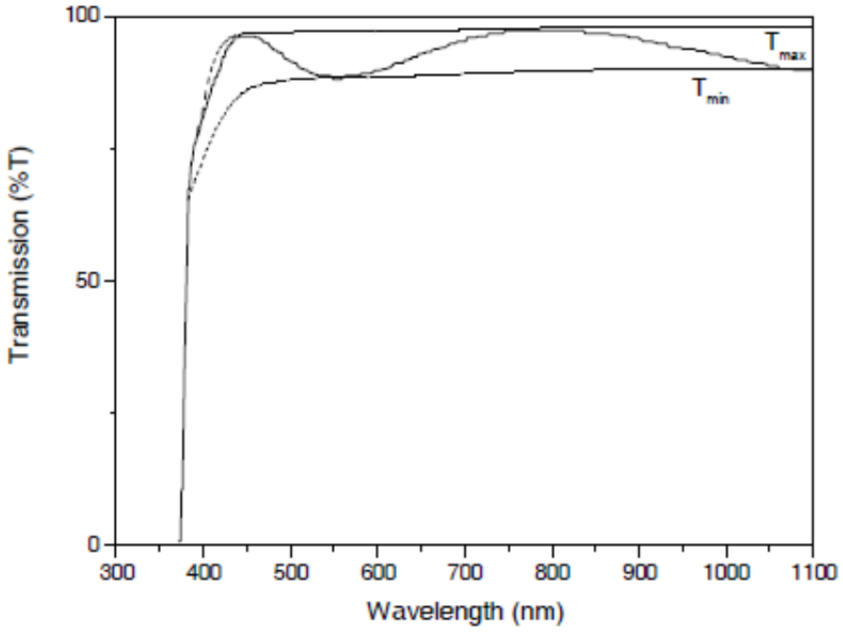

Fig. 1.4: UV/VIS/NIR transmission curve of ZnO film (UV-, VIS- and NIR- refer to ultraviolet, visible and near infrared regions, respectively) [61].

Similar results were also obtained by [62, 64, 66, 67, 78].

(V) Stability and Toxicity of ZnO

Long term stability of the ZnO is critical for stable performance of ZnO based devices and is dependent on both the thermal and chemical stability of the ZnO films. The stability

temperature for ZnO is ~ 250 ^{o}C[79]. Above this temperature, the film quality starts to degrade by thermal decomposition. Chemical stability of ZnO improves significantly with addition of dopants (such as Al, Ga, fluorine (F), Cobalt (Co)). The best results are obtained for films co – doped with (F, Ga):ZnO and (Al, Co):ZnO [80]. Similar results were presented by Minami [84] who noted that while the pure ZnO thin film is conductive, its thermal stability is not good enough. The film becomes unstable beyond a temperature of 150 ^{o}C and resistivity too may become unstable. He added Al to ZnO and found out that the thin film will becomes more stable compared with undoped ZnO thin films. He also suggested doping with Ga, In, Ti and Hf to improve on the film properties.

Comparatively, doped ZnO films are much more stable in reducing atmospheres and plasmas containing hydrogen species [79, 80]. Another important factor that contributes to the stability of ZnO and devices fabricated using these films is the scratch resistance or hardness. High hardness of the films ensures good mechanical durability and endurance. The hardness of the known TCOs increases in the following order Ag < ZnO < In_2O_3 < SnO_2 < TiN.

Meanwhile ZnO exhibits non-toxicity. The toxicity levels of elements currently used in the industry are as follows: Zn < Sn < In < Cd, Zn being the most benign, while Cd the most toxic.

III. DOPING OF ZNO

Usually pure ZnO thin films lack stability in terms of thermal edging in air or corrosive environments [10]. Besides, they have limited intrinsic electrical properties. Therefore polycrystalline ZnO films have to be doped with suitable impurity elements including group III and VII elements, among others to enhance their stability and electrical properties [79]. Extrinsic dopants play an important role of populating the conduction band so that the conductivity and carrier concentration of ZnO are improved. In particular, electrical conductivity can be readily modified by orders of magnitude by doping. The lowest resistivities reported are in the range of 1.2 to $2 \cdot 10^{-4}$ Ωcm [80-83]. Fig. 1.5 Compares the values of resistivities in impurity doped ZnO with other competing doped metal oxides-tin oxide (SnO_2), indium oxide (In_2O_3) over three decades (1970-2000). It can be seen from the figure that in the last 20 years (1980-

2000) the minimum resistivity achieved in impurity doped SnO_2 and In_2O_3 remained unchanged at 3-4 x 10^{-4} and 1-2 x 10^{-4} Ω-cm, respectively. Comparatively, the minimum resistivity achieved in doped ZnO seemed to be still decreasing and is already comparable to the lowest prevailing resistivity provided by indium-doped tin oxide (ITO) ~ 0.7 x 10^{-4} Ω-cm achieved by deposition of ITO films on glass at 300 ^{o}C by pulsed Laser Deposition (PLD) technique.

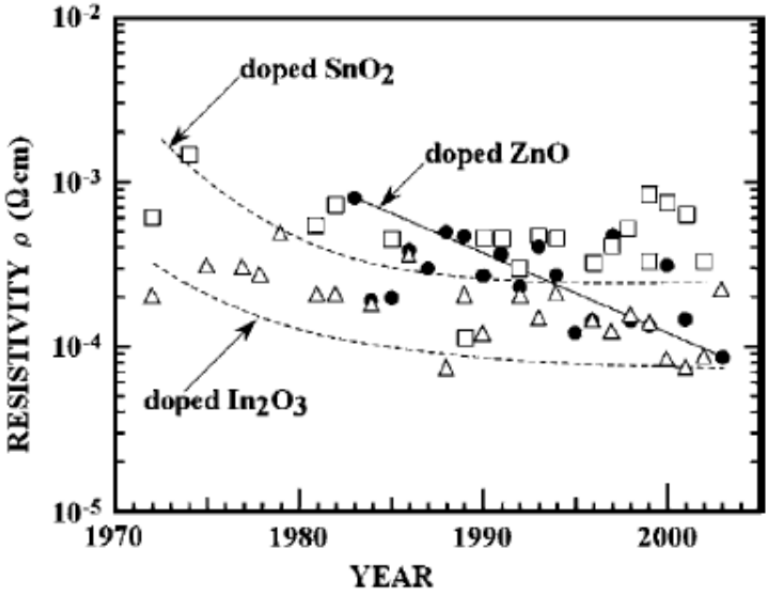

Figure 1.5: Minimum resistivity values reported for impurity doped ZnO (●), SnO_2 (□) and In_2O_3 (Δ) over the past three decades [80].

Extrinsic doping is fundamental to controlling the properties of ZnO and to obtaining of new multifunctional materials. ZnO is asymmetrically doped, that is, it can be doped easily either *n*-type or *p*-type but not both. This asymmetry has been explained with, first, the low or limited solubility of the desirable dopants; secondly, the high activation energies of these dopants; thirdly, the tendency to form spontaneously compensating defects, and lastly hydrogen acting as an unintentional extrinsic donor. n-type doping is easy while reliable p-type doping remains difficult. This problem originates from low solubility of p-type dopants and their compensation by abundant n-type impurities [82]. There is a wide variety of well developed doping methods, including sputtering, pulsed laser deposition and sol-gel [83-86].

n-type conducting ZnO can be readily obtained via either native or extrinsic donor defects. The performance of the dopant element depends on its nature, such as the electronegativity and ionic radius. In the case of using higher valence elements, named cationic impurities (such as group III elements) in ZnO, it is believed that the effective doping is achieved when Zn^{2+} ions are replaced by the impurities; whereas, if lower valence elements are used as dopants, as is the case of group VII elements, named anionic impurities, it is supposed that the oxygen ions are replaced by the impurities [87, 88]. Doping to increase and/ or control n-type electrical conductivity is commonly done with group III elements such as aluminium, boron, gallium and indium, or group VII elements such as fluorine [82]. Other dopants used include: group IV, II (Cu, Cd) elements, Y, Sc, F, V, Si, Ge, Ti, Zr, Hf [89]. These dopants act as a donor when it occupies a substitutional position for Zn^{2+} cation or an interstitial position in the ZnO lattice.

p-type electrical conductivity (where the dopant accepts electrons from the host material, leaving positive holes) is difficult to fabricate due to the native defects and self compensation that during doping resulting in lack of suitable dopants to produce reliable and reproducible films. Known acceptors in ZnO include group I elements (such as lithium), copper, and zinc vacancies, but all of these are deep acceptors and do not contribute significantly to hole conduction [90]. The main candidates are mainly group V elements, such as nitrogen [69, 70], phosphorous [23-25], arsenic [26, 27], and antimony [28, 29]. Recently, thin-film growers have focused on nitrogen as a shallower acceptor in ZnO [90]. Nitrogen is seen as the most promising candidate for successful p-type doping of ZnO films, because of its similar radius to the oxygen atom. Several groups report p-type ZnO:N films made via thermal oxidation of a Zn_3N_2 precursor [30–32], which addresses the problem of the low solubility of N acceptors in ZnO, but the resulting films are not particularly stable, and the mechanism by which N is incorporated is not clear [40].

A. ZnO n-type doping

ZnO can be doped n-type intrinsically, through native defects and extrinsically through impurity doping. For intrinsic n-type doping (unintentional doping), it is widely believed that intrinsic

defects such as the zinc interstitial (Zn_i) and oxygen vacancy (V_O) are source of donors in ZnO [91]. Vanheusden *et al.* [92] reported that the free carrier concentration was much larger than V_O in their samples, and Look *et al.* [93] suggested that Zn_i rather than V_O is the dominant native shallow donor in ZnO materials. It was also suggested that hydrogen atoms when incorporated form hydrogen-related donors, such as a substitutional hydrogen (H_O) and an interstitial hydrogen (H_i), which result in an increase in the donor concentration of ZnO [65, 94]. However, intrinsic doping remains controversial in regard to the origin of the conduction electrons [11].

On the other hand, extrinsic doping (Intentional doping) is accomplished using group III elements (such as Al, Ga, and In) as the most suitable, which can easily substitute Zn ions. Group VII elements (such as F and Cl), which substitute oxygen ion, have also been suggested for n-type dopants. Other dopants used include: group IV, II (Cu, Cd) elements, Y, Sc, F, V, Si, Ge, Ti, Zr, Hf [82 - 89].

Literature survey shows that ZnO can be extrinsically doped n-type either by mono-doping (single dopant) or co-doping (two dopants). Mono-doping is the long time dominant preference while co-doping is a recent suggestion in an attempt to improve the electrical conductivity beyond the limit of mono-doping.

1. Mono-doping of ZnO

(i) Effect of Aluminium (Al) on ZnO properties

Al doping of ZnO is favoured by both the small difference in electronegativity values of Zn (1.65) and Al (1.61) and the smaller ionic radii of Al (0.530 Å, 0.675 Å) when compared with Zn, (0.60 Å, 0.710Å) in the tetrahedral and octahedral configurations respectively[82].

Mounir [65] reported on structural and optical properties of ZnO:Al thin films prepared by the sol–gel process, in order to increase the band-gap and the optical transmittance. The best films were obtained for the ZnO films containing 2% of aluminum prepared at 550°C, with the best transmittance over the range 400-1000nm (from near ultraviolet to the near infrared, presenting an absorption cut-off at almost 290 nm). There was a change in the energy gap (E_g)

value from 3.16 eV to 3.18 eV when the ratio of Al was changed from 0% to 2%, and the best structural orientation was at (100), (002) and (101). The smoothest surface was also obtained for a dopant 2% value of the Aluminium. The optical transmittance was between 91% and 98% in the visible and near IR regions. The graphical and pictorial details of these findings are presented next.

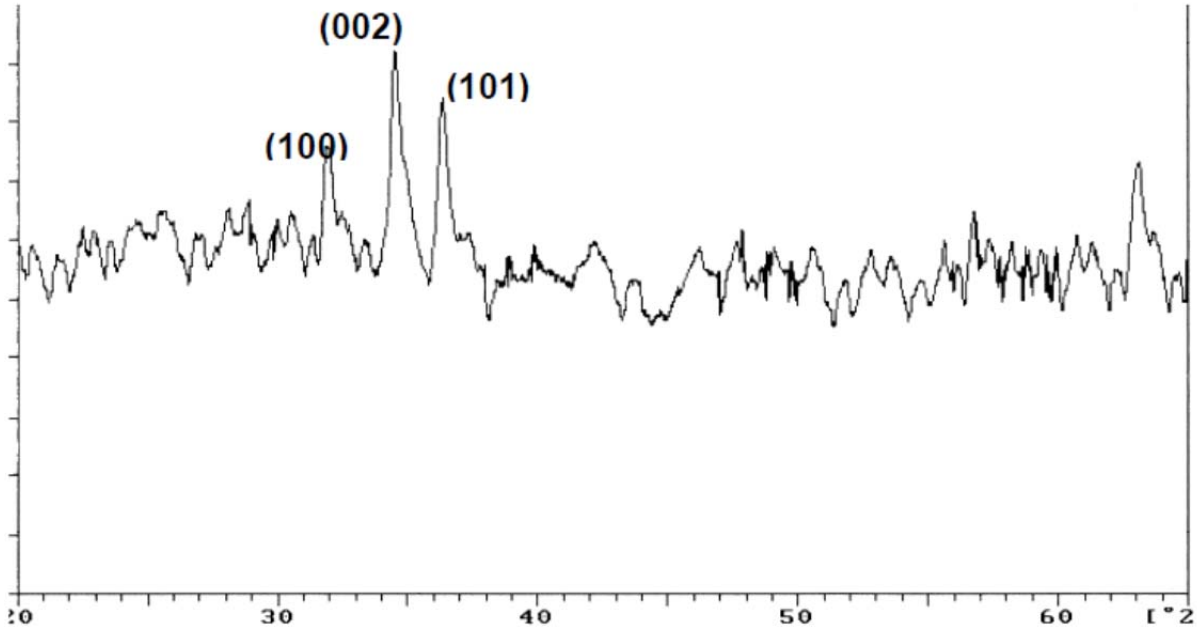

Figure 1.6: ZnO thin film XRD Spectrum[65].

Figure 1.6 displays the XRD Spectrum ZnO films. Three lines (100) at 2θ = 32°, (002) at 2θ = 34°, (101) at 2θ = 37° are pointed and considered for structural characterization of ZnO. Results of measured XRD spectra for ZnO:Al with different Al ratio (weight) from 1% to 4 % are represented in figure 1.7.

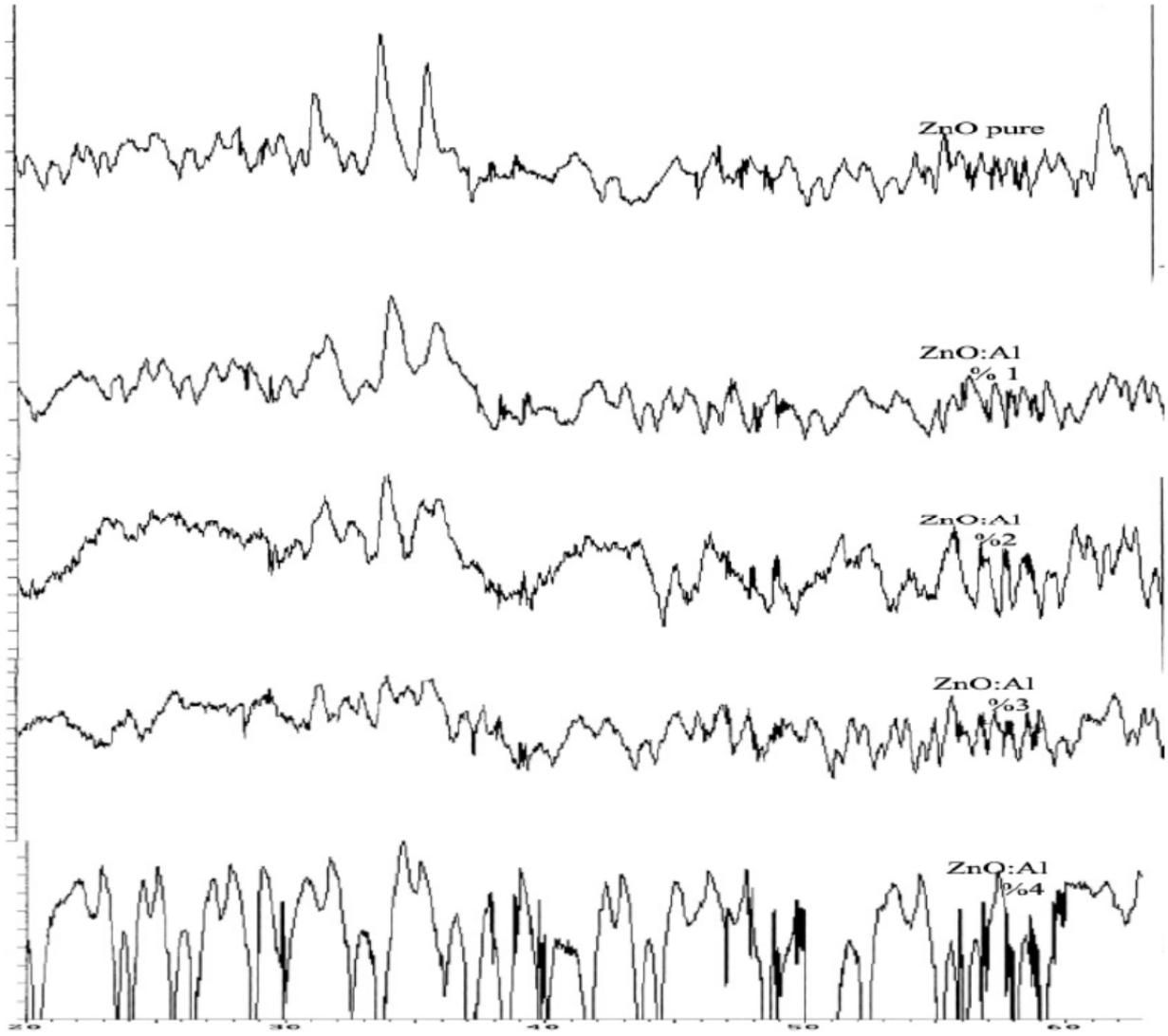

Figure 1.7: XRD Spectrums for ZnO:Al thin film. Al concentration (in weight) is indicated[65].

A significant evolution of the resolutions of ZnO (100), (002) and (101) characteristic lines is obtained. The increase of Al concentration in the starting material for the ZnO preparing process, leads to an amorphous stage of the films which appears at concentrations higher than 2%.

Characterization of surface and thickness of ZnO:Al films: Results are given in figure 1.8 for ZnO films and figure 1.9 displays the SEM observations for ZnO:Al films. The important results concern the smoothest surface (grain size) for a 2% (wt) Al impurities in ZnO:Al films, together with a first decrease of microstructures when increasing Al impurities until 2%.

Figure 1.10 displays the measured transmittance of the ZnO and ZnO:Al films in the rage 400nm to 1000 nm. Results show that the introduction of 2% of Aluminium in Zn0 films increases the film transmittance for lower values of the wavelength in the range 400 nm to 1000 nm and enable to obtain a variation of the transmittance lower than 7% in this range.

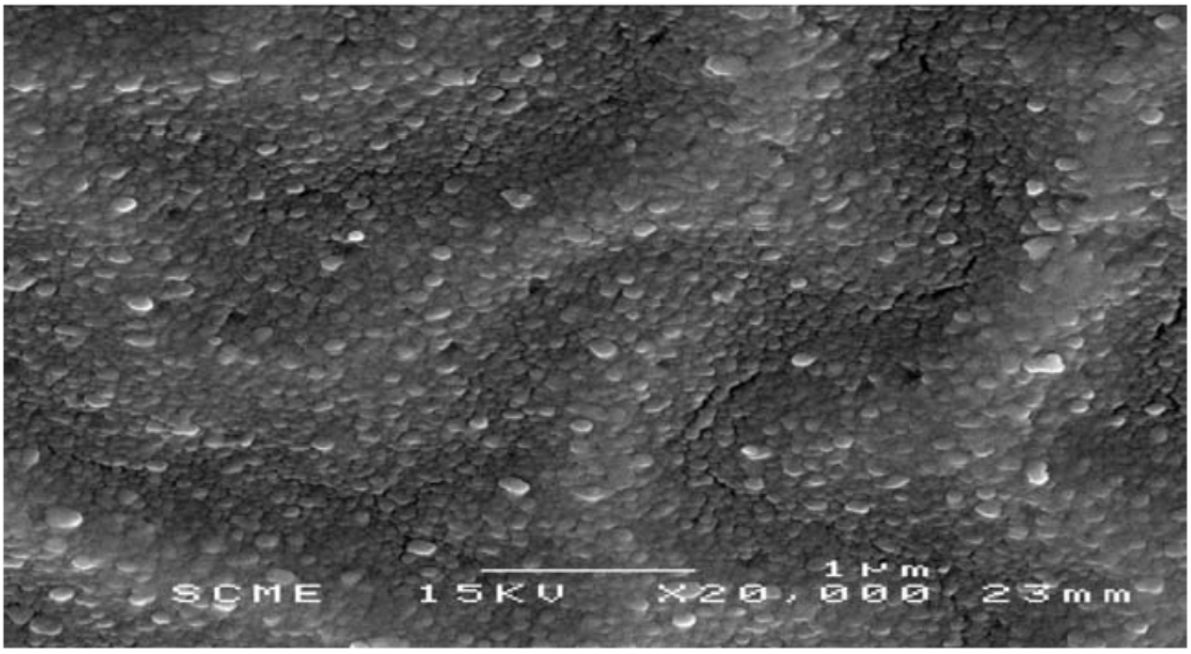

Figure 1.8: ZnO thin film observed by scanning electron microscope (SEM)[65].

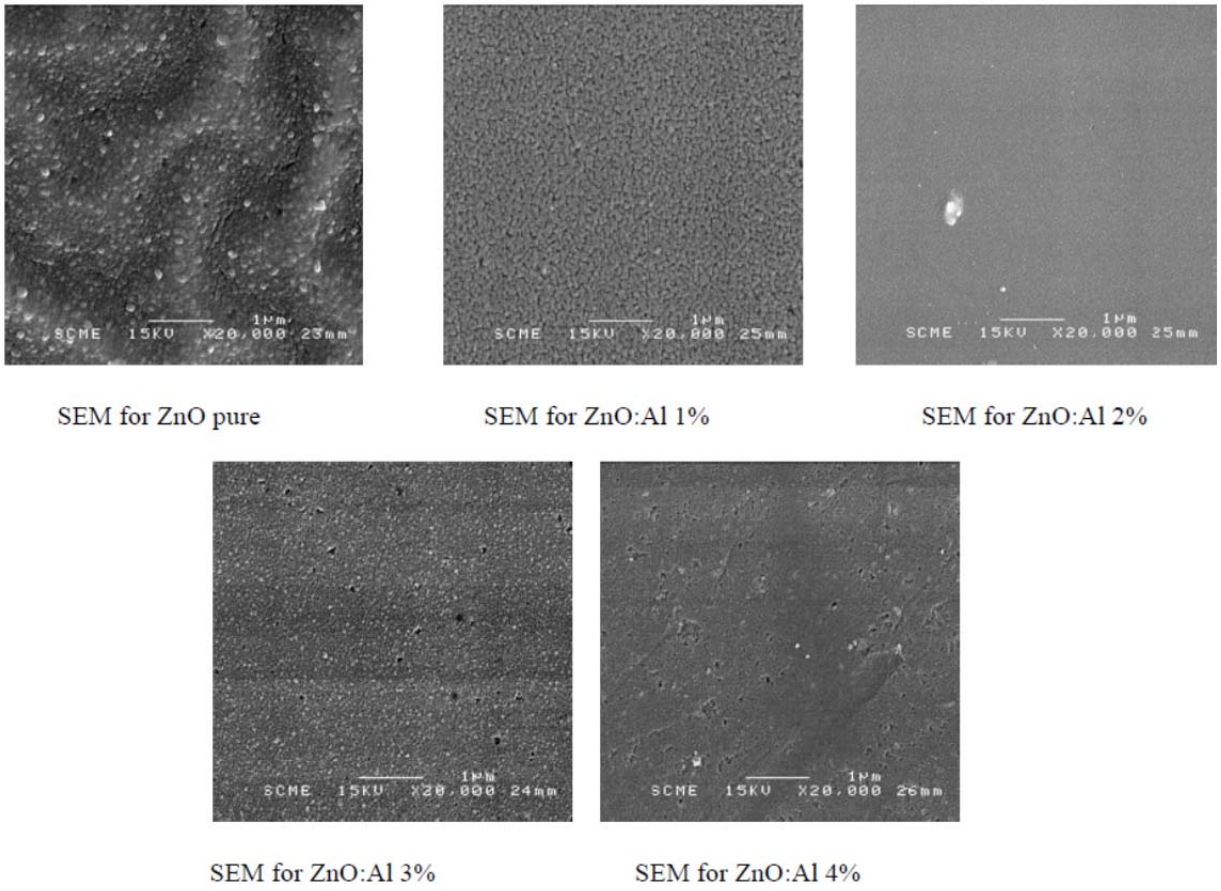

Figure 1.9: SEM pictures of ZnO:Al thin films obtained with incorporation of 1-4% (wt) Al [65].

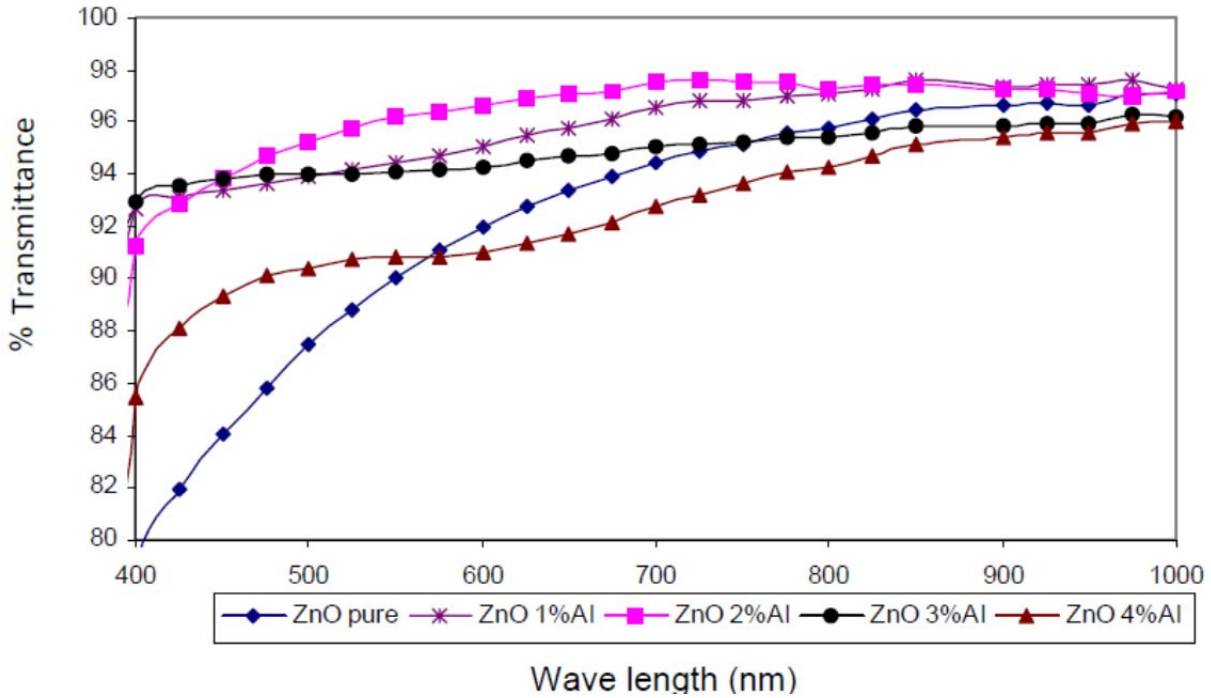

Figure 1.10: ZnO and ZnO:Al(1-4%) thin films transmittance spectroscopy [65]

Fanjie [95] doped Zinc Oxide with Aluminium (ZnO:Al or AZO) by radio frequency (RF) magnetron sputtering in order to achieve a proper resistivity and transmittance. Two primary parameters: target-substrate distance and sputtering power were optimized. The optimized parameters were confirmed as following: 8cm as the optimized distance; 200W and 250W as the optimized sputtering powers; and thickness between 300nm and 400nm as the optimized thickness. Resistivity was reported as $1x10^{-4}\Omega cm$ and transparency 90%. The AZO optimization had the follow conclusions: decreasing the distance between substrate and target will aid the production of optimized AZO; increasing sputtering power will benefit to increase the conductivity of AZO thin film, but the effect is not as significant as the target to substrate distance; increasing the sputtering power will increase the deposition rate and hence make the sputtering more efficient and the film can reach a balance between optical properties and electrical properties at a film thickness of about 300nm. The graphical and pictorials details of these results are given as below.

A series of samples were sputtered with different target to substrate distances at power levels of 50W, 100W and 150W. Table 1.1 is the sheet resistance and resistivity for the aforementioned samples. According to Table 1.3, we can conclude that for a specific power, the resistivity of the thin film is sensitive to the target to substrate distance. By decreasing the distance from 19cm to 8cm, the sheet resistance and resistivity can be decreased dramatically. Thus we can conclude that shorter target to substrate distance is better.

From Figure 1.14, we know that the resistivity decreases in similar fashion for different power. We also know that the deposition power also plays a role in determining the electrical properties. From the above curve, we can observe that the resistivity will decrease as power increase with distances kept the same. Generally speaking, higher power can contribute to decrease in resistivity.

In order to better understand the correlation between the thin film properties and target-substrate distance, a curve of resistivity as a function of distance of different power levels as shown in figure1.11, was plotted.

Table 1.1 the sheet resistance and resistivity as a function of distances for different power levels[95].

Power(W)	Distance(cm)	Thickness(nm)	Sheet Resistance(Ω/□)	Resistivity(Ωcm)
50	8	2170	6.7	1.45E-3
50	12	1580	90	1.42E-2
50	16	1015	6330	6.3E-1
50	19	533	49900	2.6
100	8	2170	8.3	1.8E-3
100	12	1580	14.8	2.4E-3
100	16	1015	285	2.9E-2
100	19	533	34900	1.86
150	8	2170	7.74	1.67E-3
150	12	1580	6.4	1.01E-3
150	16	1015	191	1.93E-2
150	19	533	13200	0.7

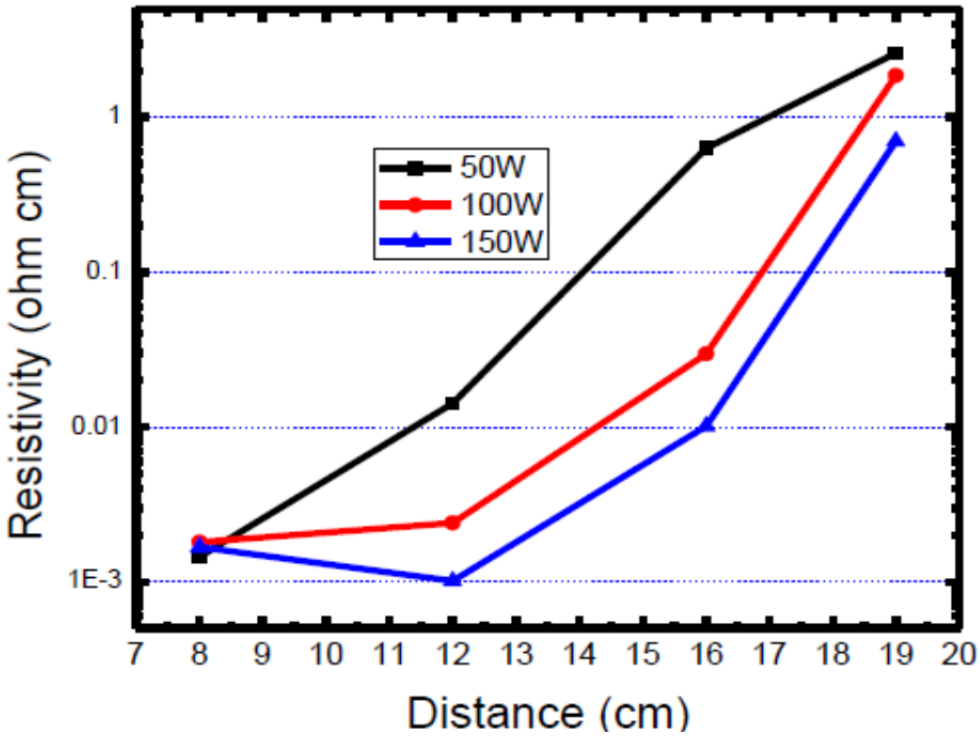

Figure 1.11: Resistivity as a function of target to substrate distance for different power levels[95].

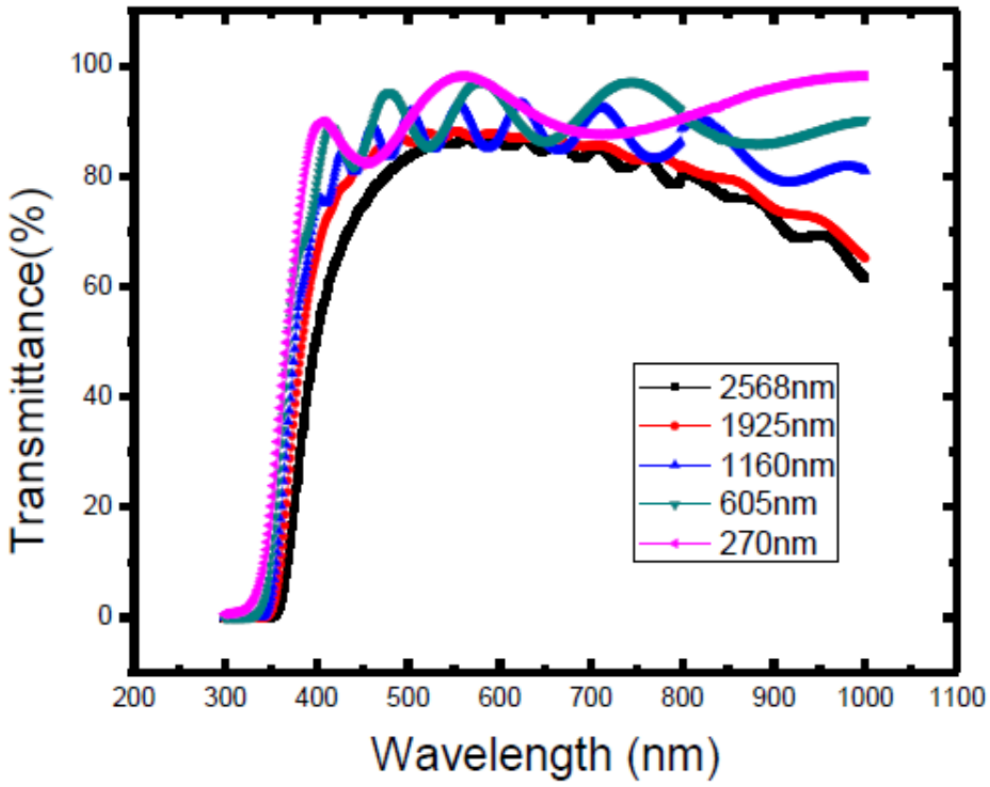

Figure 1.12: Transmittance spectrum in the visible range (150W 8cm)[95].

Figure 1.12 shows the transmittance spectrum for AZO thin film prepared at a 150W and a deposition distance 8cm; this shows that the AZO thin films are fairly transparent. Even when we increase the film thickness from 270nm to 2568nm, the transmittance will only decrease slightly, from about 90% to 80% in the visible range.

Table 1.2 shows the surface resistance and resistivity as a function of thickness for a particular target-substrate distances and power of 50W. A curve of resistivity as a function of thickness is plotted in Figure 1.13. According to the curve, 8cm is the optimized target substrate distance. And for a specific distance, during the first few hundreds of film thickness, the resistivity decreased dramatically, but it will become relatively stable if we continue increase the device thickness. This suggests that the optimized device is in the circle zone.

From Figure 1.13, we confirm that at the same target-substrate thickness and the same power, the resistivity will decrease as the film thickness increases. On the other hand, when thickness

and deposition power are kept the same, the target-substrate distance also plays an important role in decreasing the resistivity.

Table 1.2 Surface resistance and resistivity as a function of thickness for particular target-substrate distances and power of 50W[95].

50W 8cm	280nm	539nm	855nm	1800nm	2950nm
S.R(Ω/□)	1200	1150	91	12	4.1
Resistivity (Ωcm)	3.36E-2	6.19E-2	1.80E-3	2.1E-3	1.2E-3
50W 12cm	184nm	397nm	737nm	1126nm	1869nm
S.R(Ω/□)	350000	25000	804	108	91
Resistivity (Ωcm)	6.4	1.0	5.9E-2	1.2E-2	1.7E-2

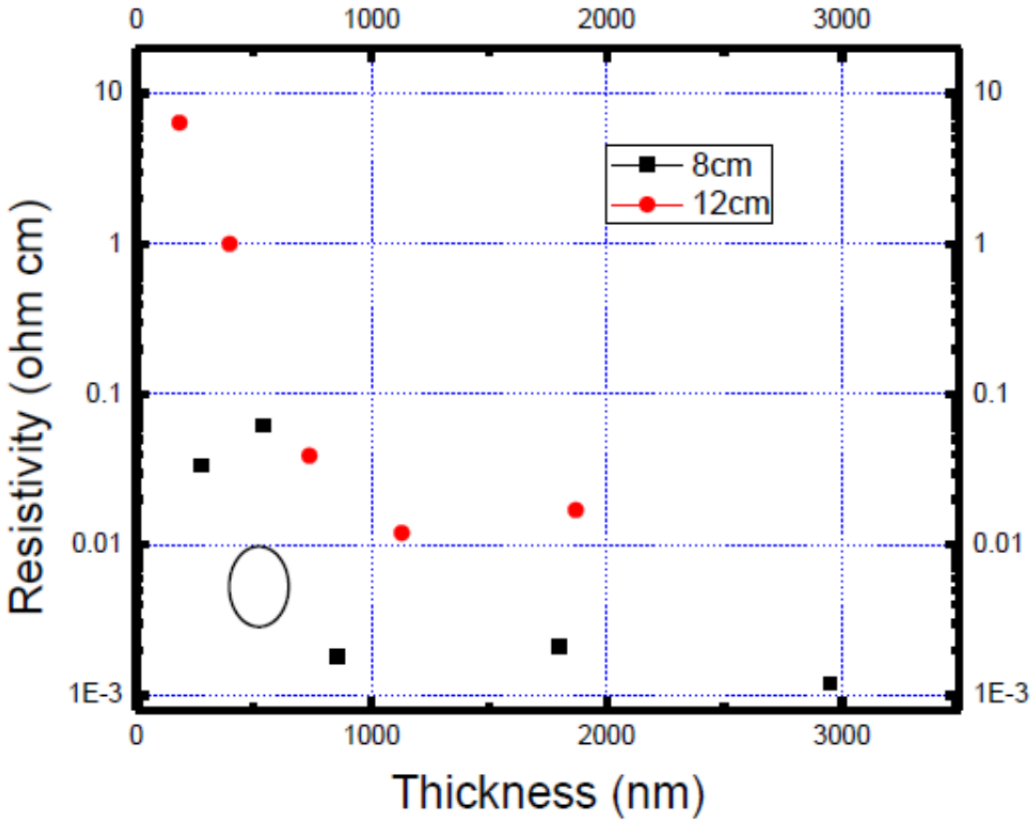

Figure 1.13: Resistivity as a function of film thickness for material deposited in 50W[95].

Table 1.3 shows the resistivity as a function of substrate-target distance with the same thickness and deposition power. The curve is plotted in Figure1.14.

.

Table 1.3 Resistivity as a function of substrate-target distance with the film thickness 600nm and deposition power 100W[95].

100W 600nm	8cm	12cm	16cm	19cm
S.R(Ω/□)	600	1150	7800	29900
Resistivity(Ωcm)	3.6E-3	6.9E-3	4.7E-2	1.8E-1

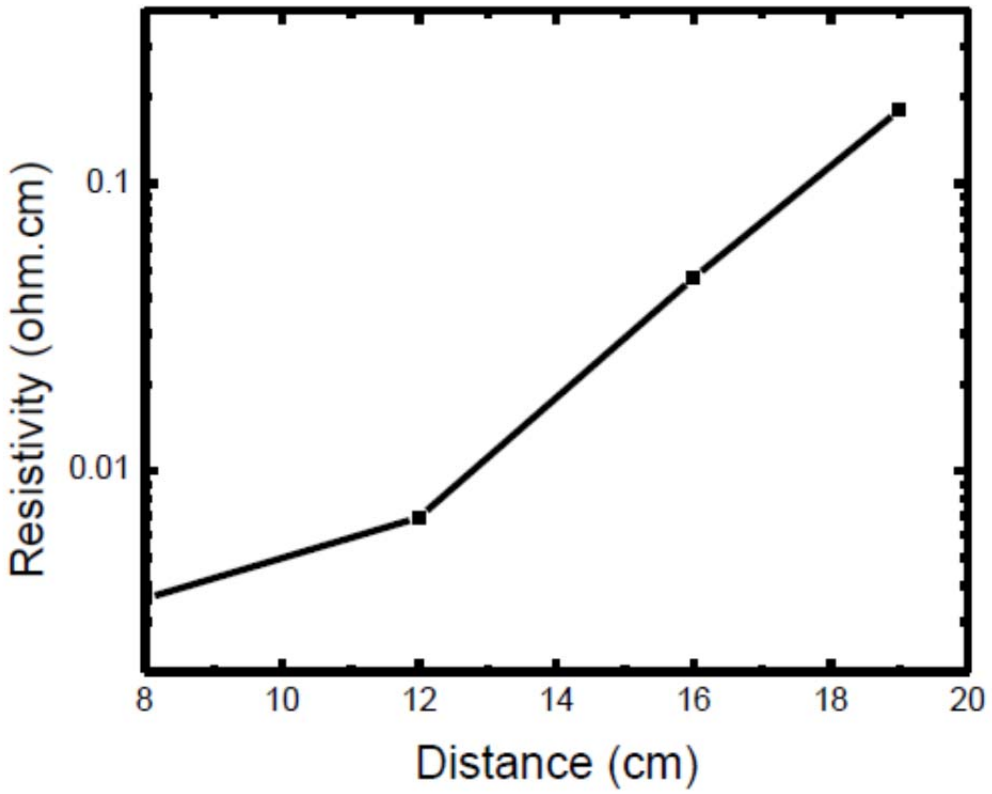

Figure 1.14: Resistivity as a function of substrate-target distance for a 600nm thick film at 100W[95].

According 1.14, when power and film thickness are kept unchanged, the target to substrate distance will play an important role in determining the film resistivity. The resistivity will

increase from 3.6E-3Ωcm at the distance 8cm to 1.8E-1Ωcm at the distance 19cm. In conclusion, the resistivity will decrease dramatically as the target-substrate distance decrease and other parameter are kept the same. The target-substrate distance is a primary parameter determining the electrical property of the AZO thin film. As the distance is shortened, the distance between target and substrate and a more conductive thin film anode can be achieved.

Figure1.15 shows the transmittance spectrum in the visible range for 600nm AZO thin films deposited at 100W at different target to substrate distances. We can conclude that in the visible spectrum, the transmittance does not change when we change the target-substrate distance. At all four distances, the transmittances are more than 90% in visible spectrum.

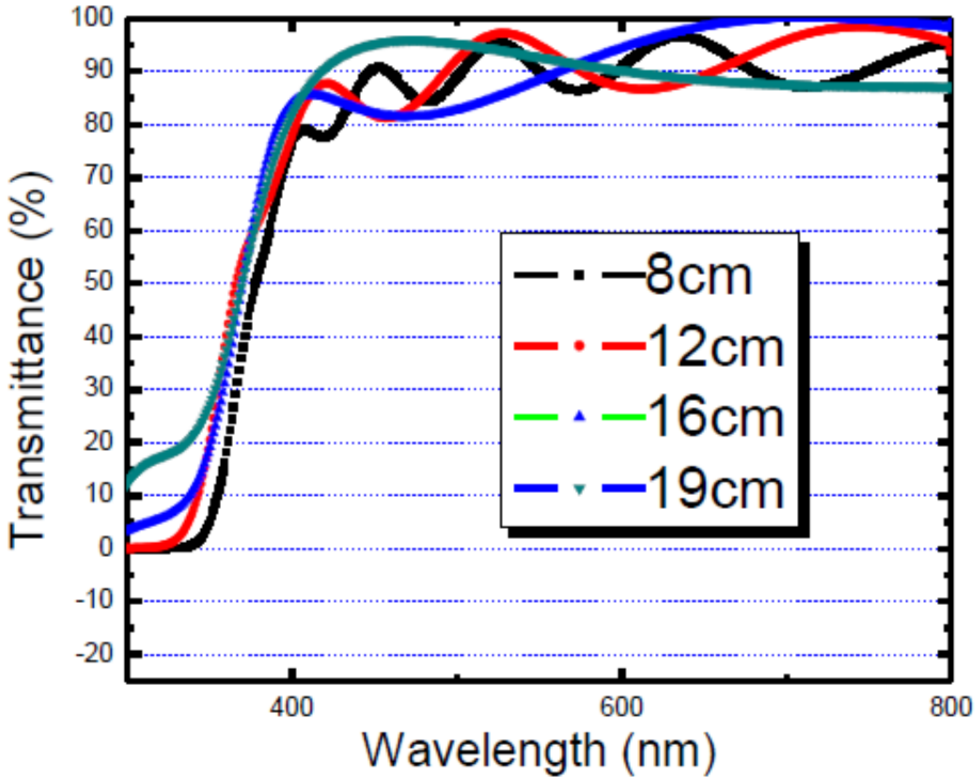

Figure1.15 The transmittance spectrum in the visible range for 600nm thick AZO thin films deposited at different target to substrate distances with power of 100W[95].

Aluminum doped zinc oxide films were prepared by reactive mid frequency magnetron sputtering. The idea was to characterize the electrical and optical properties [96]. The carrier mobility could be increased up to 42 cm^2/Vs and the transmission between 400 nm and 1100

nm was enhanced by the reduction of aluminum content in the targets. ZnO:Al films with high conductivity and excellent transparency in the visible and also NIR were developed at high dynamic deposition rates of up to 115 nm*m/min by mid frequency magnetron sputtering. An optimization of the aluminum concentration and the substrate temperature leads to high carrier mobility of 42 cm²/Vs.

Table 1.4: Thickness, aluminum concentration, resistivity ρ, carrier concentration N and mobility μ of ZnO:Alfilms shown in Fig. 1.17 and Fig. 1.18 [96].

Film	Thickness (nm)	Al-concentration (at%)	ρ (10^{-4} Ohmcm)	N (10^{20} cm^{-3})	μ (cm^2/Vs)
A	620	2.3	3.3	4.4	42
B	870	2.7	2.8	5.3	41
C	896	3.8	2.6	8.0	30
D	866	6.0	5.2	9.	13
E	906	1.1	17630	0.12	0.3
F	809	Not available	4.4	3.4	42
G	793	3.0	2.4	6.8	38

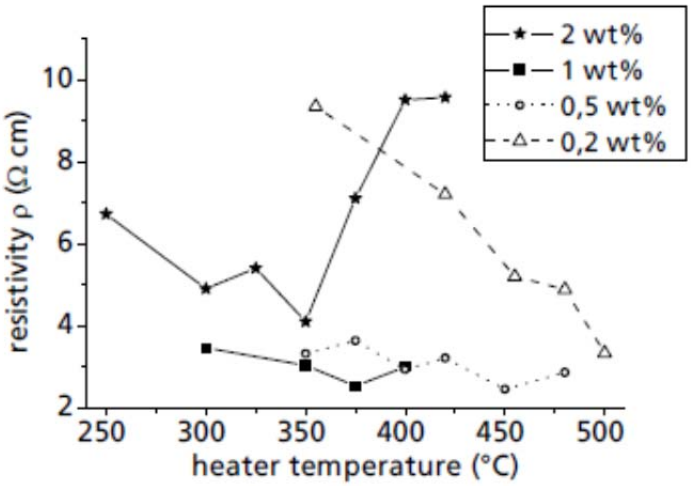

Fig. 1.16. Resistivity ρ of ZnO:Al films as a function of the heater temperature. The different curves correspond to films prepared from targets with different aluminum content given in the legend [96].

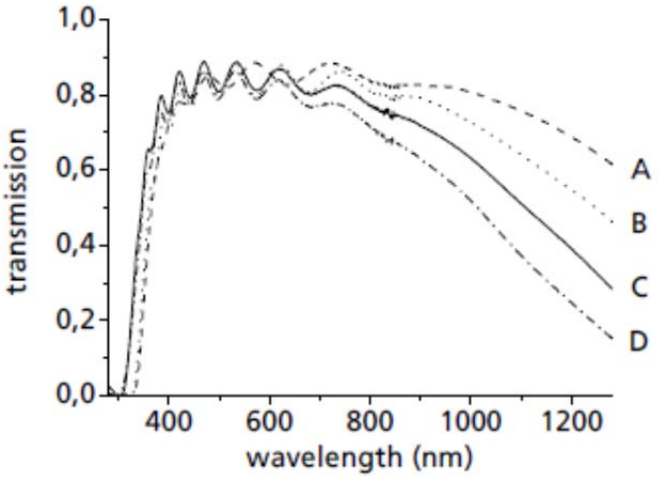

Fig. 1.17. Spectral transmission of ZnO:Al for targets with different Al concentrations using optimized sputtering conditions. Some film properties are given in Table 1.4 [96].

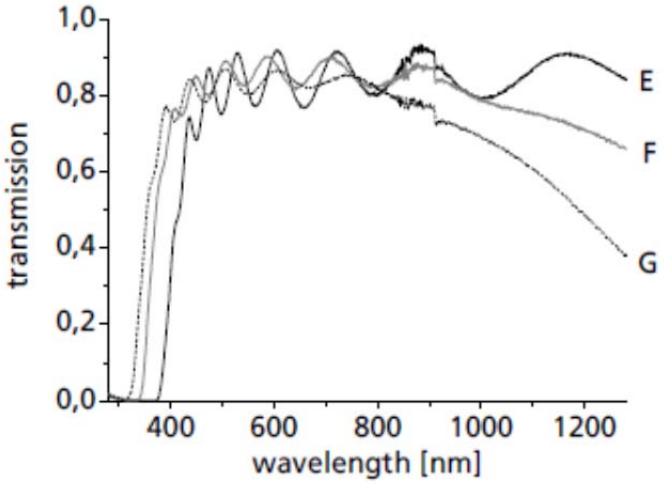

Fig. 1.18. Transmission of ZnO:Al coated glass for films from targets with different Aluminum content. The electrical properties of the films are shown in Table 1.4 [96].

Jae Keun Seo [97] deposited AZO films on glass substrates by the RF magnetron sputtering method using an AZO target (Al: 2 wt.%) at room temperature. The effect of RF power on structural, electrical, and optical properties of 150- nm-thick AZO films was investigated. XRD results showed that AZO films have highly preferred orientation (002) peaks. The grain size of the AZO film in the cases of 150 W and 200 W RF power were 27.6 and 34.2 nm, respectively. Also, RF powers of 150 W and 200 W provided good electrical and optical properties. The

resulting values for 150 W and 200 W are summarized as a resistivity of 0.017 Ω·cm and 0.014 Ω·cm, a sheet resistance of 510 Ω·sq and 411 Ω·sq, and a transmittance 94.59% and 94.53%, respectively. The pictorial and graphical details are presented in figures 1.22 – 1.26.

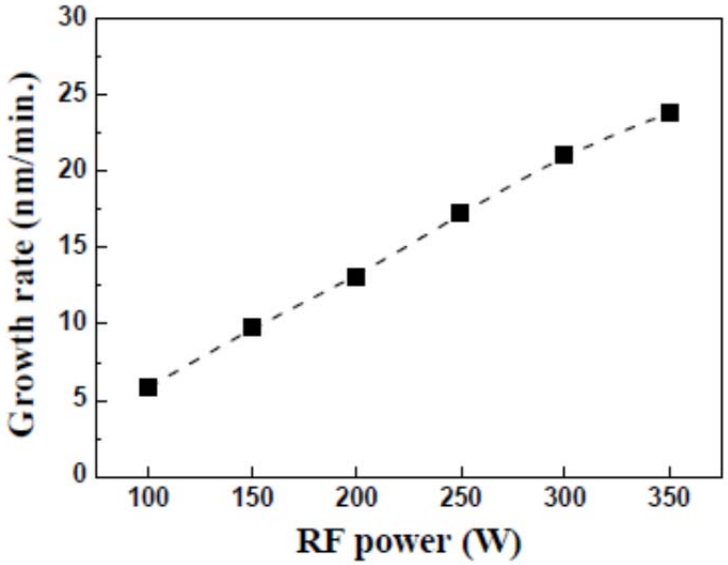

Figure 1.19: The growth rate of Al-doped zinc oxide films as a function of radio frequency (RF) power [97].

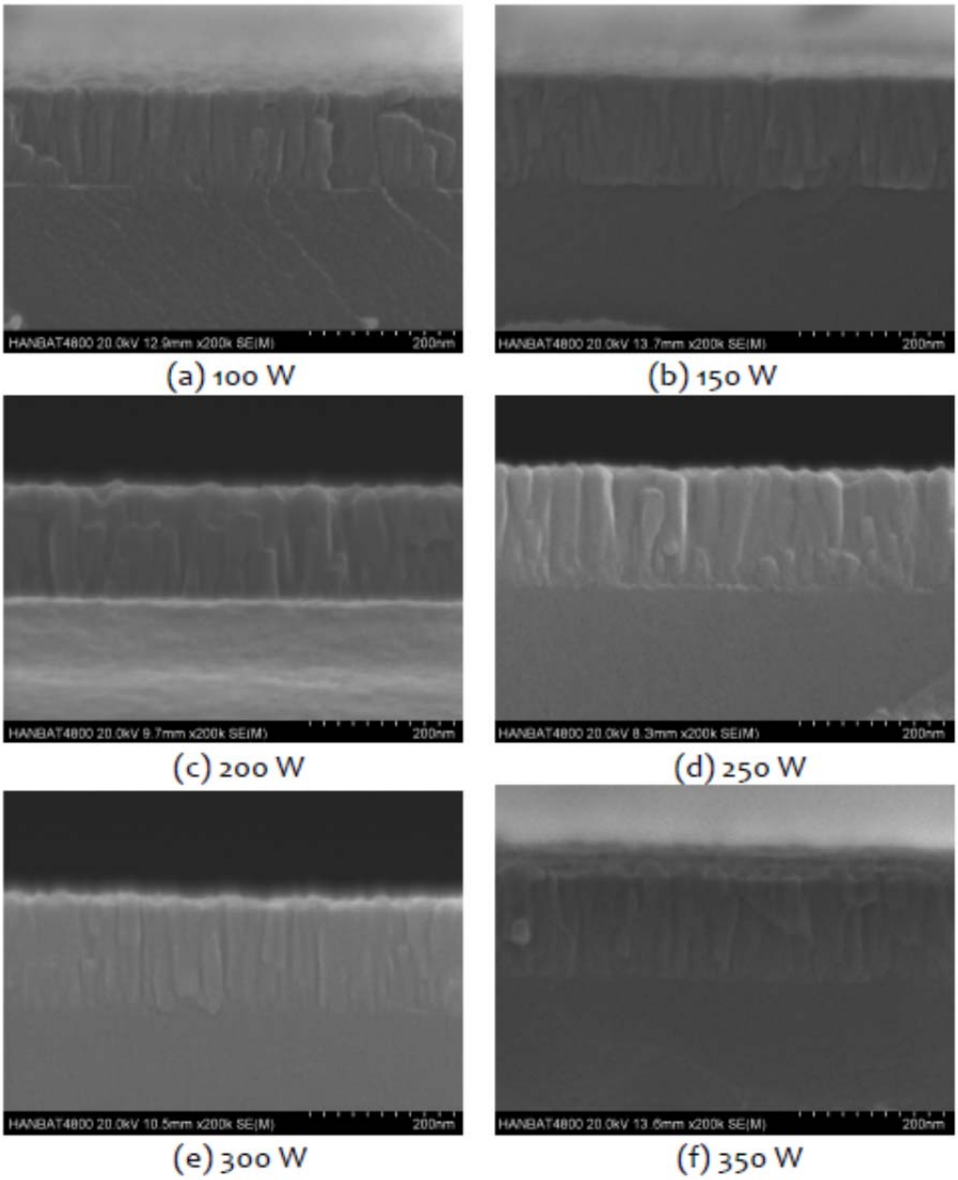

Figure 1.20: The cross-sectional scanning electron microscopy images of Al-doped zinc films as a function of radio frequency [97].

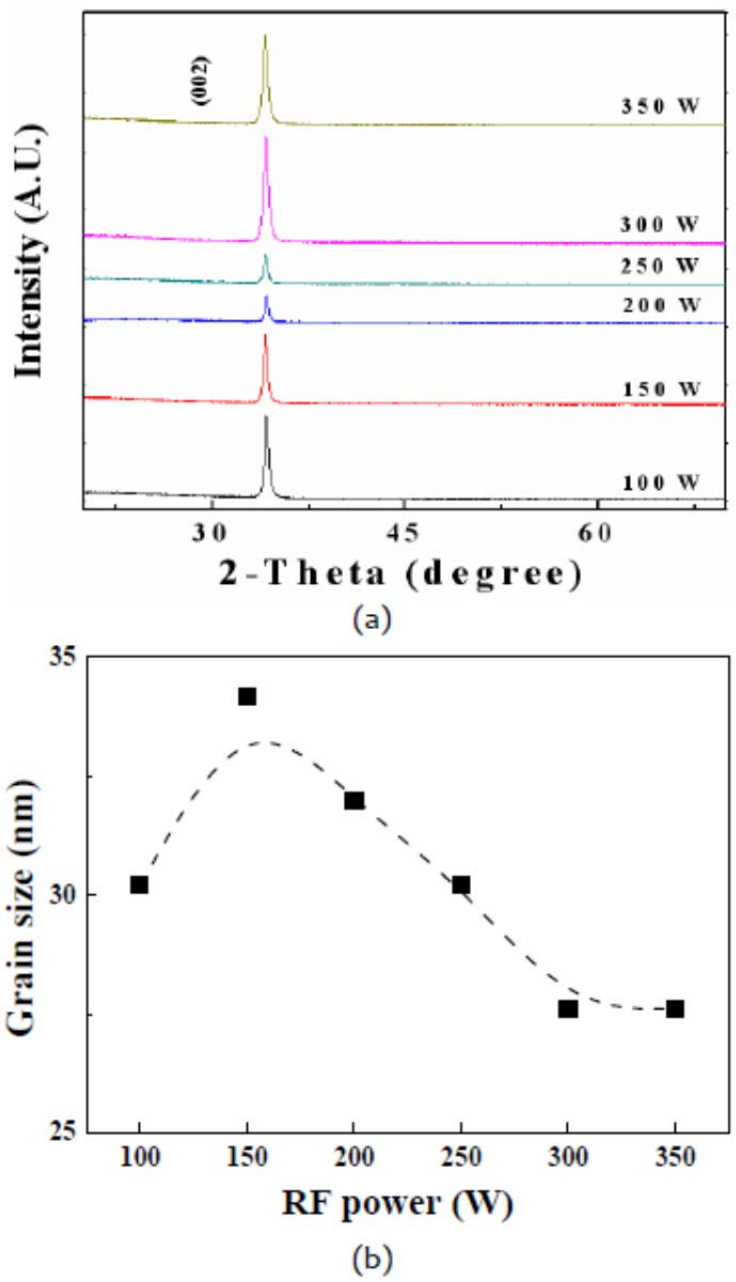

Figure 1.21: X-ray diffraction results of Al-doped zinc oxide films deposited on a glass substrate, (a) X-ray spectra and (b) grain size. RF: radio frequency [97].

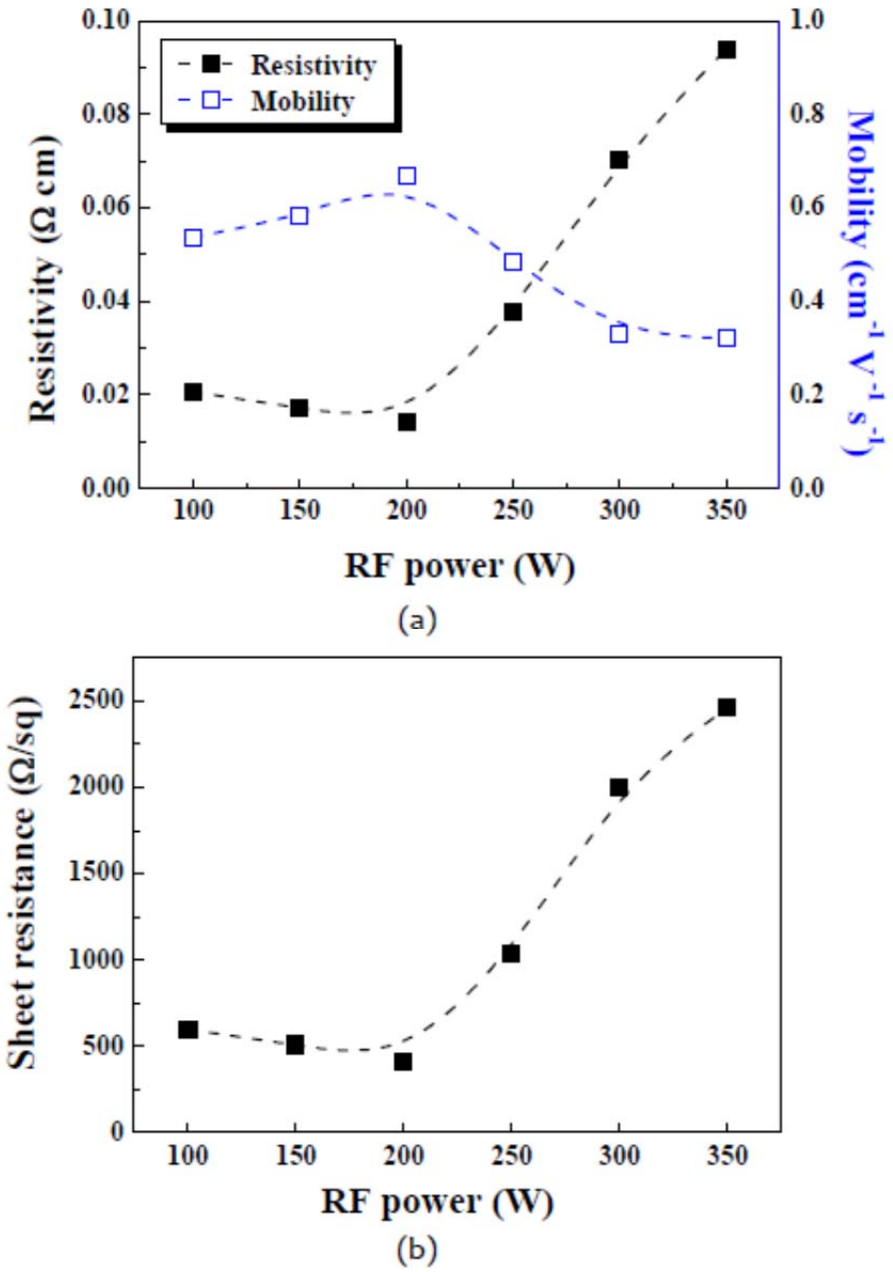

Figure 1.22: Electrical properties of Al-doped zinc oxide films as a function of radio frequency(RF) power, (a) resistivity and mobility by Hall measurement and (b) sheet resistance by four-point probe [97].

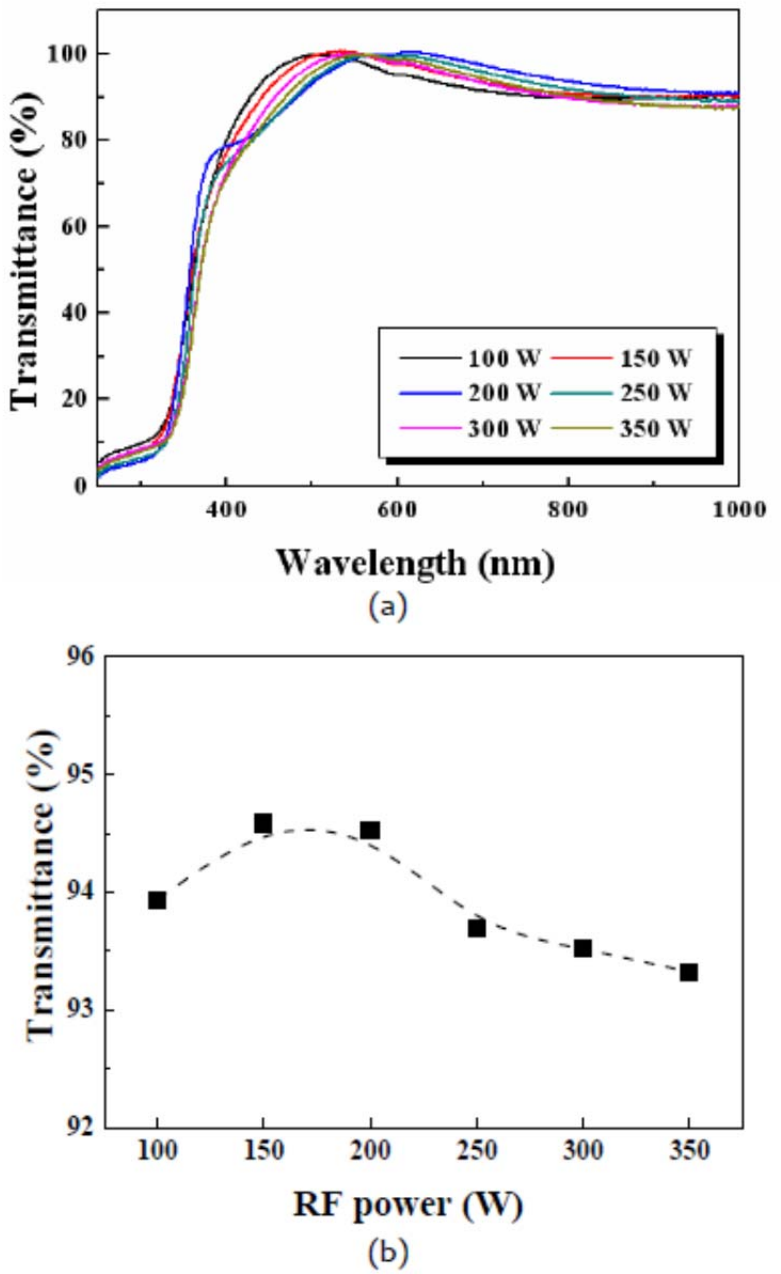

Figure 1.23: Optical properties of Al-doped zinc oxide films as a function of radio frequency (RF) power, (a) transmittance spectra and (b) average transmittance (400 – 800 nm) [97].

Dong-Hyun Hwang *et. al*. [78] deposited Al-doped Zinc Oxide (AZO) on glass substrates by radio frequency (R.F.) magnetron sputtering technique. The properties of the films were controlled by adjusting the oxygen flow contents as a mixture of Ar and O_2 gases. The structural, electrical and optical properties of the films were characterized by X-ray diffraction (XRD), atomic force

microscopy (AFM), a UV-visible spectrometer, as well as Hall effect measurements. Results revealed that a film deposited with an oxygen partial pressure content of 0% had a hexagonal structure, a strongly preferred orientation with the c-axis perpendicular to the substrate and the lowest resistivity of about 6.9×10^{-4} Ω cm. The optical transmittance spectra showed more than 80% transmittance in the visible region, and the band gap was found to be direct. Strong violet emission located at 2.96 eV was observed in the AZO films deposited with an oxygen partial pressure content of 0%. Figures 1.24- 1.26 show the results.

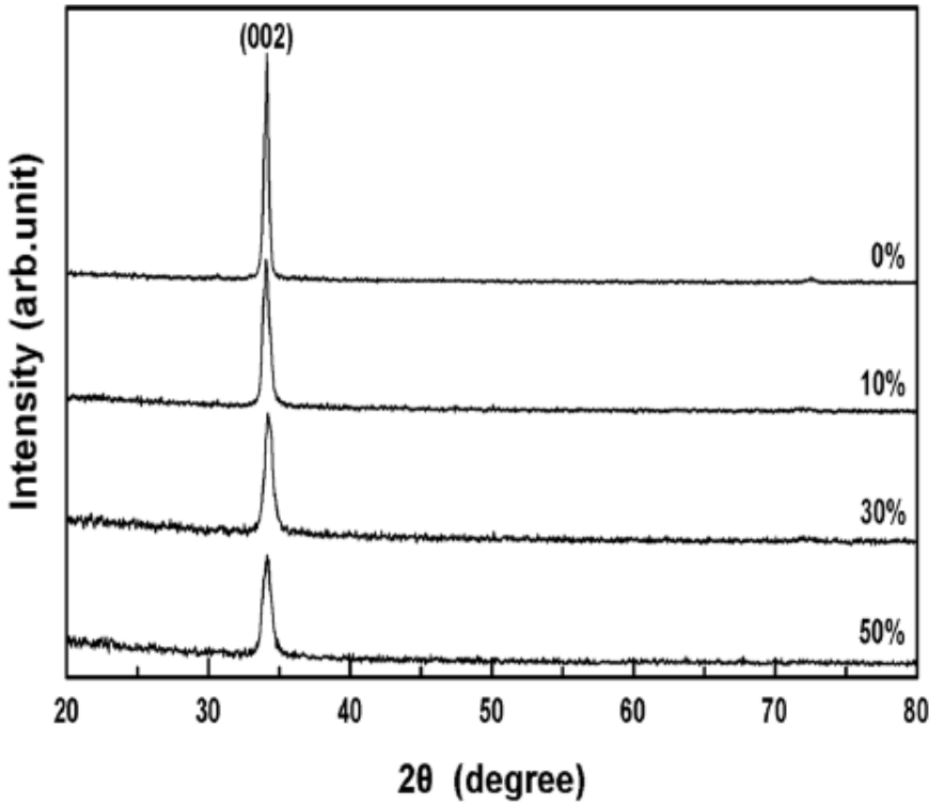

Fig. 1.24: XRD spectra of AZO films grown at various oxygen flow contents of 0%, 10%, 30% and 0% [78].

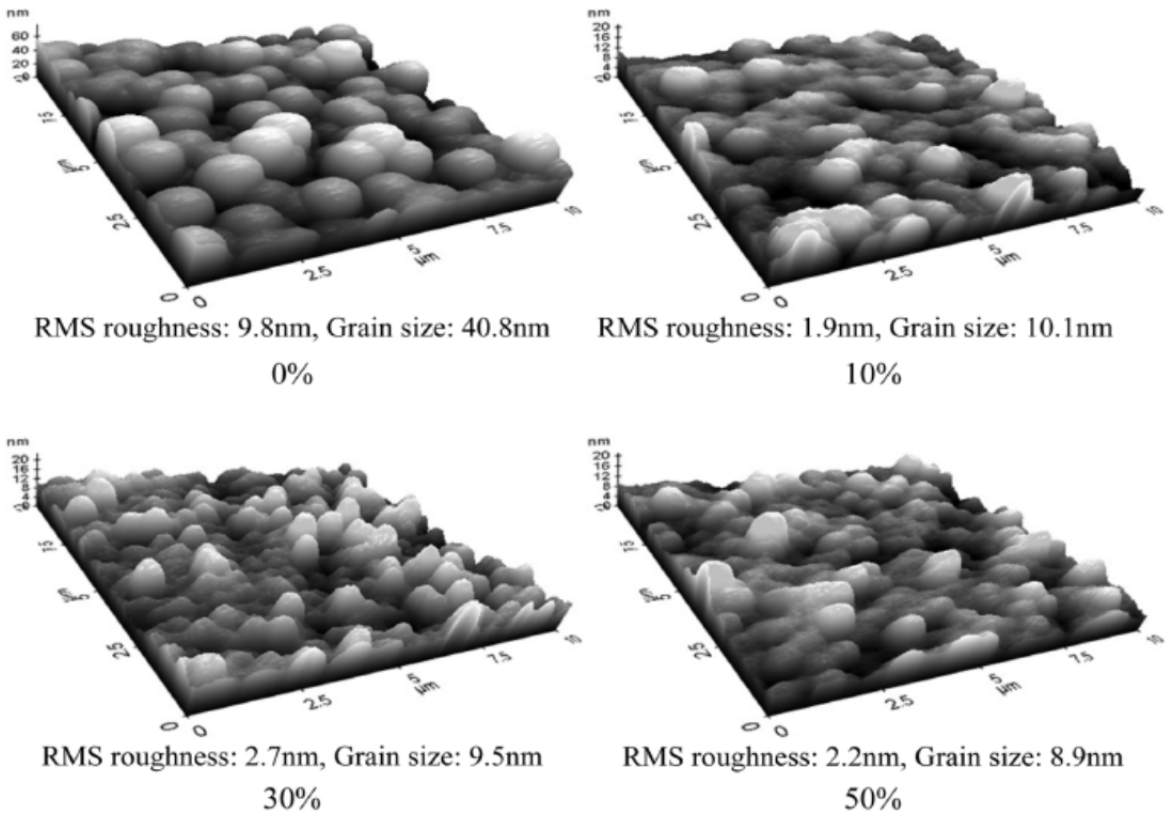

Fig. 1.25. AFM surface images of AZO films deposited at different oxygen flow contents of 0%, 10%, 30% and 50% [78].

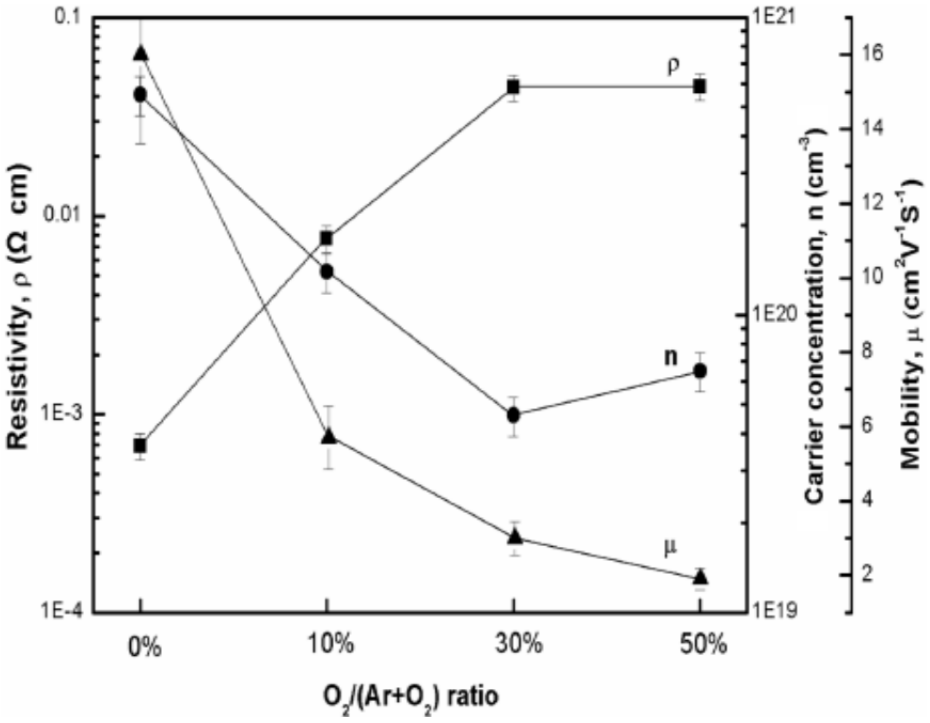

Fig. 1.26: Electrical properties of AZO films prepared at several oxygen flow contents [78].

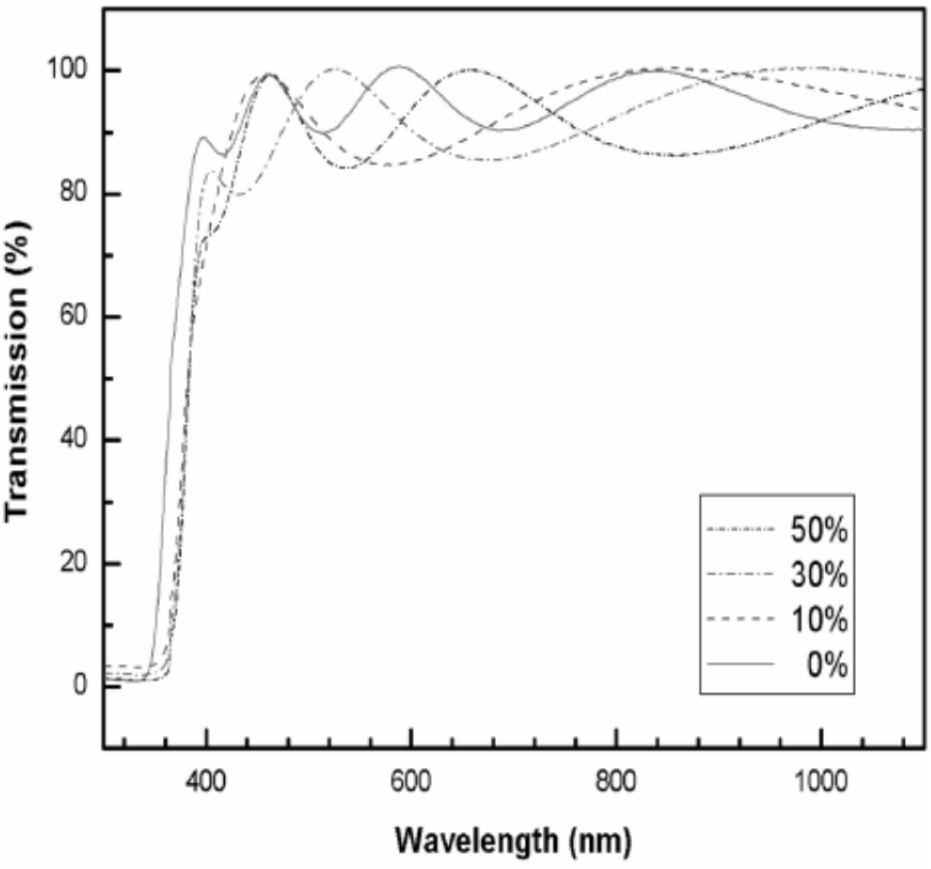

Fig. 1.27: Optical transmittance spectra of AZO films grown at various oxygen flow contents[78].

Aluminum doped zinc oxide (AZO) thin film was deposited on microscopic glass substrate following a chemical technique called successive ion layer adsorption and reaction (SILAR) [63]. The technique involves multiple dipping of the substrate in an aqueous solution of sodium zincate kept at room temperature and deionized water kept near boiling point. Al doping was found to increase the film growth rate. It was approximately 0.20 μm/mole/dipping for ZnO film and 0.22 μm/mole/dipping for AZO film. Structural characterization by X-ray diffraction (XRD) technique confirmed incorporation of aluminum in ZnO lattice. The c-axis orientation was significantly enhanced due to Al incorporation which was revealed from marked increase of (002) peak intensity compared to other peaks of hexagonal ZnO. The cross sectional view in SEM (Scanning electron micrograph) also reveals growth of large crystallites perpendicular to the substrate. The resistance of the film decreased about one order in magnitude due to Al

doping. The activation barrier value of 0.31 eV for ZnO film was however found to be unaffected due to aluminum incorporation. The results are shown in figures 1.28 – 1.33.

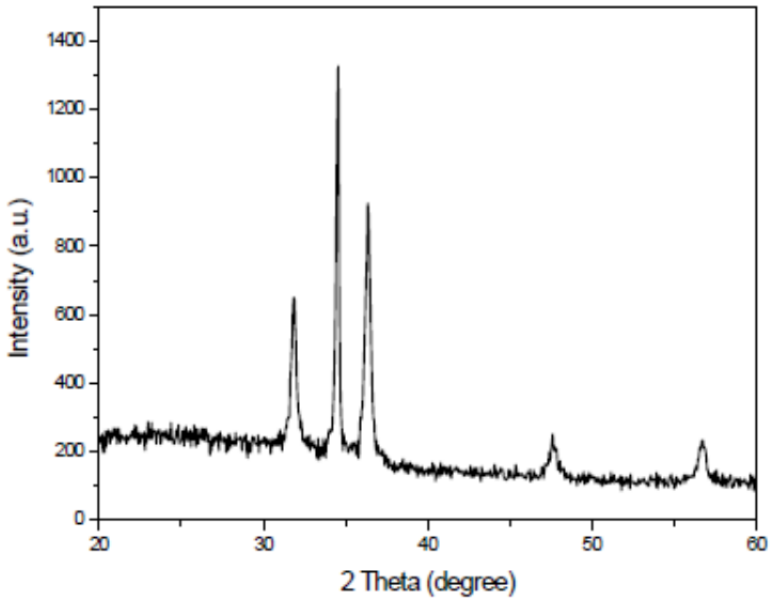

Figure 1.28: XRD pattern of undoped ZnO film(5.0 µm thick) [63].

It is seen from Figure 1.28, the (002) peak appears with maximum intensity at 34.55^0. The other peaks at 31.85^0, 36.35^0, 47.6^0 and 56.85^0 can be associated with (100), (101), (102) and (110) peaks of ZnO, as is expected for hexagonal ZnO structure [98]. The strong preferred c-axis orientation is evident from the figure.

Figure 1.29, on the other hand, shows the XRD pattern of AZO film. The figure indicates clearly that Al-doping promotes c-axis orientation. Figure 1.30 shows the pattern of the AZO film heat treated at 400 ^oC for 1 hour. Heating at 400^0C did not produce any modification in the structural orientation. The invariance in structure indicates that incorporation of aluminium was complete after 200 ^oC heat treatment. The location of the diffraction pattern peaks is shifted slightly to the high diffraction angle. It is evident that aluminium doping increases the intensity of (002) peak and decreases the intensity of all other peaks. No metallic Al characteristic peak was observed. This may be due to Al replacing zinc substitutionally in the lattice or aluminum segregation to the non-crystalline regions in the grain boundary.

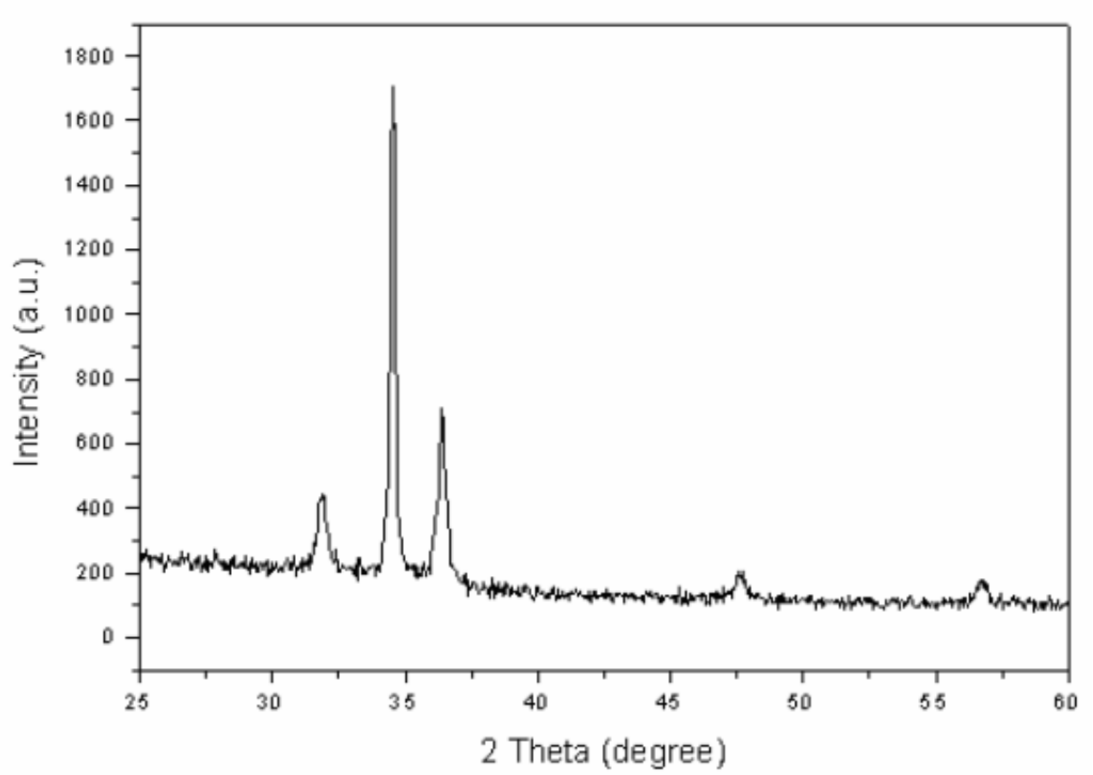

Figure 1.29: XRD pattern of 7% Al-doped ZnO film treated at 200 ^{o}C [63].

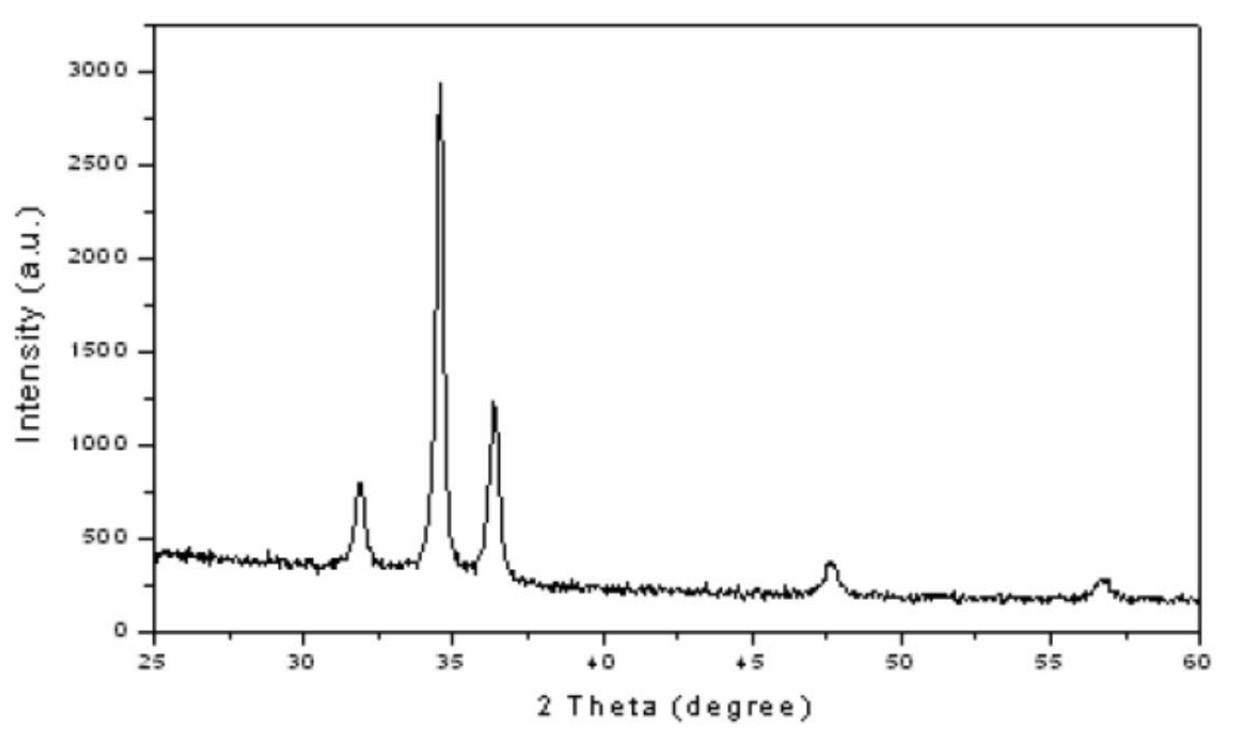

Figure 1.30: XRD pattern of heat treated (400^{o}C, 1 hr.) Al-doped ZnO film [63].

Fig.1.31: SEM pictures of ZnO film on glass [63].

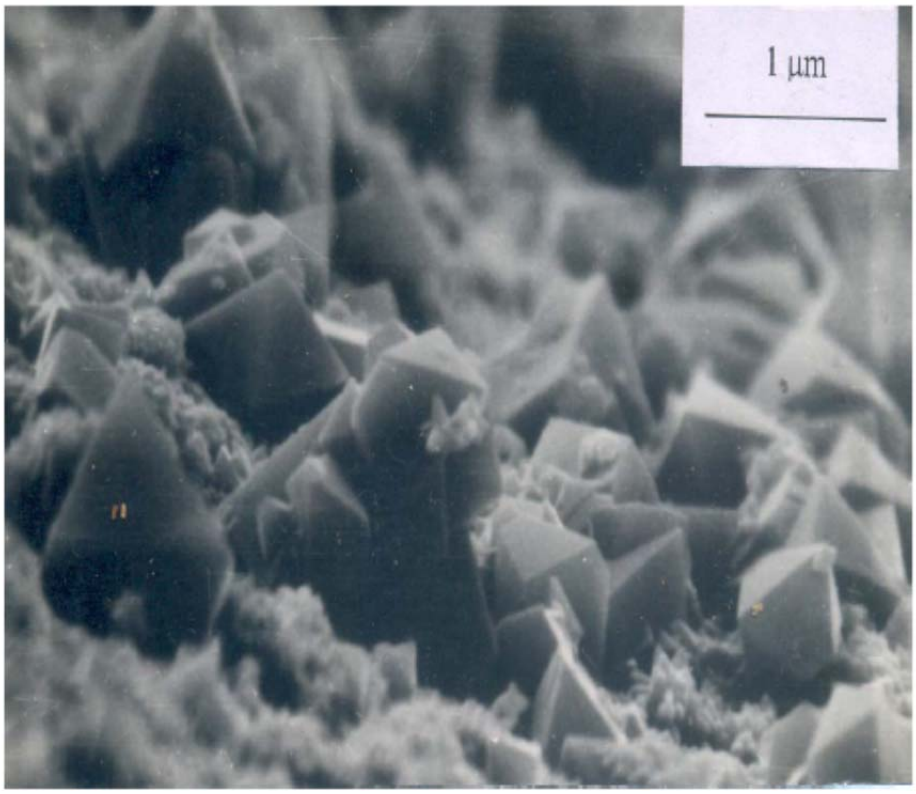

Fig.1.32: SEM pictures of AZO film on glass(cross sectional view) [63].

Electrical resistance versus temperature for ZnO and Al-ZnO films: A dark electrical resistance measurement was carried out in the temperature range 380-480K using the DC two-point probe method. Figure 1.33 shows the variation of resistance with temperature. In the figure, lnR (in kilo-ohms) is plotted against temperature. The decrease in resistance with increasing temperature following semiconducting behaviour of ZnO is observed.

The activation energy was determined by using the equation

$$R = R_o e^{E_a/KT}$$

where R is the resistance at temperature T , R_o is a constant, E_a is the activation energy and k is the Boltzmann constant

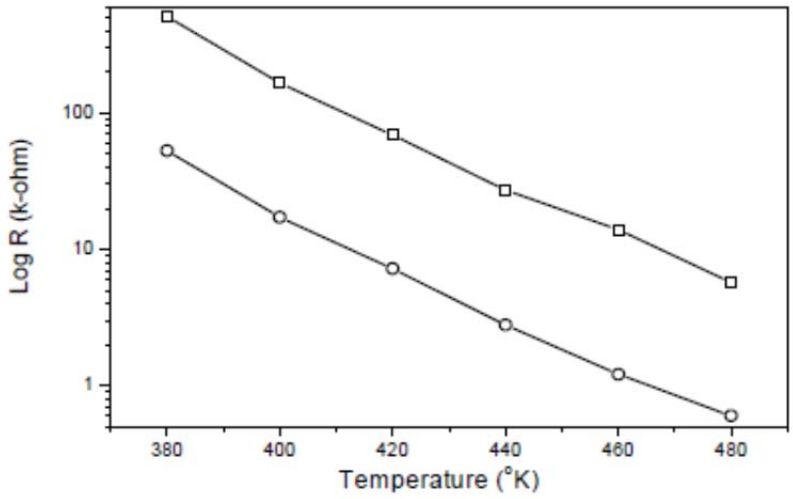

Figure 1.36: Variation of electrical resistance of ZnO and AZO film [63].

Jeong [99] deposited Al- doped ZnO (AZO) films by RF magnetron sputtering system and investigated the physical properties of the films. AZO film showed a preferred orientation in the [001] direction. As amounts of Al in the target were changed (0-10 wt.%), the crystallinity and the transmittance as well as the optical band gap were changed. The electrical resistivity was also changed according to the Al doping amounts.

Fu [100] reported almost metal conductivity (ρ = 4.6x10^{-4} Ωcm, sheet resistance *RS* = 32 Ω/) and high visible transparency (85 – 90 %) for aluminum - doped ZnO films (ZnO:Al), deposited by middle-frequency (MF) alternative magnetron sputtering.

Guillen [101] doped ZnO with aluminium using direct current (DC) magnetron sputtering and produced resistivity of ρ = 9x10^{-4} Ωcm and visible transparency exceeding 85%.

Myong [102] grew Al-doped ZnO films by photoassisted Metal Organic Chemical Vapour deposition (MOCVD) method and obtained highly conductive films with a minimum resistivity of 6.2x10^{-4} Ωcm.

Zhitomirsky *et. al* [103] reported a very high conductivity of ZnO doped with Aluminum. Compared with undoped ZnO, the Al-doped ZnO (AZO) films had a lower resistivity and better stability.

Jeong[104] suggested aluminium is particularly a suitable dopant for high transparency, stability and high conductivity of ZnO. Because aluminium doped ZnO (AZO) thin films have high transmittance in the visible region, and a low resistivity; consequently, the optical band gap can be controlled by using Al doping.

Minami [105] also added Al in Zinc Oxide and found that the thin film becomes more stable compared with un-doped zinc oxide thin film. He also noted that adding (doping) other elements such as Ga, In, Ti, Ge and Hf to ZnO also helped modify the properties of the thin film.

(ii) Effect of Gallium (Ga) on ZnO properties

Transparent conductive Ga-doped zinc oxide (ZnO:Ga) films have been extensively studied due to their low material cost, relatively low deposition temperature, and stability in hydrogen plasma compared to other metal oxides such as indium tin oxide. Its n-type conductivity is

mainly caused by substitution of Zn^{2+} ions by Ga^{3+} ions releasing excess electrons into the conduction band.

Addition of Ga to ZnO leads to a significant increase in the conductivity of ZnO without compromising the transmittance in the visible region. Among Group III elements, Ga is an excellent *n*-type dopant in ZnO, with distinctive advantages over the other group elements (such as Al, In). It has a more compatible covalent bond length (1.92 Å for Ga-O and 1.97 Å for Zn-O) than that of Al or In (2.7 Å for Al-O and 2.1 Å for In-O); that is, that the value of ionic/atomic radii of Ga is very close to that of Zn ions/atoms, which results in very little strain in the ZnO film upon doping with Ga [106-108]. In terms of affinity towards oxygen, the Ga has relatively lower affinity compared to Al [106-107]. Lower affinity of Ga towards oxygen is especially important because it lowers the possibility of formation of gallium oxide precipitates / clusters, which can affect the electrical properties of the film. It is also known that the Ga:ZnO are more resistant to moisture and have shown higher stability in humid atmosphere [109]. Ga-doped ZnO has been widely studied. However, among the Ga-related excitonic transitions, only excitons bound to neutral GaZn donors have been commonly reported..

Bhosle Vikram [110] deposited gallium doped ZnO thin films by Pulsed laser deposition (PLD) technique and provided the results presented below.

Structural characterization: Fig. 1.34 shows XRD results (θ-2θ scans) of the films with different concentrations of Ga grown at 400 ^{0}C and 2 x 10^{-2} torr. These patterns show that the films are highly textured along the c-axis which is designated as the (0006) peak of sapphire. The absence of additional peaks in the XRD pattern excludes the possibility of any extra phases and/or large-size precipitates in the films.

Electrical and optical properties: The effect of doping was studied by measuring the electrical and optical properties of the films with different concentrations of Ga. Fig. 1.35 shows the effect of film composition on the temperature dependence of resistivity for Ga doped ZnO films. Figs. 1.35 (a – e) correspond to gallium concentrations of 0%, 2%, 3.65%, 5% and 7%, respectively. Pure ZnO shows relatively high resistivity at room temperature (RT) and a negative

temperature coefficient of resistivity (TCR), characteristic of semiconducting behavior. However, with the addition of Ga, the room temperature (RT) values of resistivity decrease by two to three orders of magnitude. It can be seen from figs. 1.35 (b), (c), (d) and (e) that the RT resistivity decreases continuously as the Ga concentration is increased up to 5%, beyond which the resistivity was found to increase again.

The values of resistivity for different Ga doped ZnO films are listed in table 1.5. The increase in conductivity can be explained by the increase in carrier concentration due to Ga addition. The increased carrier concentration also leads to a metallic behavior at temperatures closer to the ambient temperature, which is not observed in pure ZnO. Metallic conductivity is observed in samples containing 2%, 3.65% and 5 % Ga, due to the formation of a degenerate band appearing in heavily doped semiconductors, as suggested by Mott [111, 112]. The increase in carrier concentration is also consistent with the results, shown in fig. 1.36. This figure illustrates transmission spectra of ZnO films with different concentrations of Ga. The absorption edge shows a continuous shift towards higher energy with the increase in Ga concentration according to the Burnstein-Moss effect [113, 114]. The shifts observed in the transmission spectra are in good agreement with observations reported by other researchers [115].

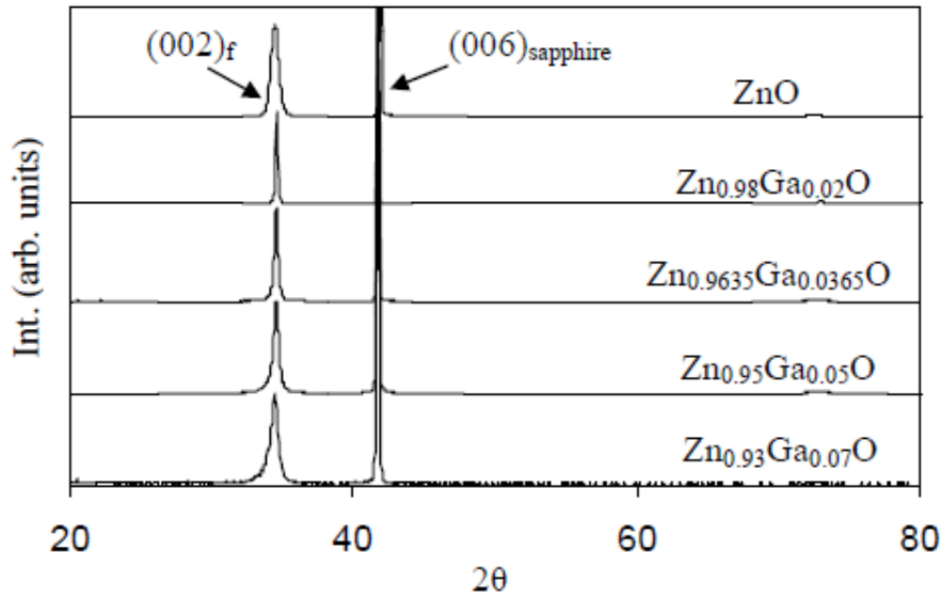

Figure 1.34: XRD of ZnO films with different concentrations of Ga deposited at 400^0C and 2 x 10^{-2} torr of oxygen pressure [110].

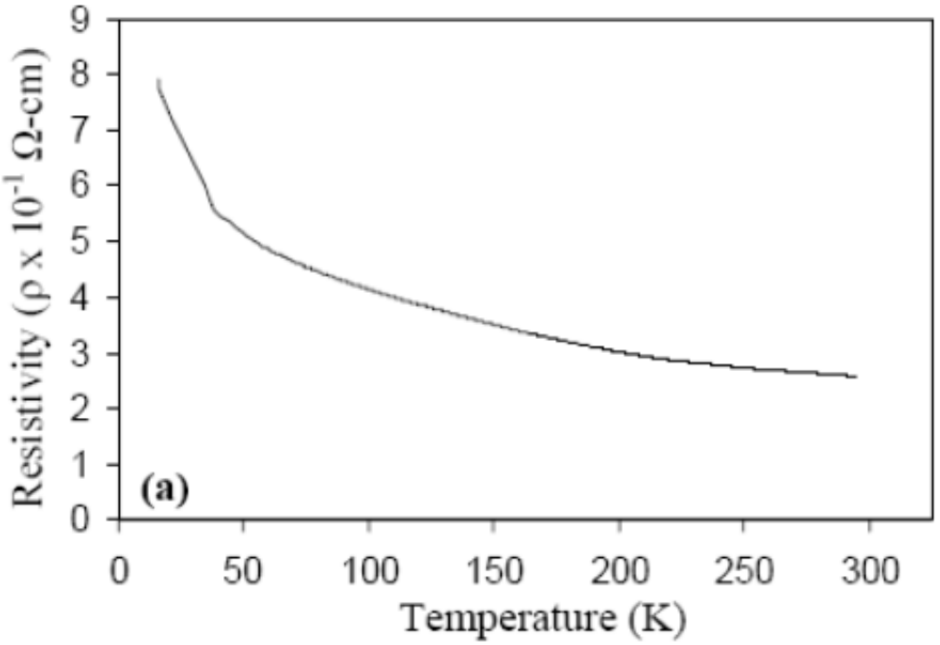
Resistivity (ρ x 10^{-1} Ω-cm)
9
8
7
6
5
4
3
2
1
0
(a)
0
50
100
150
200
250
300
Temperature (K)

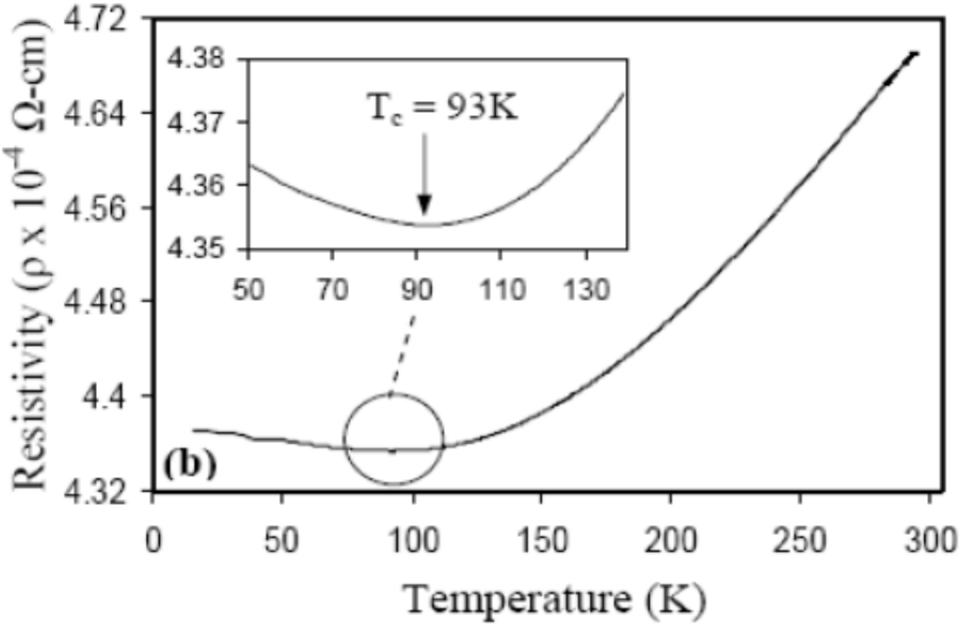
Resistivity (ρ x 10^{-4} Ω-cm)
4.72
4.64
4.56
4.48
4.4
4.32
4.38
4.37
4.36
4.35
T_c = 93K
50
70
90
110
130
(b)
0
50
100
150
200
250
300
Temperature (K)

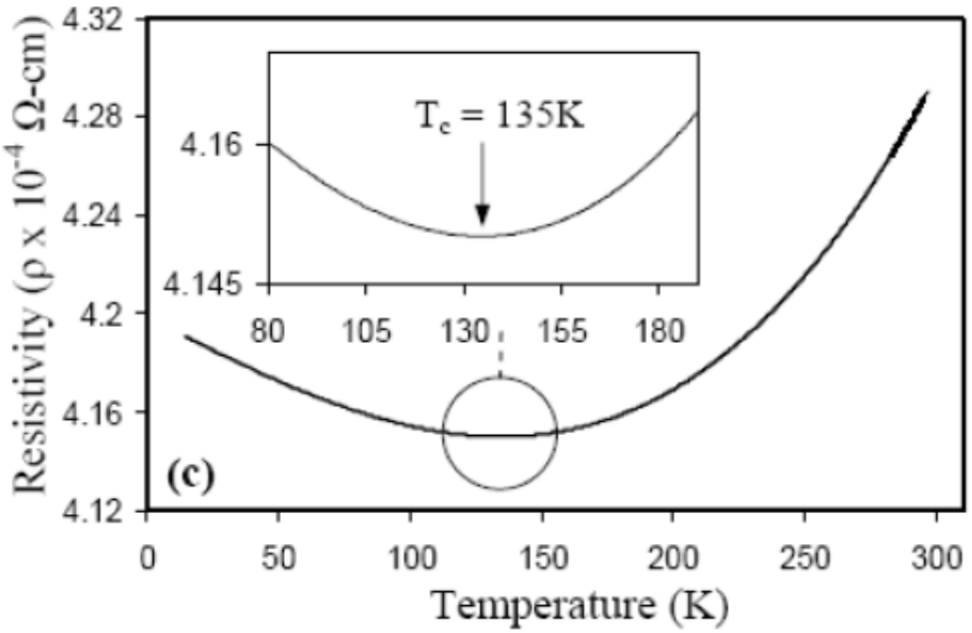
Resistivity (ρ x 10⁻⁴ Ω-cm)
4.32
4.28
4.24
4.2
4.16
4.12
0
50
100
150
200
250
300
Temperature (K)
T_c = 135K
4.16
4.145
80
105
130
155
180
(c)

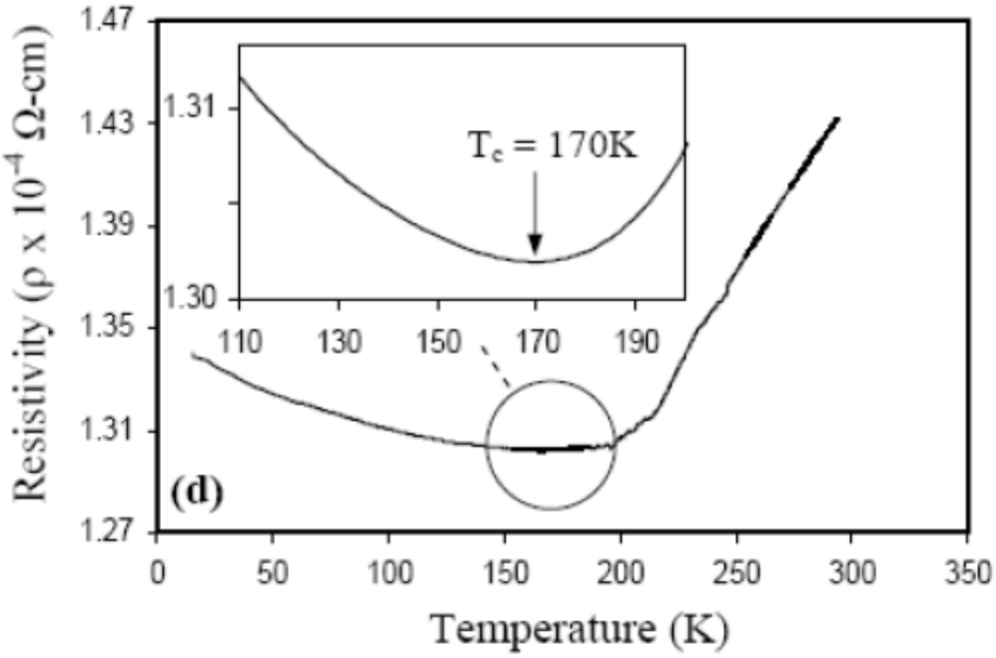
Resistivity (ρ x 10⁻⁴ Ω-cm)
1.47
1.43
1.39
1.35
1.31
1.27
0
50
100
150
200
250
300
350
Temperature (K)
T_c = 170K
1.31
1.30
110
130
150
170
190
(d)

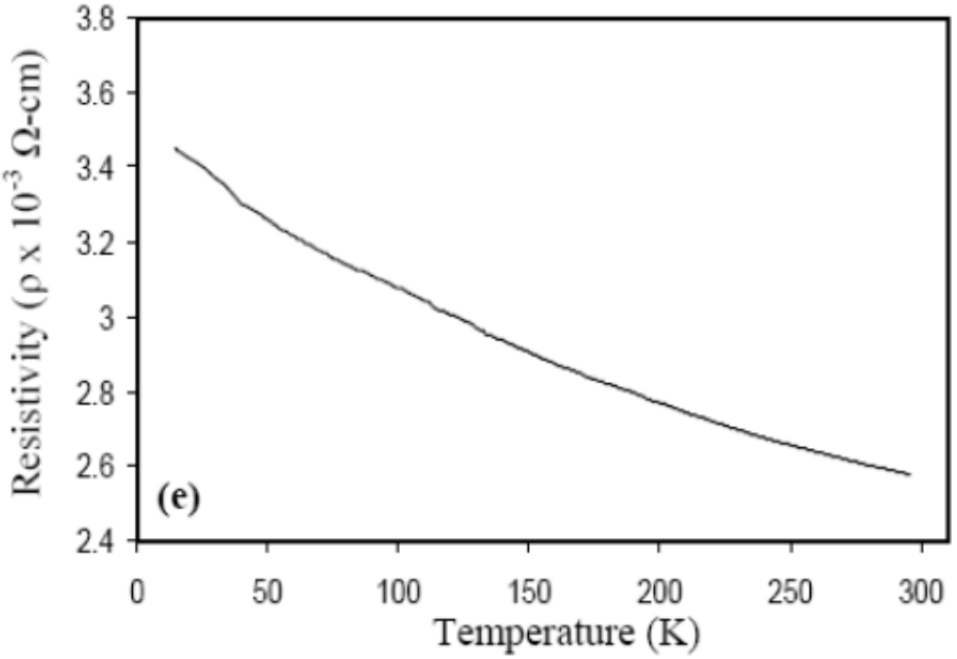

Figure 1.35: Plot of resistivity vs temperature for (a) undoped ZnO film, (b) $Zn_{0.98}Ga_{0.02O}$ (c) $Zn_{0.965}Ga_{0.0365}O$ (d) $Zn_{0.95}Ga_{0.05}O$ (e) $Zn_{0.93}Ga_{0.07O}$ [110].

Table 1.5: List of values of resistivity and the metal – semiconductor transition temperature of ZnO films with varying Ga concentrations [110].

%Ga	Resistivity (Ω-cm)	T_c (measured) K	$Li = d_{Ga}$ (nm)	T_c (calculated) K
0	2.59×10^{-1}	-	-	-
2	4.71×10^{-4}	93	1.33	92
3.65	4.29×10^{-4}	135	1.10	134
5	1.40×10^{-4}	170	0.98	171
7	2.57×10^{-3}	-	-	-

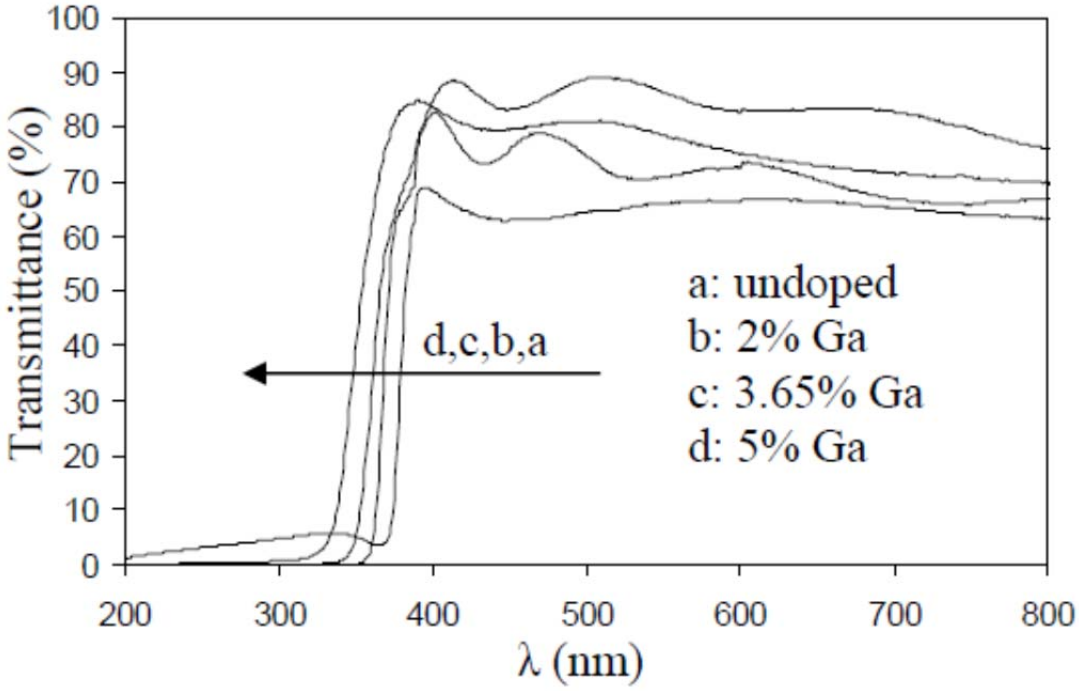

Figure 1.36: Transmission spectra of films with different concentrations of Ga [110].

Quan-Bao [5] deposited transparent conductive Ga-doped zinc oxide (ZnO:Ga) films with highly preferred orientation of (002). The films were deposited on glass substrates by DC reactive magnetron sputtering. An investigation into the variation of structural, electrical, and optical properties with Ga content revealed as follows: the peak position of the (002) plane is linearly shifted to the lower 2θ value with the increase of Ga content; the lowest resistivity of the ZnO:Ga films is 3.51×10^{-4} Ωcm and the average transmittance of the films is over 90% in the visible range. The optical band gap of the films is in the range of 3.58–3.74 eV. The optimum growth condition was obtained by using the Zn–Ga alloy target of 3.0 at.% Ga content. The pictorial and graphical presentation of results is given in figures 1.40 – 1.42.

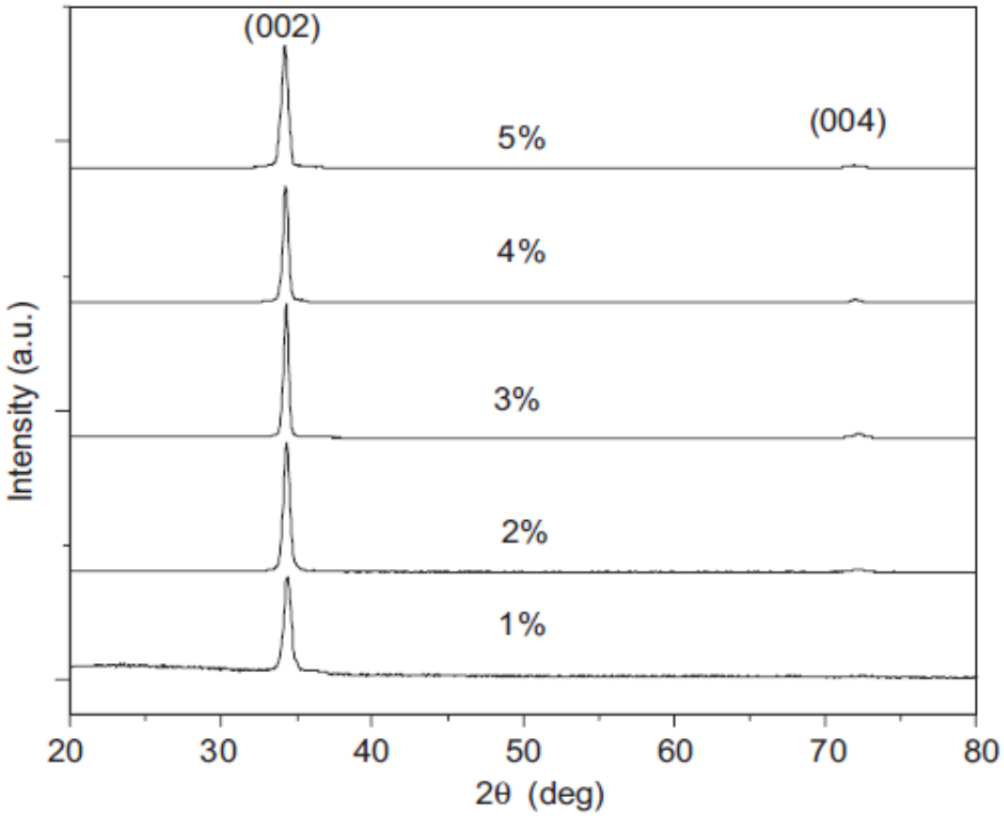

Fig. 1.37: X-ray diffraction patterns of ZnO:Ga films deposited under different Ga content (at%)[5].

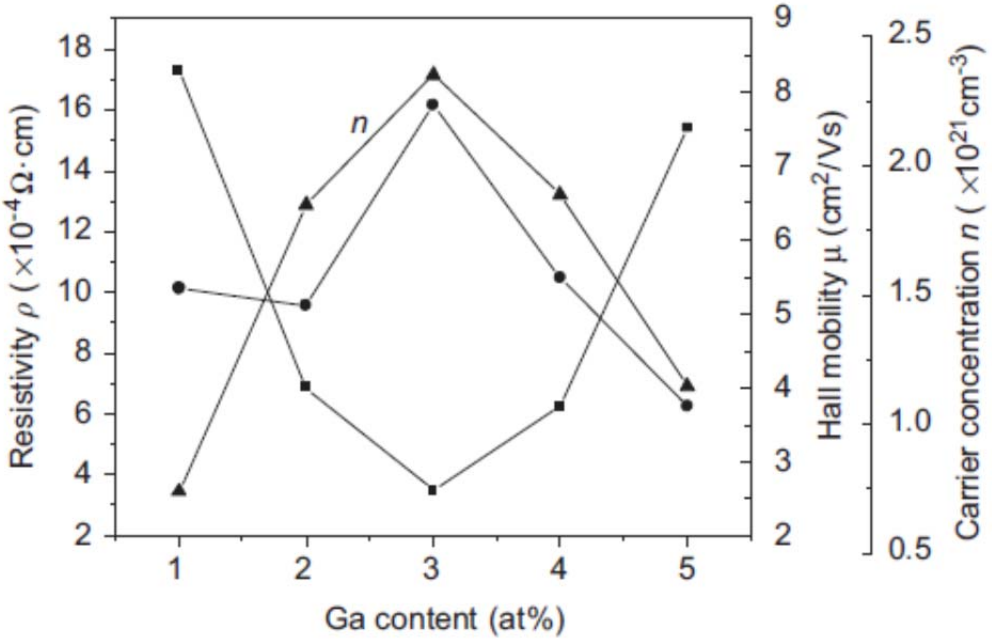

Fig. 1.38: Resistivity, Hall mobility and carrier concentrations as a function of Ga content for ZnO:Ga films[5].

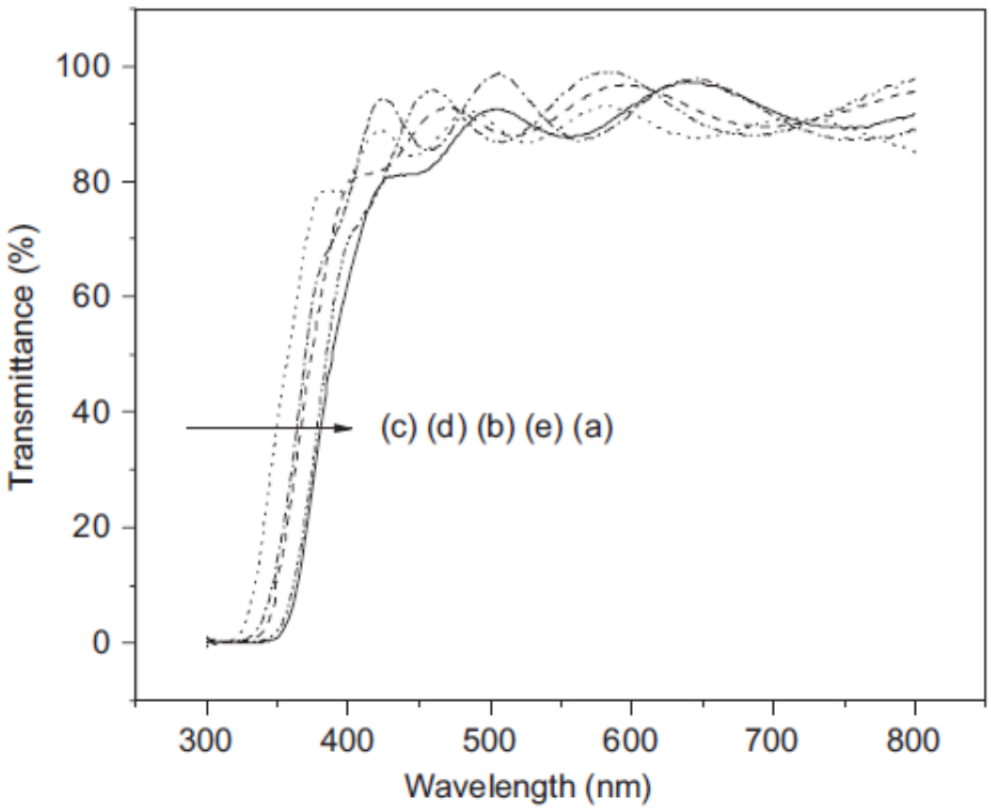

Fig.1.39: Spectral dependence of the transmittance of ZnO:Ga thin films prepared under different Ga contents: (a) 1.0 at%; (b) 2.0 at%; (c) 3.0 at% (d) 4.0 at%; and (e) 5.0 at% [5].

Hirata [116] reported high transmittance, low resistivity, and *c*-axis highly oriented ZnO:Ga thin films deposited on glass by laser ablation at different deposition temperatures. The surface morphology, crystalline structure, optical and electrical properties were found to depend directly on substrate temperature. Optical and electrical analysis revealed that the optical transmittance, carrier concentration, and optical energy gap of the ZnO:Ga transparent conductive oxides increased when the deposition temperature was raised from 150 to 300 ^{o}C. Films grown on 300 °C substrates showed a low resistivity value of 3.6×10^{-4} Ωcm, a carrier concentration of 8.7×10^{20} cm^{-3}, a band gap of 3.81 eV, and a visible transmission of 85%. These films were deposited with an excimer (KrF) laser beam of wavelength 248 nm operated under optimized conditions of 2.7 mJ/cm^2 energy density and 30 Hz repetition rate.

The electrical resistivities as a function of deposition temperatures are plotted in Fig.1.40. All samples had the same thickness (200 nm) as measured by a conventional stylus surface

roughness detector. As can be observed from Fig. 1.42, the resistivity decreases as the substrate temperature increased from 150 to 300 °C. Similar behavior has been reported for Al- or Ga-doped zinc oxide TCOs deposited by other techniques [117, 118].

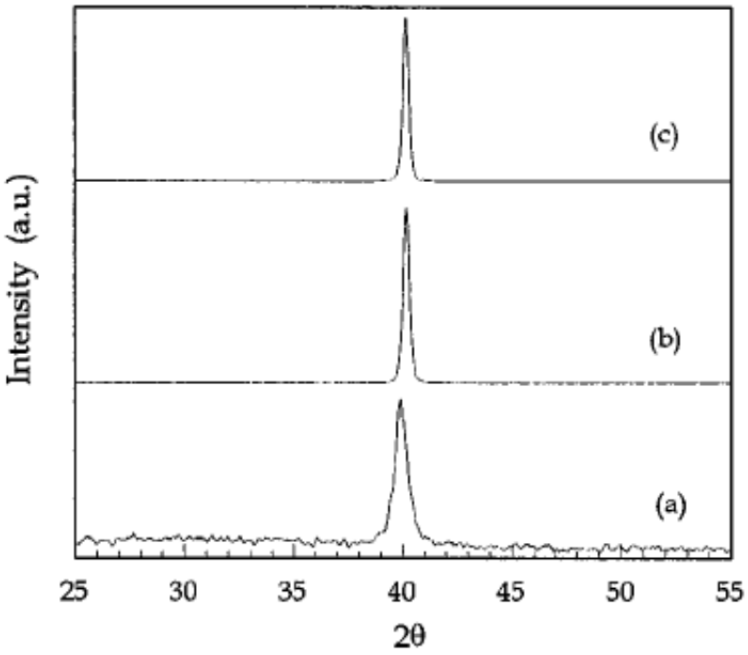

Fig. 1.41: X-ray diffraction patterns measured on ZnO:Ga films deposited at (a) 150, (b) 250, and (c) 300 °C substrate temperatures, respectively [116].

Table 1.6 Resistivity and band gap values for ZnO:Ga grown at four different deposition temperatures [116].

T (°C)	$\rho(\Omega\,\mathrm{cm})\times10^{-4}$	E_g (eV)
150	20.0	3.68
200	6.4	3.71
250	5.2	3.78
300	3.6	3.81

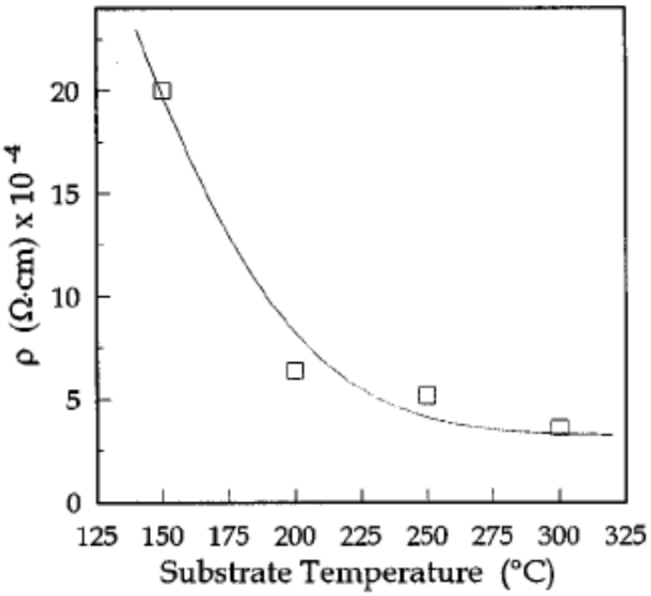

Fig. 1.42: Resistivity values of ZnO:Ga films as a function of substrate temperature [116].

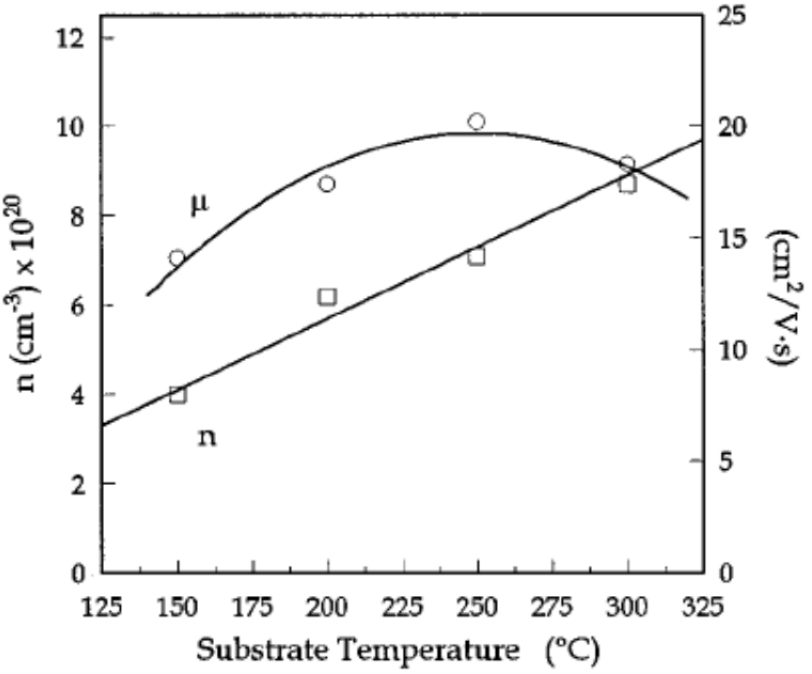

Fig.1. 43: Electron concentration and Hall mobilities for ZnO:Ga films deposited by PLD at different temperatures [116].

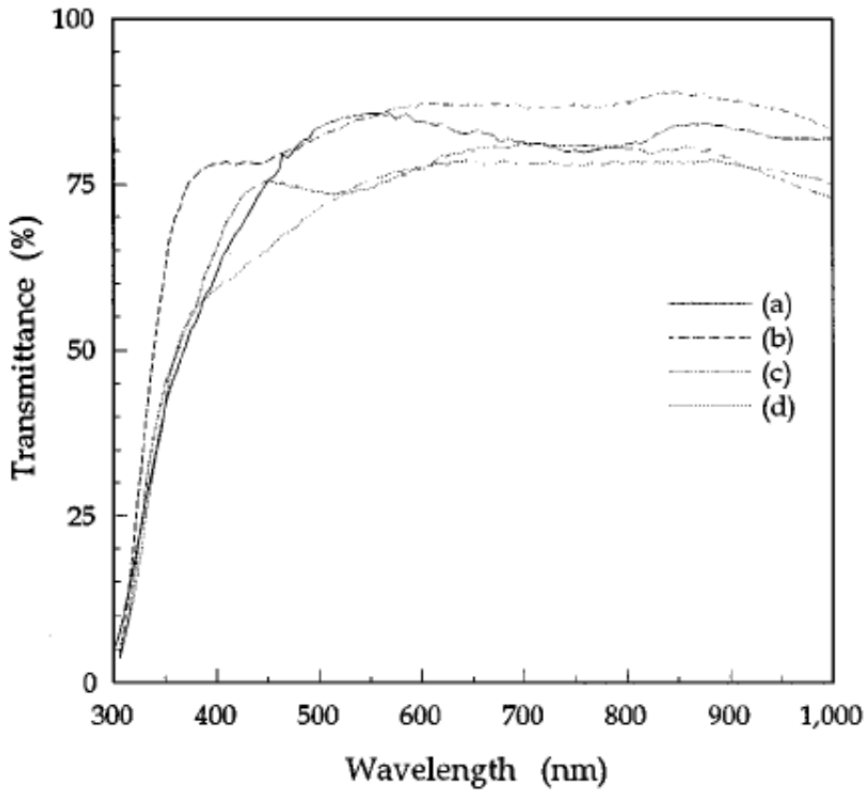

FIG. 1.44: Transmittance spectra of 200 nm films of (a) Indium doped tin oxide (ITO) and three ZnO:Ga films grown by PLD at (b) 300, (c) 250, and (d) 150 °C, respectively [116].

Christopher [119] employed a high-throughput combinatorial approach to explore a range of Ga doping levels from ≈2- 7.5 at.% gallium in materials sputtered from ceramic oxide targets on glass substrates. Using the combinatorial approach this compositional spread was examined over a range of substrate temperatures and sputtering atmospheres. Structural, optical, and electrical analysis was then performed using the suite of combinatorial characterization tools. In parallel, pulsed laser deposition (PLD) from ceramic targets was used to produce state of the art Ga:ZnO films on glass at a variety of substrate temperatures for comparison to the combinatorial studies. The best PLD materials were deposited at a nominal substrate temperature of 300 ^{o}C and resulted in a film with a resistivity of 7.7 × 10^{-5} Ω·cm and transparency in excess of 85% in the visible. The results are also presented in figures 1.45 – 1.47.

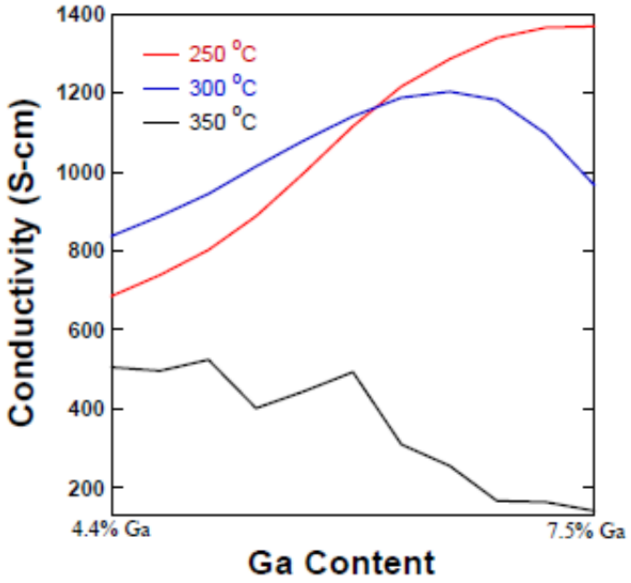

Fig.1.45: Conductivity across several Ga:ZnO compositional libraries at substrate temperatures ranging from 250 to 350^{0}C [119]

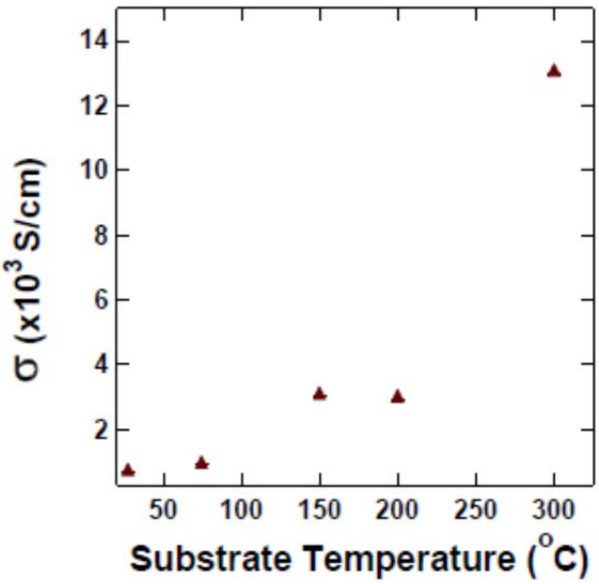

Fig.1.46: Conductivity for Ga:ZnO (2 at% Ga) deposited on glass using pulsed laser deposition as a function of substrate temperature [119].

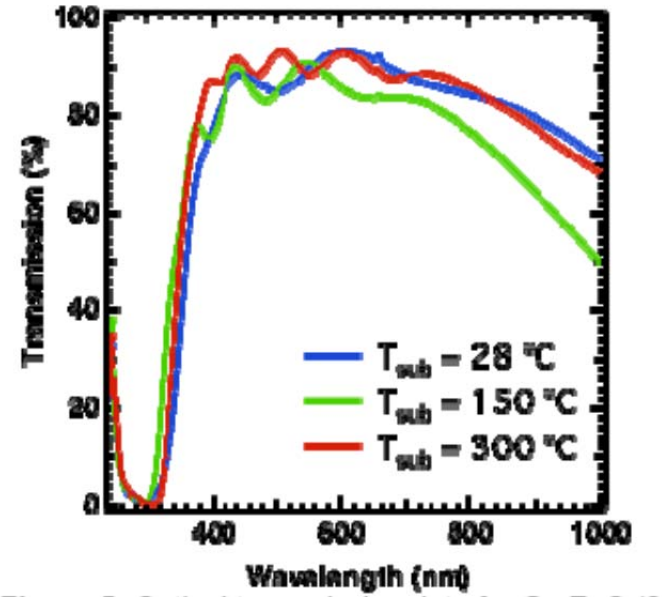

Fig. 1.47: Optical transmission data for Ga:ZnO (2 at.% Ga) films and glass substrate. Inset shows image of Ga:ZnO deposited at 300^0C [119].

G.K Paul [120] prepared gallium-doped zinc oxide (ZnO) films with different concentrations by sol–gel technique. The films were optically transparent and electrically conducting. It was observed that band gap initially increased with gallium doping from 3.281 to 3.328 eV up to a doping concentration of 2 at.%. Further doping had an adverse effect with respect to both electrical and optical properties. The lowest resistivity obtained for the 2 at.% doped sample was $6.3x10^{-3}$ Ω cm, which still was one order of magnitude higher than the films prepared by vapor-phase techniques.

Hirata [121] did pulsed laser deposition of gallium–doped zinc oxide (ZnO:Ga) transparent-conducting films and grew the films on glass at different substrate temperatures. A widening in the optical band gap and a good gallium doping efficiency were observed in the films when the substrate temperature was raised from 150 ^{o}C to 300 ^{o}C, as determined from optical and electrical measurements. X-ray diffraction measurements revealed that the films grow preferentially oriented in the (002) crystallographic direction of zinc oxide grains. The crystallinity of the films was also found to be strongly dependent on the substrate deposition

temperature. The ZnO:Ga films had an excellent transmittance (80%) in the visible spectrum and a low resistivity value (7×10^{-4} Ωcm) in 200 nm thickness samples deposited on glass substrate by laser ablation at 300 ^{o}C.

Highly conducting and transparent gallium doped ZnO thin films were grown on sapphire by PLD [122]. For 5 at.% Ga doped samples, the resistivity value was close to 1.4×10^{-4} Ω-cm and the transmittance was ~ 80%. Such low resistivities and high transmittances were achieved with an optimized combination of dopant and oxygen vacancy concentration. In addition, it was the first time, metallic conductivity with a metal-semiconductor transition (MST) had been observed in gallium doped ZnO. Detailed structural characterization confirmed the epitaxial nature of the films and also suggested the absence of extra phases and/or nanoclusters.

In another research study, Ga-doped ZnO thin films were deposited by DC magnetron sputtering [123]. It was found out that variation in the sputter pressure and film thickness modified the physical properties. Films with lowest resistivity of 2.6×10^{-4} Ωcm, Hall mobility of 18 cm^2/Vs and carriers concentration of 1.3×10^{21} cm^{-3} were obtained. Mobility and grain size were found to be linearly dependent, which resulted in high mobility in films with larger crystalline grain size. Optical transmittance (80 – 90 %) depended on both, thickness and sputtering pressure and its changes were consistent with the changes of the electrical parameters. Other deposition parameter with major influence on the film's properties was the substrate temperature (T_S).

Ataev *et al.*[124] reported resistivities as low as 1.2×10^{-4} Ωcm for Ga-doped ZnO films grown by chemical-vapor deposition.

Gotoh and Yanokura [125] doped ZnO with with varying concentrations of Ga and confirmed that although carrier concentration is instrumental in decreasing the resistivity, at very high carrier concentration the resistivity tends to increase. Fig. 1.49 shows the variation of resistivity of ZnO with %Ga concentration. It can be seen that the resistivity initially decreases with

increasing Ga/Zn ratio up to 2-3%, and increases further with %Ga additions. A similar trend is observed with other dopants such as Al doped ZnO, where the lowest resistivity is achieved for a critical concentration of the dopant, and then the resistivity again rises above that critical concentration [126]. The lowest value of resistivities reported for Al:ZnO is 8.5×10^{-5} Ω-cm. [127,128]. It is believed that the increase in resistivity beyond a critical concentration of dopant is related to the increase in ionized impurity scattering.

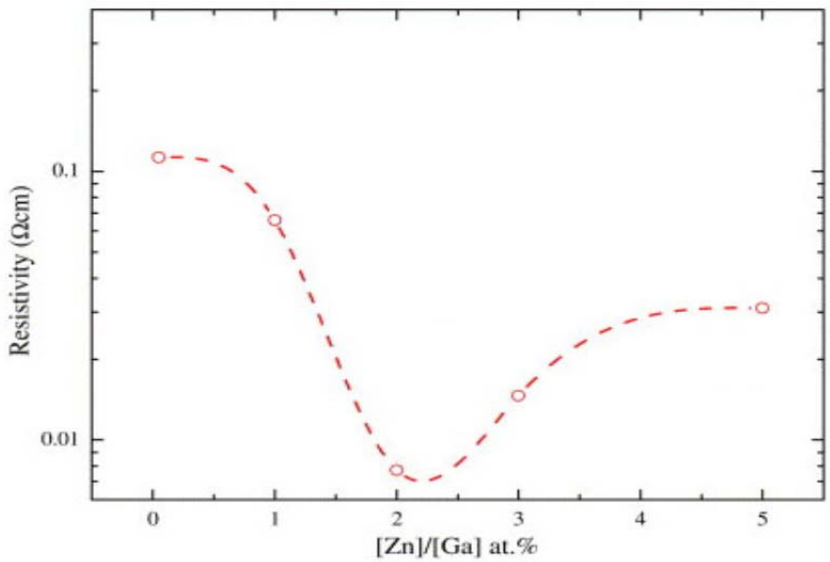

Figure 1.48: Resistivity versus %Ga [125]

ZnO:Ga films were also deposited by spray pyrolysis(figs. 1.49, 1.50)[129]. In Fig. 1.49, it can be observed that the electrical resistivity decreases as the substrate temperature increases, until a minimum resistivity value is reached. This result is associated with a improved film formation; beyond this optimal temperature the film resistivity increases due to both the zinc oxide formation with a better stoichiometry (a highly resistivity phase) and the out-diffusion of alkaline ions, Potassium (K), Calcium (Ca), Sodium (Na), and Silicon (Si) coming from the glass substrate into the film, which compensate the free electrons. The electrical resistivity as a function of the [Ga]/[Zn] ratio in the starting solution shows a decrease as the [Ga]/[Zn] rate is increased, reaching a minimum value at a certain [Ga]/[Zn] ratio (2-3 at.%), further increase in the resistivity values is observed when the [Ga]/[Zn] ratio increases. For low [Ga]/[Zn] ratios the resistivity decrease is due to the increase of the Ga atoms that are incorporated into the lattice

ZnO in the Zn sites, supplying one electron to the conduction band for each Ga atom, until the maximum solubility of Ga into the ZnO lattice is reached (minimum value of the resistivity curve).

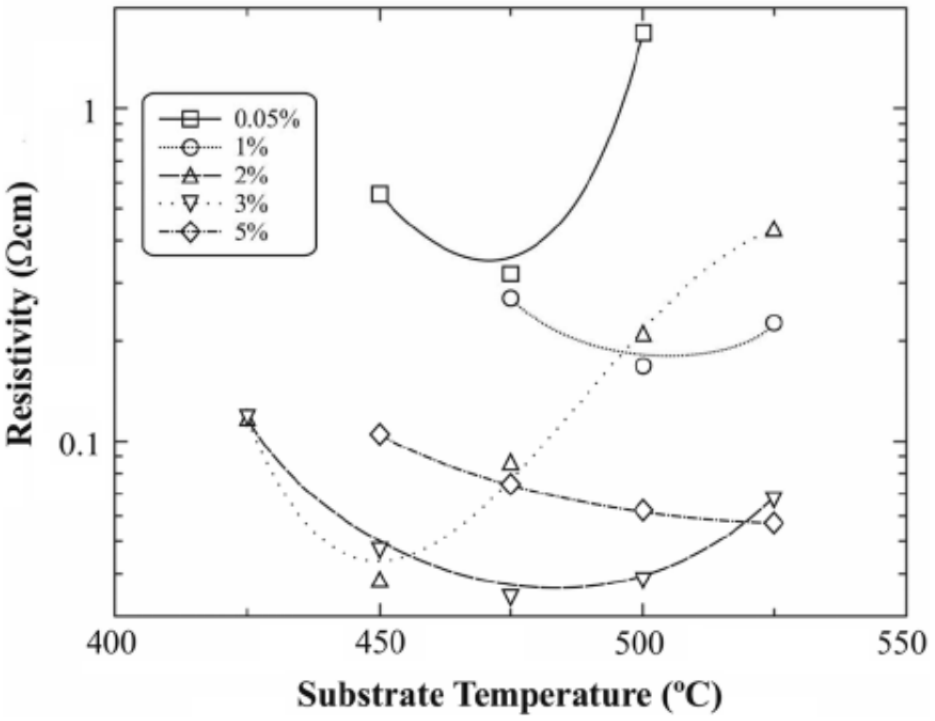

Fig.1.49: Variation of the electrical resistivity with the substance temperature for as-deposited ZnO: Ga films at different [Ga]/[Zn] (at.%) ratios [129].

In Fig. 1.50*a*, a SEM micrograph shows the surface of a ZnO : Ga film deposited with a [Ga]/[Zn] = 0.05 at. % ratio, and deposited at substrate temperature (T_S) = 475 ^{o}C. This micrograph shows a regular surface morphology formed of small and large rounded grains with sizes running from 110 to 260 nm. The 1.50*a* and 1.50*b* images suggest a film with a low roughness and porosity. The HREM micrograph displayed in Fig.1.50*b* shows ZnO : Ga grains in different orientations with not well defined grain boundaries among them.

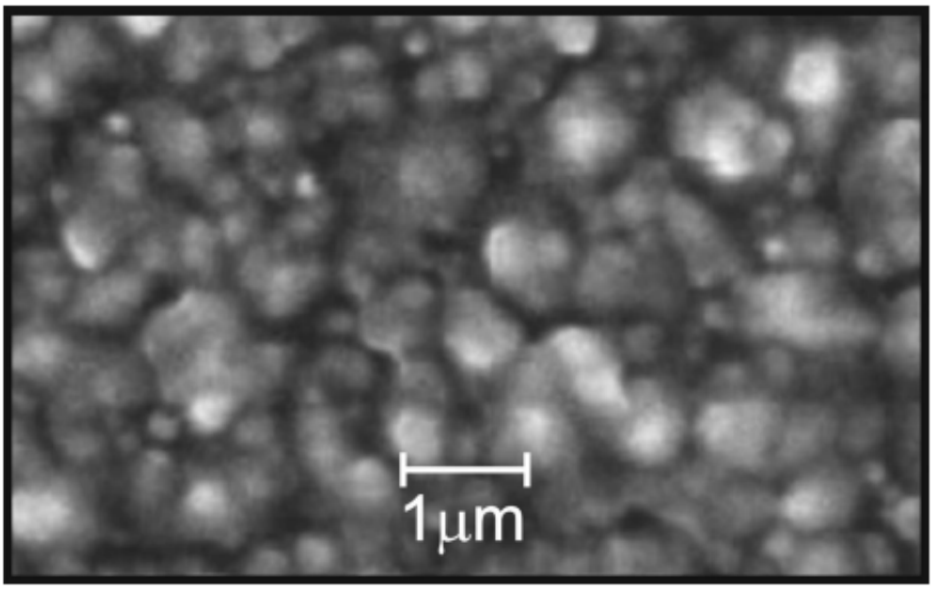

Fig.1.50*a*: SEM micrograph from a ZnO : Ga film deposited at T_S = 475 ^{0}C from a O.2M starting solution. A regular surface with two grains sizes of rounded grains is observed [129].

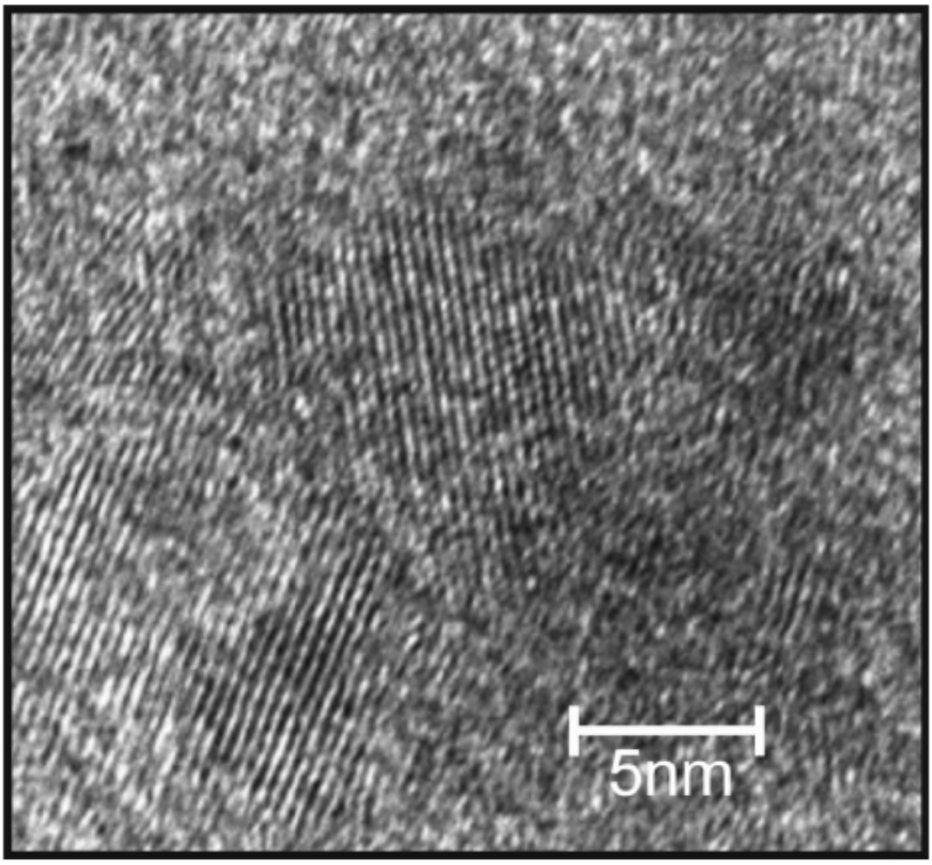

Fig. 1.50*b*. HREM micrograph showing the structure of one of the large grains observed in Fig. 1.50*a* [129].

(iii) Effect of Indium (In) on ZnO properties

On adding indium impurity to the ZnO semiconductor, it substitutes Zn (because of their similarity of ionic radius). Since Indium has one more electron than Zn, it acts as donor impurity and creates an n-type semiconductor [130].

Indium doped zinc oxide (ZnO:In) thin solid films were deposited on soda-lime glass substrates by the ultrasonic spray pyrolysis technique [131]. The effect of the substrate temperature on the electrical, morphology, and optical characteristics of ZnO:In thin films was studied. It was found that, as the substrate temperature increased, the electrical resistivity decreased, reaching a minimum value in the order of 7.3×10^{-3} Ω cm, at 415 ^{o}C. Further increase in the substrate temperature resulted on an increment on the electrical resistivity of the thin solid films. All the samples were polycrystalline with a well- defined wurtzite structure. The preferred growth showed a switching from a random orientation at low substrates temperatures to (002) in the case of films deposited at the highest substrate temperature used. As the substrate temperature increases, the corresponding surface morphology changes from an almost faceted pyramidal to round-shaped form. The optical transmittance of the films in a interval of 400 to 700 nm is around 70%, with a bandgap value in the order of 3.45 eV. Further presentation of the results is shown in Figures 1.51 – 1.54.

Fig.1.51 also reports the corresponding measurements of carrier concentration and mobility of ZnO:In thin films as a function of the substrate temperature. For all cases, varying between 1 and 2 $cm^2/V\text{-}s$ the magnitude of the electron mobility is very low, then the increase of carrier concentration due to the formation of InZn point defects could be considered as the main reason for the decrease of the electrical resistivity of ZnO:I n thin films.Then again the carrier concentrations oscillate between 1.96 and 4.44×10^{20} cm^{-3}. Table 1.7 summarizes the results of the electrical characterization of the thin films.

Table 1.7 Hall effect measurements of the ZnO:In thin films deposited at different substrate temperature [131].

Substrate temperature ± 0.5 (°C)	Electrical resistivity Ω cm ($\times 10^{-2}$) $\pm$ 5%	Carrier mobility $cm^2/(V\text{-}s) \pm 5\%$	Carrier concentration cm^{-3} ($\times 10^{20}$) $\pm$ 5%
385	1.41	1.7	2.63
400	1.29	2.0	2.45
415	0.73	1.9	4.44
430	0.90	1.8	3.74
445	3.11	1.0	1.96

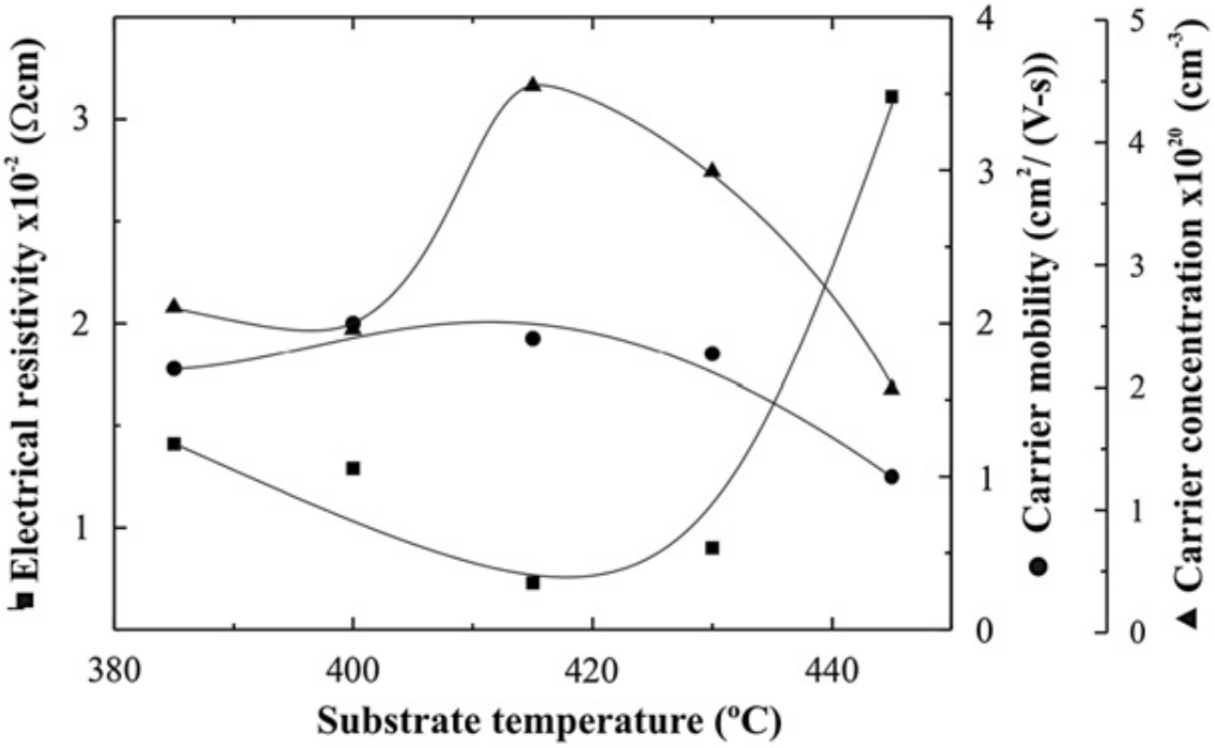

Fig.1.51. Variation of the electrical resistivity, carrier mobility and concentration of ZnO:In thin films as a function of the substrate temperature [131].

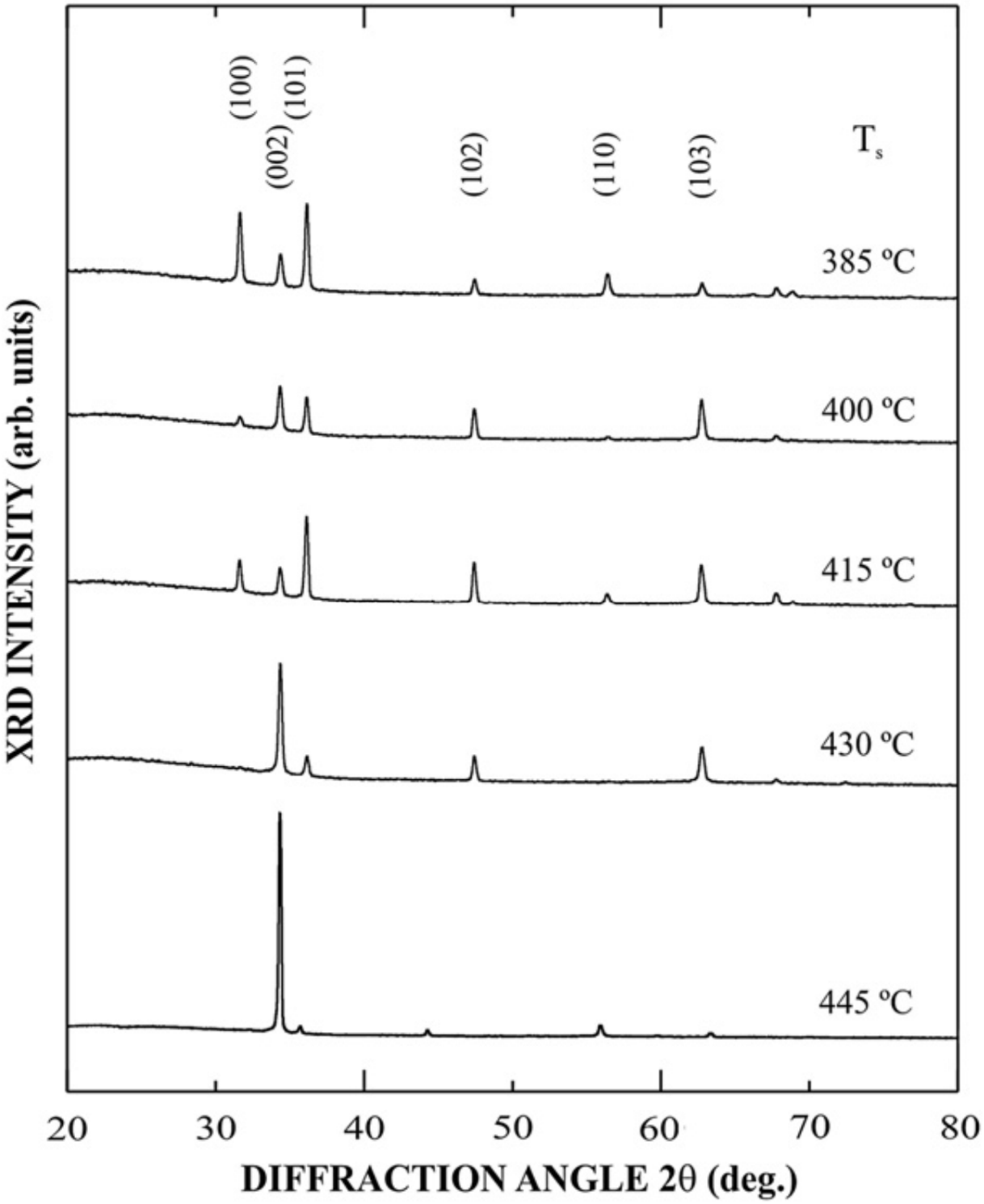

Fig.1.52: X-ray diffraction patterns of ZnO:In thin films deposited at different substrate temperatures [131].

Fig.1.53 shows the SEM images of ZnO:In thin films deposited at different substrate temperatures. As the substrate temperature increases, changes in the morphology of the films are observed. It is interesting to note that, in the case of the films deposited at 385 ^{o}C, grains with pyramidal-shape are formed, see Fig.1.53(a).

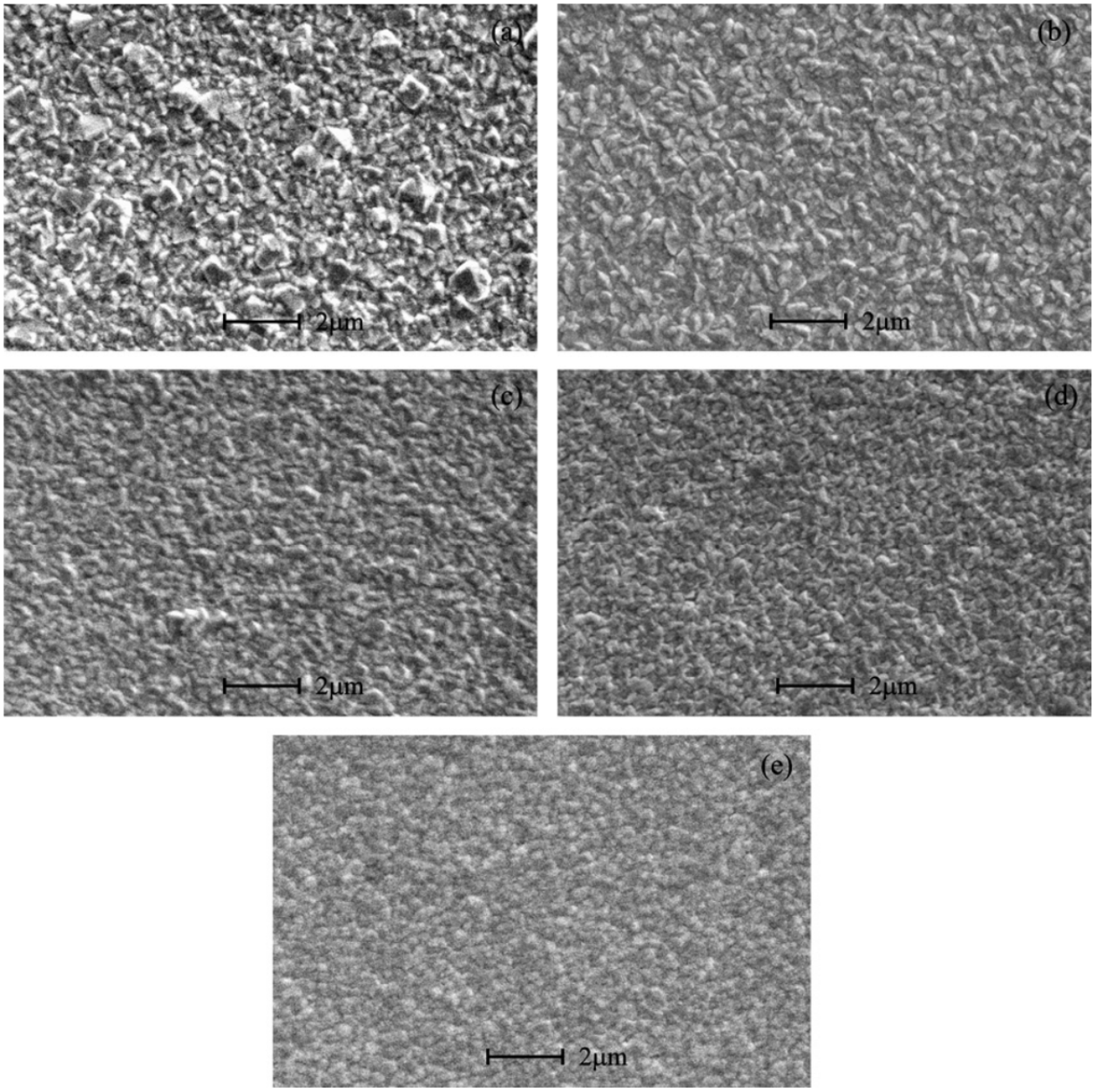

Fig.1.53: Scanning lectron micrographs of ZnO:In thin films deposited at different substrate temperatures; (a)385, (b)400, (c)415, (d)430 ,and (e) 445 ^{o}C [131].

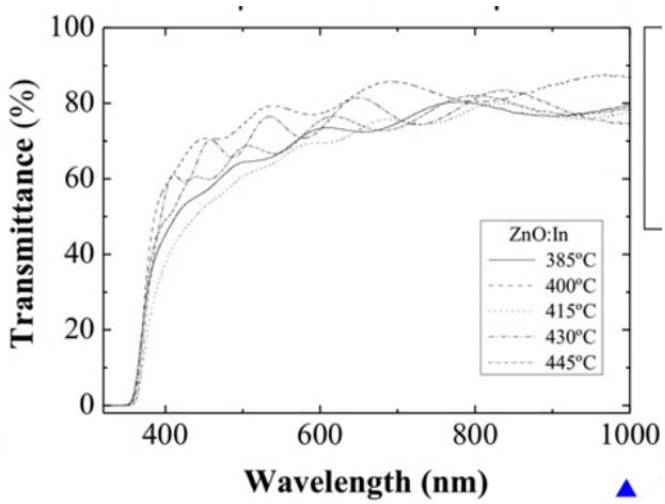

Figure 1.54: Transmittance spectrum of ZnO:In thin films deposited at different substrate temperatures[131].

Razaee [130] deposited high quality sol-gel derived indium doped ZnO (IZO) thin films on glass substrates by spin coating at 2000 rpm. Zinc Acetate and indium Chloride were used as precursor materials. The effect of dopant concentration and annealing in different temperature on the electrical, optical and structural properties of produced thin films were investigated. The optical transmittance spectra showed a very good transmittance of 99.5% within the wavelength of 540 nm for the film doped with 2 wt.% In . Increased dopant (more than 6 %) changed n-type semiconductor to p-type. This phenomenon was not been reported before. The reason of this changing might be a decrease in donor property of indium following an increase of impurity. So indium acts as acceptor impurity and substituted for oxygen. Indium has electron less than Oxygen and could absorb radical electron that lead to increased pores. Therefore, change in carriers type resulted in change of n-type semiconductor to p-type. Results showed that the c-axis orientation was determined by annealing temperature and that the grain size and resistance of the IZO thin films were mainly influenced by the annealing temperature. Conductivity initially decreases as converting semiconductor and decreasing carrier concentration (resistivity 3.05 $x10^{-2}\Omega cm$). But following the increasing impurity, the carrier concentration increases so that the lowest resistivity was observed with impurity of 3.2%. The details of these findings are also presented below.

Structural properties (fig.1.55): The XRD pattern have been recorded in the 2theta range of 30-40, where the peak of hexagonal wurtzite type In doped ZnO structure is present. This indicated that films have polycrystalline structure. The XRD patterns also showed a high preferential c-axis oriented structure. Diffraction peak (002) had considerable growth, but decreased when dopant concentration increased. It was similar to other reports. Crystal quality of samples with lower dopant concentration was higher.

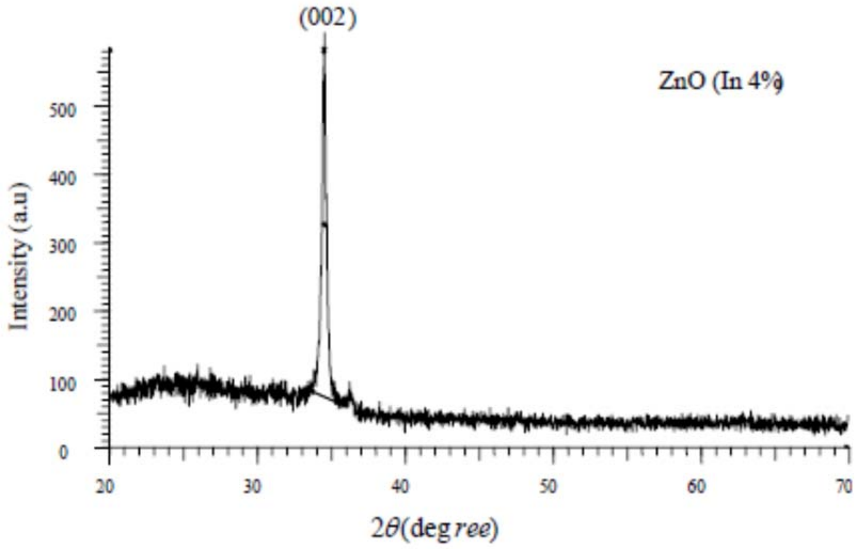

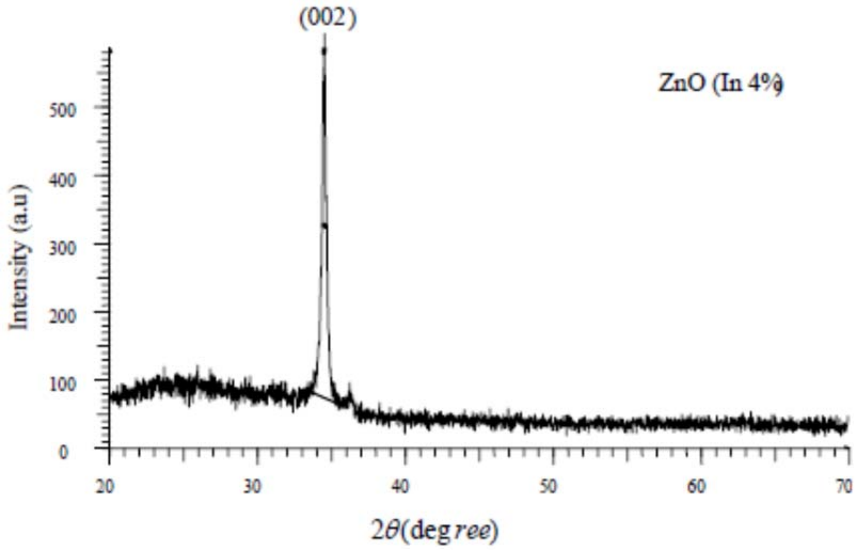

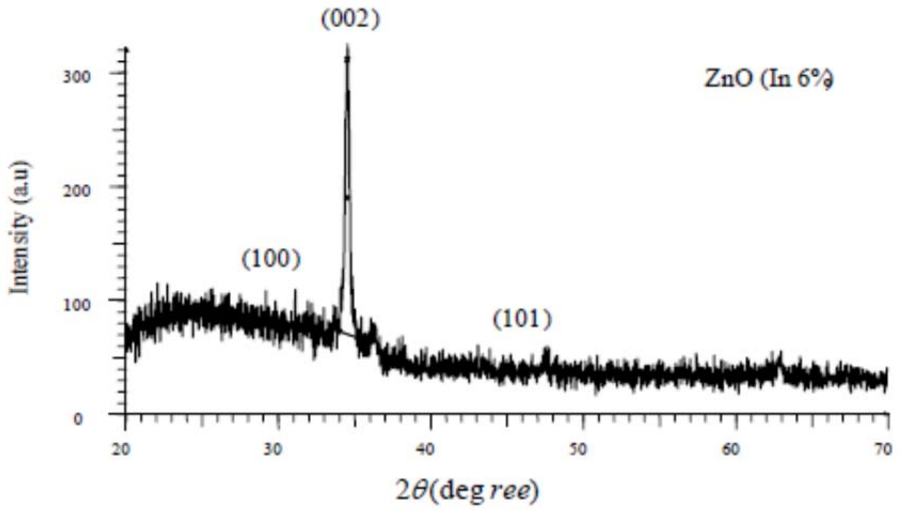

Fig.1.55: XRD pattern of Indium (various wt.%) ZnO thin films [130].

Optical properties (figures 1.56, 1.57): Some samples showed transmittance of 99.5% (In ,2 wt.% and ZnO in 540 nm). There is no report for such a transmittance of ZnO films. High percentage of visual spectrum pass through films. The highest transmittance related to In (4 wt.%) ZnO sample. Increased dopant concentration reduces transmittance of samples. The reasons for reduced transmittance of visual spectra are incident diffraction caused by Indium atoms surrounded by ZnO (Indium atom a little larger than Zn) and crystal imperfection.

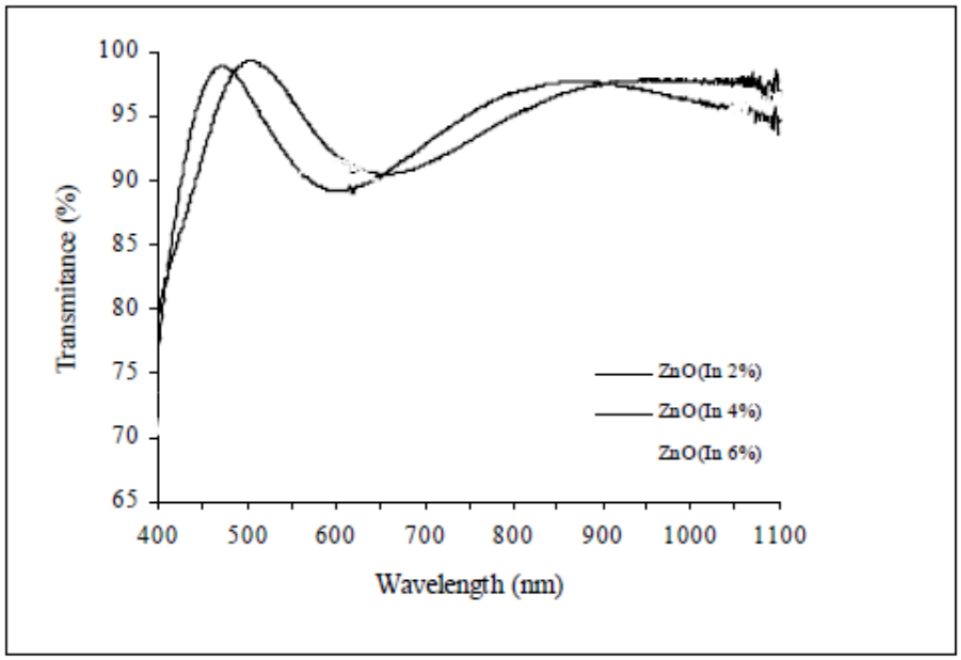

Fig.1.56: Visual transmittance spectra for Indium ZnO thin film [130].

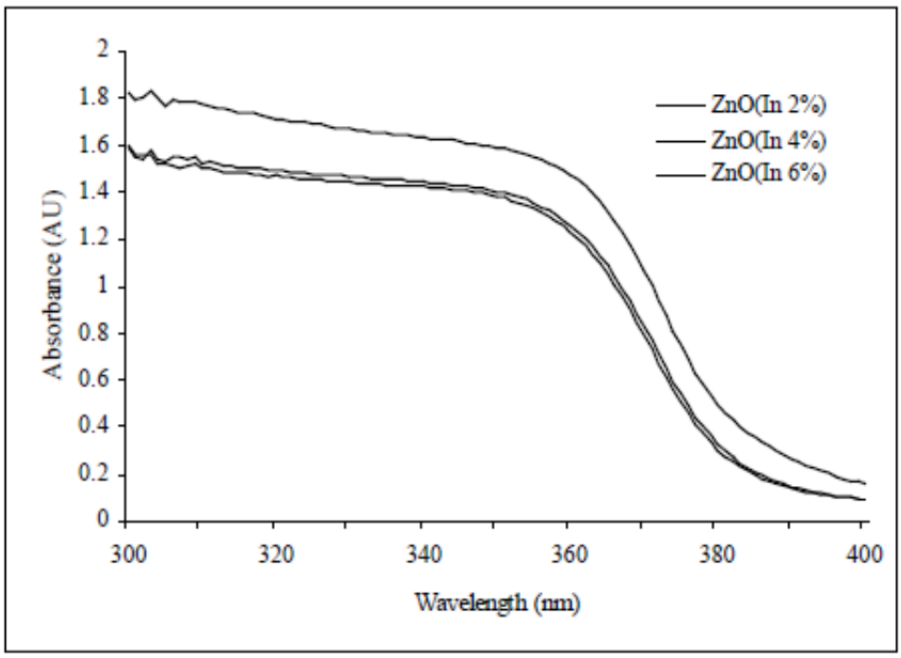

Fig.1.57: UV absorbance spectra for Indium (various wt%) ZnO thin film [130].

Electrical properties (table 1.8): Pure ZnO is a well-known n-type transparent semiconductor and has a high resistivity. Adding indium impurity to semiconductor, it substitutes Zn (because of their similarity of ionic radius). Since Indium has one more electron than Zn, acts as donor impurity and creates an n-type semiconductor. Hall effect measurements certify this issue. This substitution lead to an increase of electron concentration and a very high decrease of electrical resistivity. So we have a semiconductor of high conductivity. Values in table 1.8 shows how surface resistivity decreases (less than half) with increasing of impurity percentage. Increasing impurity (higher than 6%) lead to change ntype semiconductor to p-type. This phenomenon has not been reported so far. The reason of this changing might be a decrease in donor property of Indium following an increase of impurity. So Indium acts as acceptor impurity and substituted for Oxygen. Indium has 3 electron less than Oxygen and could absorb radical electron that lead to increased pores. Therefore, changing in carriers type resulted in changing of n-type semiconductor to p-type. At the initiation of changing, decreased carriers lead to decreased resistivity, because the number of pores was few. But increase of impurity lead to increased carriers concentration, so that the least resistivity was observed at impurity of 32%.

Table 1.8. Calculated value for resistivity, carriers concentration and mobility for Indium (various wt.%) ZnO samples [130].

Dopant concent ratio	Surface resistivity	Special resistivity	Carriers concentratin	Mobility
0	5763.97	-	-	-
2	400.64	1.09E-2	-1.15E19	49
4	406.69	1.34E-2	-9.55E18	48
6	422.51	3.05E-2	-8.72E17	234
8	2175.81	-	-	-
16	1086.66	-	-	-
32	222.39	-	-	-

Sali [66] grew indium-doped zinc oxide (ZnO: In) thin films on Si substrates using the chemical spray technique. The effects of thickness (e), as well as the substrate temperature (Ts), were studied. It was revealed by X-Ray diffraction that the preferred orientation of polycrystals is along C-axis, with hexagonal wurtzite structure. Two important facts were calculated from measurements: the dopant concentration throughout the film and the thickness of the films. It was found that the thickness increased with time of deposition. The corresponding characteristics of the films as a function of the substrate temperature and thickness were reported. As the substrate temperature increases, a decrease in the resistivity value for the films was observed. Under optimum deposition conditions a low resistivity and a high optical transmittance of the order of 2.8×10^{-4} Ω.cm and 85 %, respectively, were obtained.

The pure zinc oxide was first studied separately and the when indium doped**.**

Pure zinc oxide:

The figure 1.58 shows typical X-ray diffraction of the ZnO films. It was observed that the preferred orientation of polycrystals is along C-axis, with hexagonal wurtzite structure. Whose cell parameters are 3.24992 Å and 5.20658 Å for A and C, respectively.

The two spectra of figure 1.60 exhibit the transmittance and reflectance results obtained from the ZnO films deposited on glasses substrate at 480 °C. Both of them show the normal transmittance of more than 90 %.

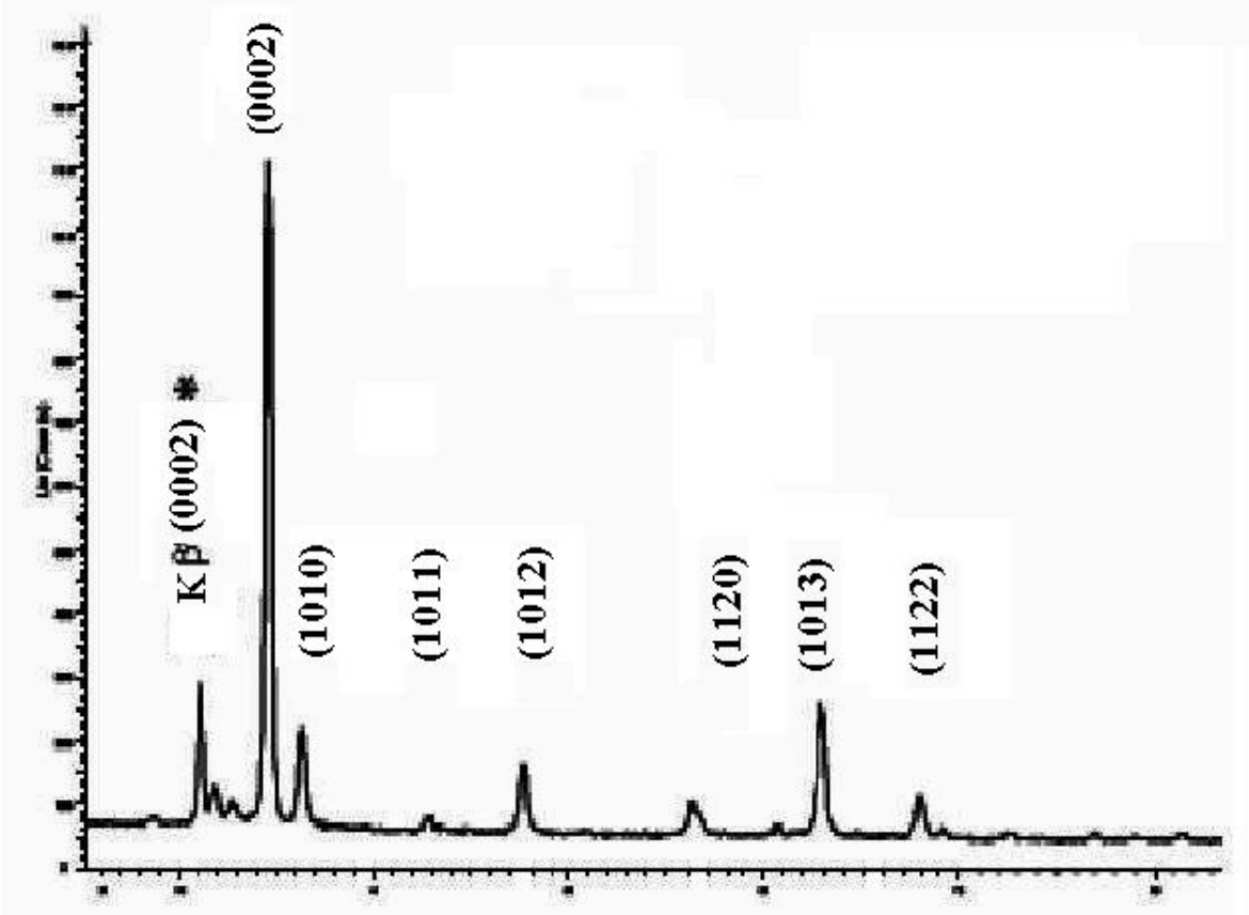

Fig. 1.58: the typical X-ray diffraction of the ZnO thin film [66].

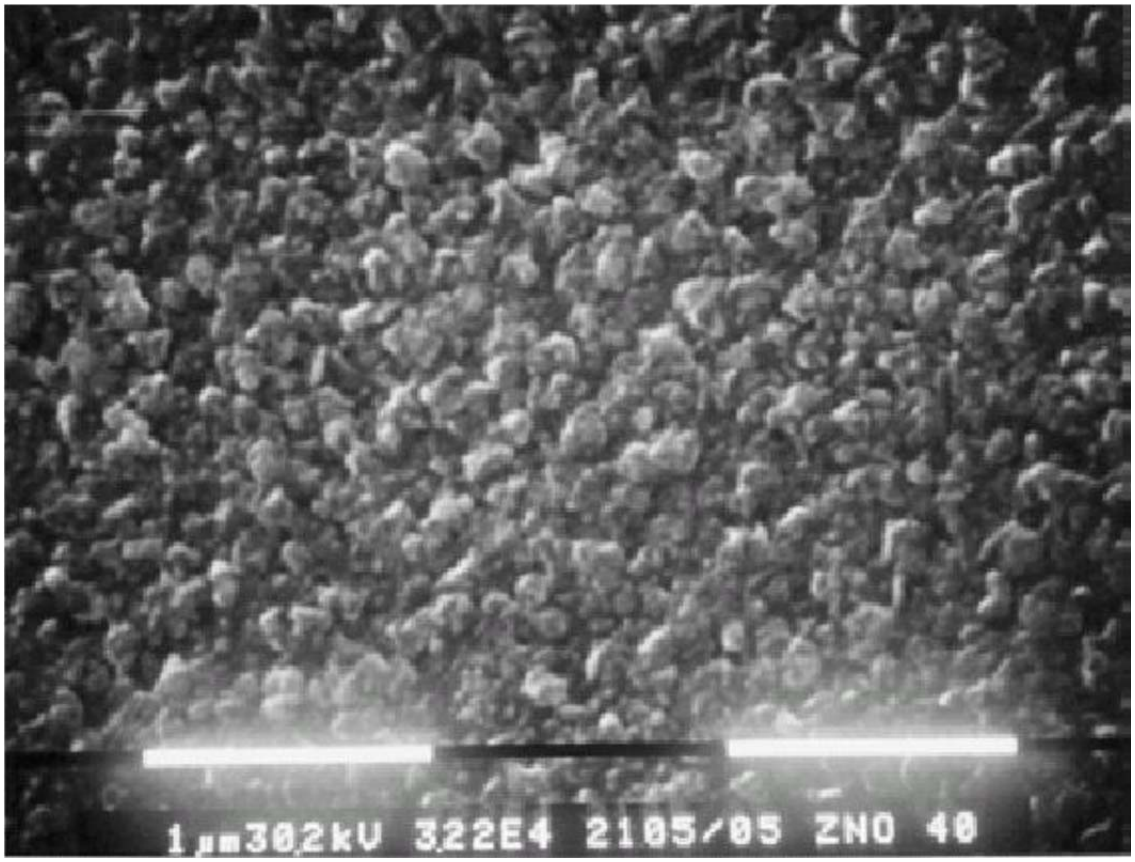

Fig.1.59: MEB of surface of the layer of ZnO [66].

Indium-doped zinc oxide:

The chemical composition of the elements is: 50.57 % Zn, 48.33 % O and 1.1 % In. The observation with the MEB of surface of the layer of ZnO: In deposited on silicon deposited by spray making it possible to visualize the grains. The image of fig. 1.61 shows a little disturbed surface of the layer obtained.

The spectra of transmission (t) and reflexion (r) are represented in Fig. 1.62. The transmission (t) and reflexion (r) are cancelled below approximately 366 nm. This cut corresponds to the optical gap of ZnO, which is approximately 3.4 eV

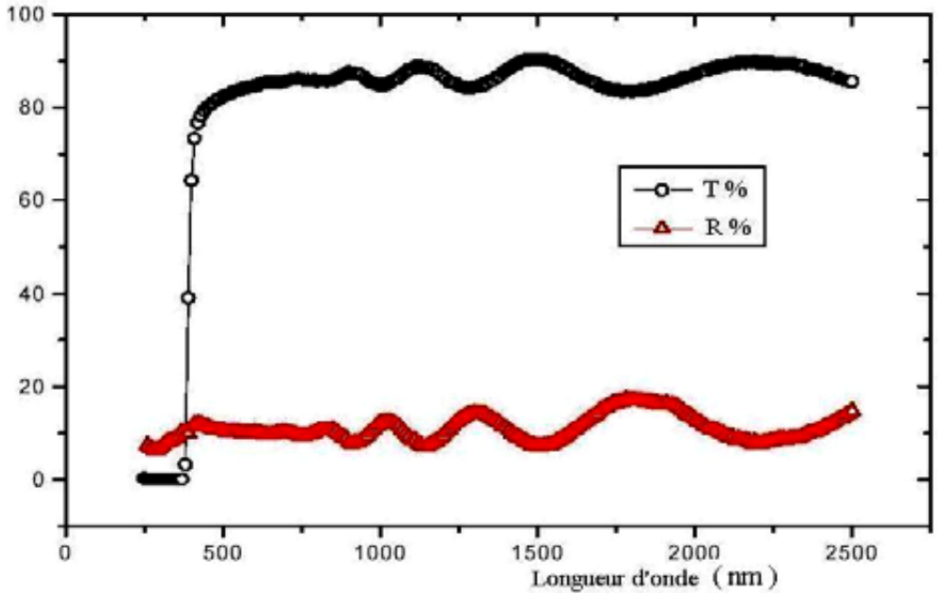

Fig.1.60 : the transmittance and reflectance spectra obtained from the ZnO films deposited on glasses substrate at 480 °C [66].

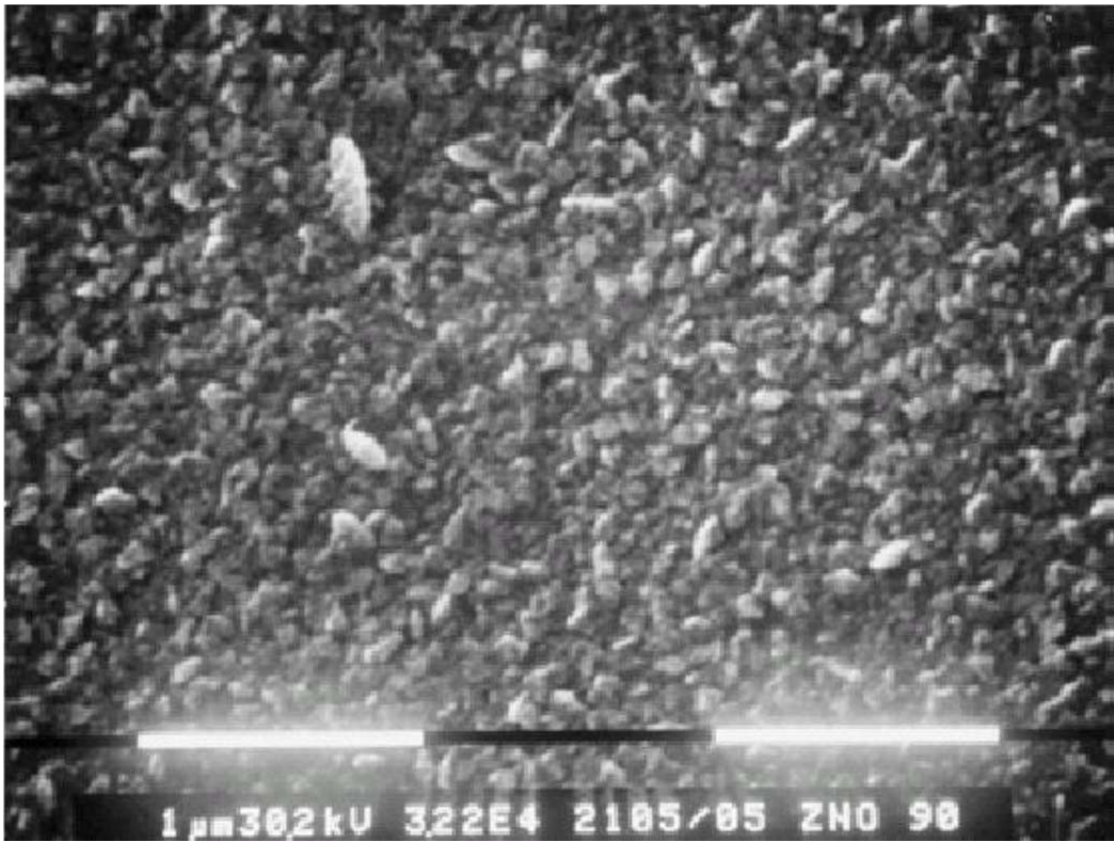

Fig. 1.61: MEB of surface of the layer of ZnO:In [66].

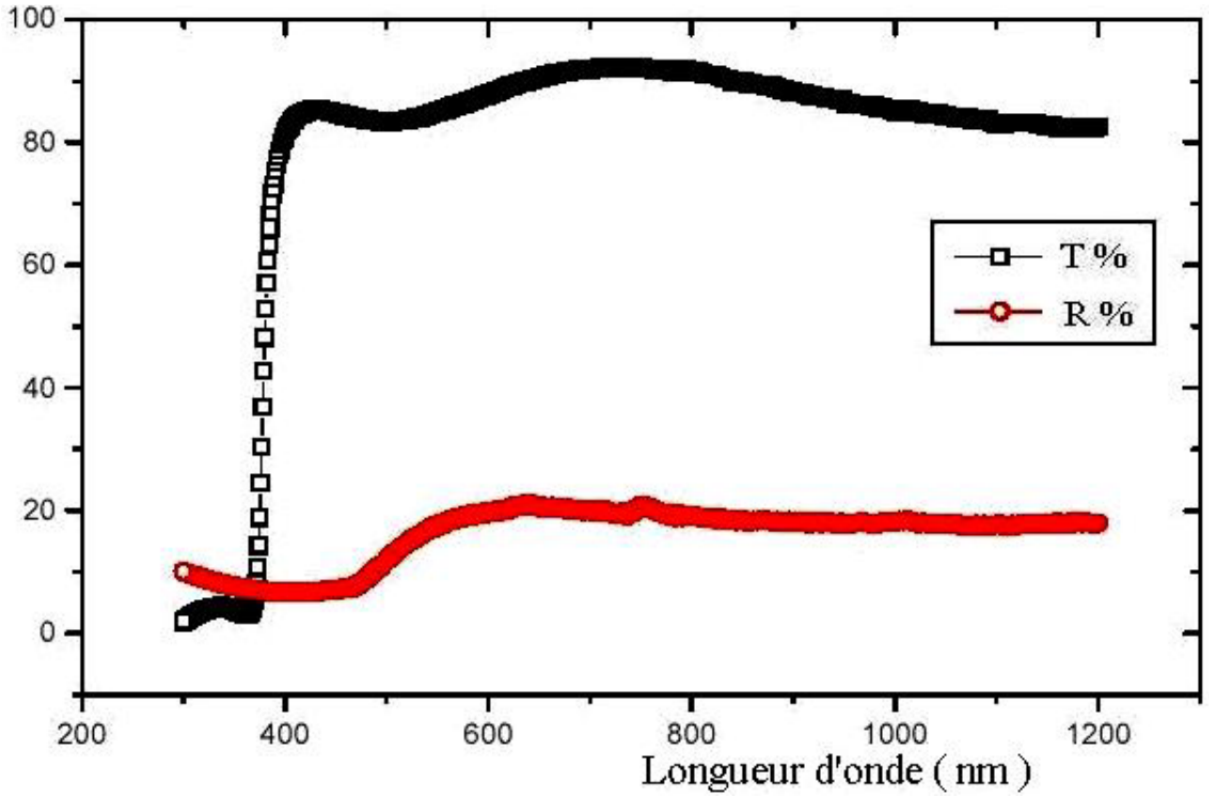

Fig. 1.62: the transmittance and reflectance spectra obtained from the ZnO:In films deposited on glasses substrate at 480 °C [66].

Effect of the temperature on the resistivity: The main interest was to study the resistivity of the layers as function of the temperature of the substrate. The figure 1.63 shows the evolution of the resistivity of the layers according to the temperature of the substrate. The resistivity passes by a minimum for a temperature which increases. This figure shows that the resistivity of the doped samples decreases compared To ZnO un-doped. This reduction in the resistivity can be interpreted by the increase in the number of the charge carriers (electrons) coming from the ions In^{3+} donors incorporated in the substitutional or interstitial sites from cation from Zn^{2+}. The increase in the temperature of deposit produces a rise in the resistivity, which is probably due to a reduction in the mobility of carriers resulting from excess from Zn and In.

Effect of the thickness on the resistivity: Fig. 1.64 shows the variation of the resistivity of the layers according to the thickness, the resistivity decreases with the thickness. This reduction can be due to the increase in the mobility and the concentration of the electrons in the layers.

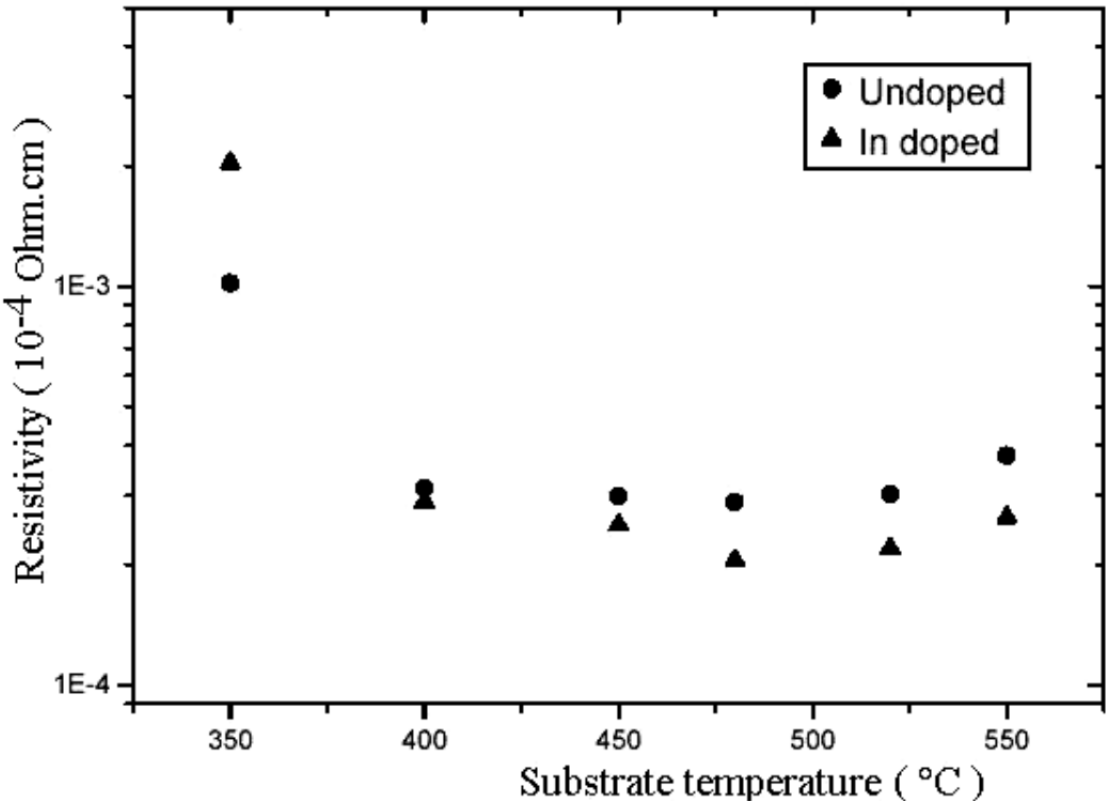

Fig.1.63: Evolution of the resistivity of the layers according to the temperature of the substrate [66].

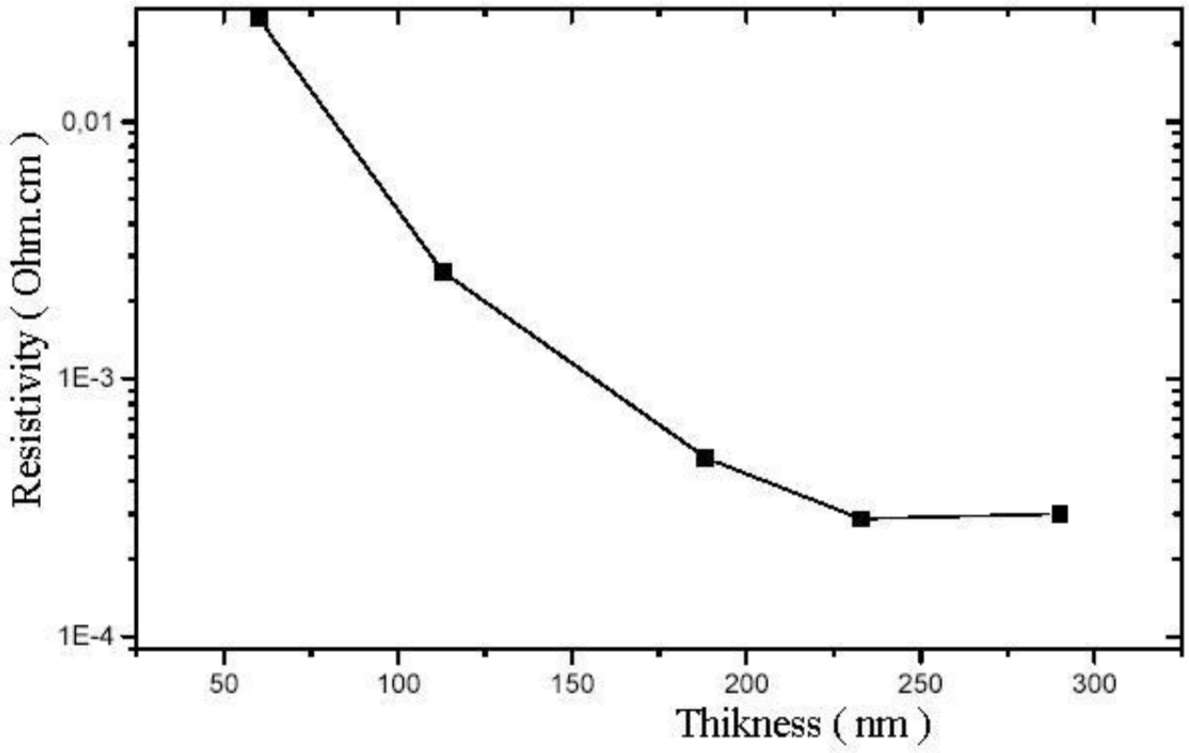

Fig. 1.64: variation of the resistivity of the layers according to the thickness [66].

Girjesh [67] particularly studied the structural, morphological, electrical and optical properties of IZO films deposited onto glass substrate at a temperature of 380 ± 5°C. Effects of indium concentration on the structural, morphological, electrical and optical properties were studied. These films are found to show (002) preferential growth at low indium concentrations. An increase in In concentration causes a decrease in crystalline quality of films as confirmed by X-ray diffraction technique which leads to the introduction of defects in ZnO. Indium doping also significantly increased the electron concentrations, making the films heavily n-type. However, the crystallinity and surface roughness of the films decreased with increase in indium doping content likely as a result of the formation of smaller grain size. Typical optical transmittance values in the order of (80%) were obtained for all films. The lowest resistivity value of 0·045 Ω-m was obtained for film with 5% indium doping. Details of these results are given below.

Structural studies: The X-ray diffraction spectra of IZO films deposited at 380°C for various dopant concentrations are shown in figure 1.65. Undoped ZnO film shows a preferential orientation along the (0 0 2) plane at 2θ = 34·3°. The other peaks observed in the X-ray diffractogram are (1 0 2), (1 1 0) and (1 0 3), but intensity of these peaks are found to be too less as compared to the preferentially oriented peak.

The 2θ values were compared with the standard JCPDS data card (80-0075). With the increase in indium doping percentage, the intensity of the peak corresponding to the plane (0 0 2) is found to decrease and that corresponding to (1 0 1) and (1 0 0) plane increase. Similar behavior has been reported by other workers [132, 133]. The results of IZO allow us to state that there is a predominant growth of ZnO microcrystal with the c-axis tilted around 58 degree towards the plane of substrate at higher doping while for lightly doped samples c-axis is perpendicular to the plane of the substrate [134].

Morphological studies: Figure 1.66(a–f) shows the AFM of IZO deposited at 380°C on glass substrate with different indium dopant concentrations. The micrograph shows uniform polycrystalline nature of the IZO films. Undoped ZnO film has a uniform surface morphology with many voids. When a small amount of indium (1%) was doped, numbers of voids are found

to decrease. The particle size and roughness of IZO are found to decrease with the indium doping percentage.

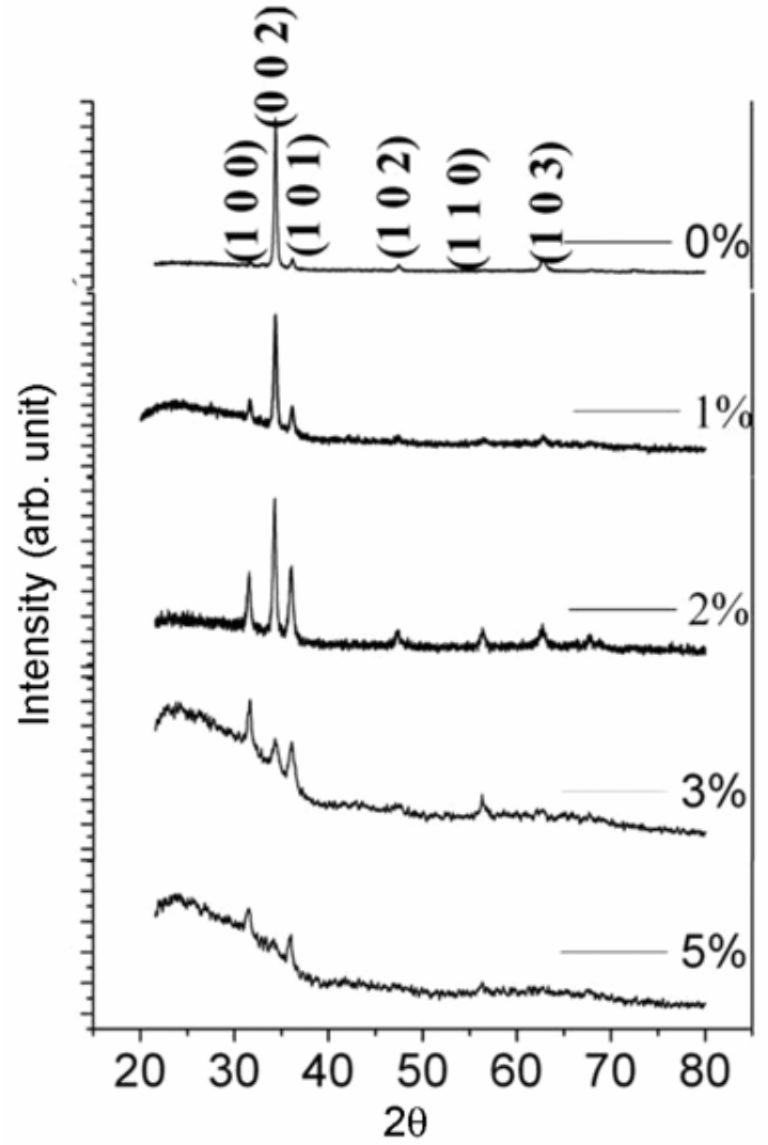

Fig. 1.65: XRD spectra of undoped and indium doped ZnO films [67].

In addition the density of the features increases as the doping concentration increases. The AFM image (figure 1.66b), corresponding to the lowest IZO (1%) exhibits grains of size 156·36 nm (calculated from the statistical distribution curve). As the indium content increases, the grain size decreases, the lowest grain size has been obtained for 5% IZO film, that is, 112·23 nm. This reveals that doping with indium leads to the formation of the films with bigger

smoothness or we can say that the indium atoms distributed uniformly in ZnO film making an orderly arrangement.

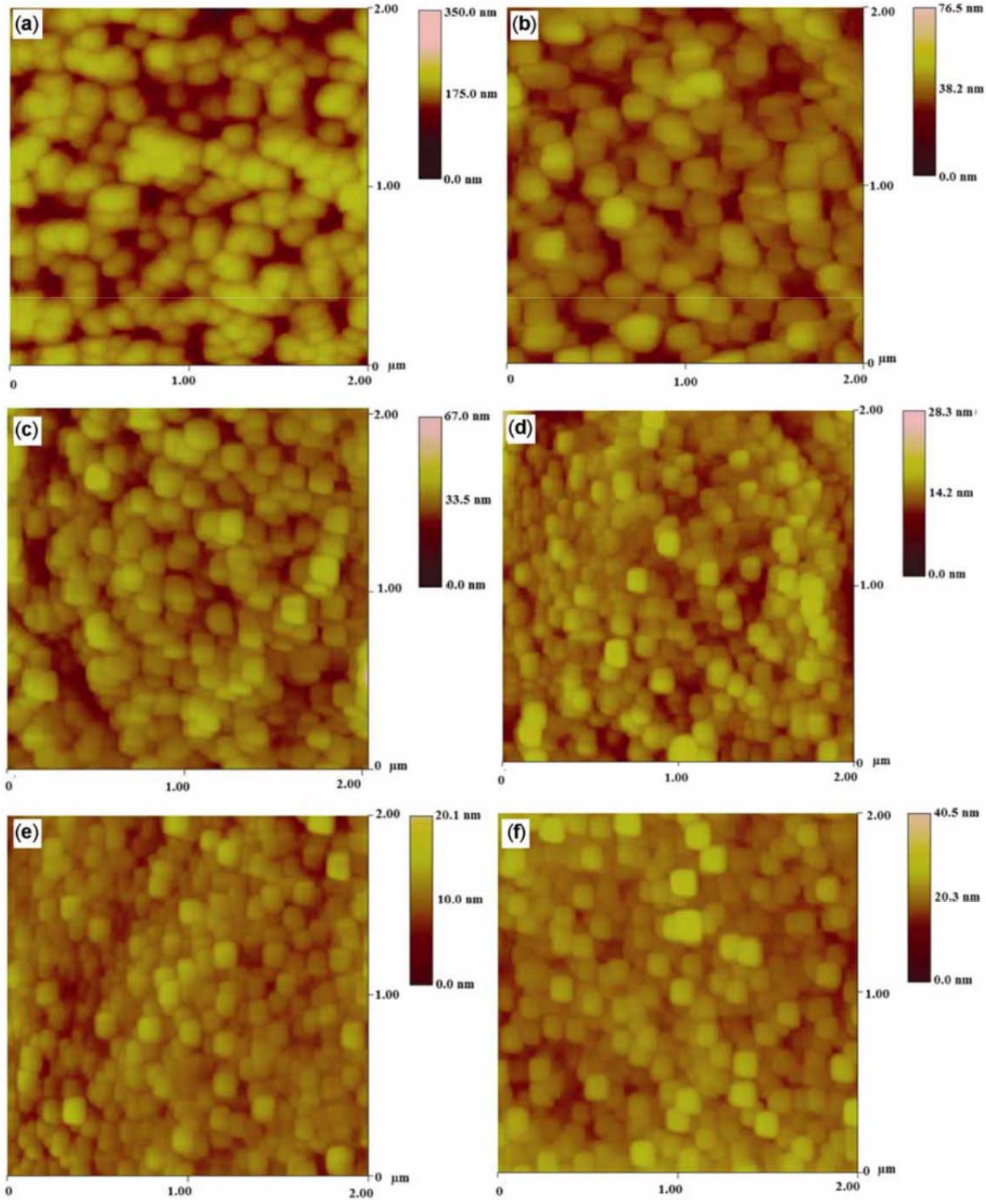

Fig. 1.66: AFM micrographs of IZO films at (a) 0%, (b) 1%, (c) 2%, (d) 3%, (e) 4% and (f) [67].

Optical studies: The absorbance spectra of IZO in the UV–Vis region are shown in figure 1.67(a). From the figure it is clear that there was no optical absorption in the visible region. However, the UV region of the absorbance versus wavelength curve shows a split peak for undoped and lightly indium doped ZnO films. This may be due to the fact that the Zn^{+2} with d electron energy level could be split by the effect of the crystal field, resulting in the split peak in the UV spectrum [135]. Beyond the absorption edge figure was not symmetric for the undoped and lightly indium doped film. This could be related to the oxygen and metal charge transfer. The energy at which charge transfer occurs between oxygen and metals depends on the cations and the symmetry of its coordinate site [136]. As the indium doping increases, the figure was found to be more symmetric. Thus we can say that for lightly doped film there is less charge transfer, while at higher doping better charge transfer is seen between oxygen and zinc. Symmetry of the absorption spectrum could be related to the transfer of electron to the conduction band and hence to the variation in resistivity. Optical transmittance spectra (figure 1.67(b)) of IZO show excellent transmittance (> 80%) and a sharp cut off between 360 and 375 nm. It is clear from the transmittance spectra that increment in doping percentage slightly affects the transmittance of the film. This might be due to the formation of grainy surface leading to large scattering loss.

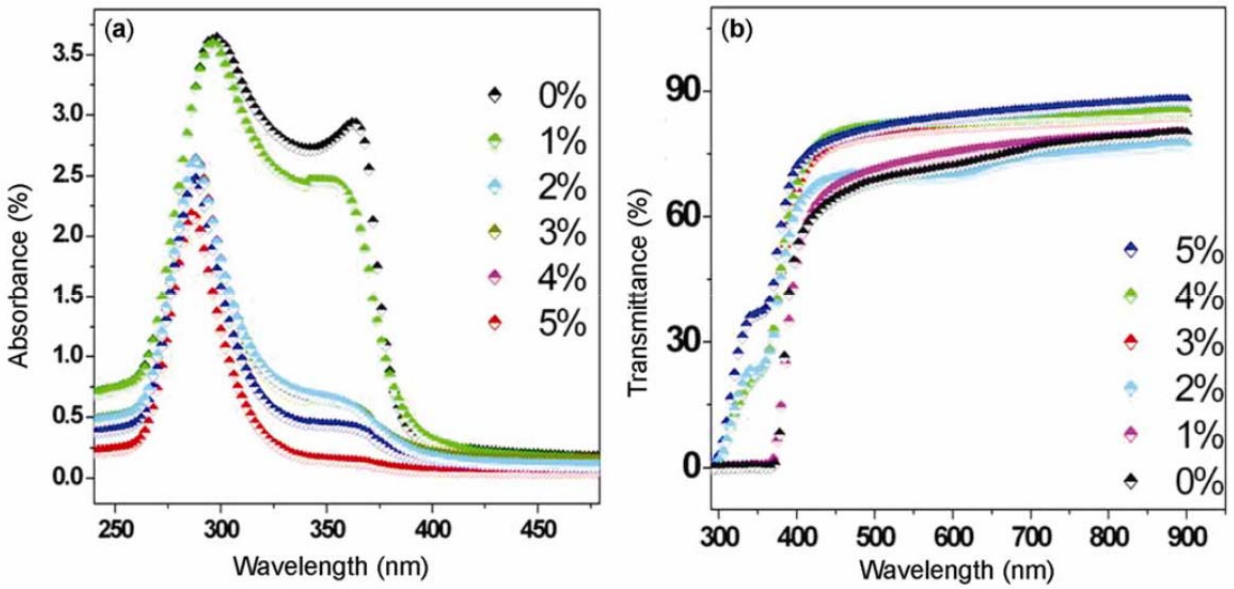

Fig. 1.67:(a) Optical absorbance spectra and (b) optical transmittance spectra of IZO films [67].

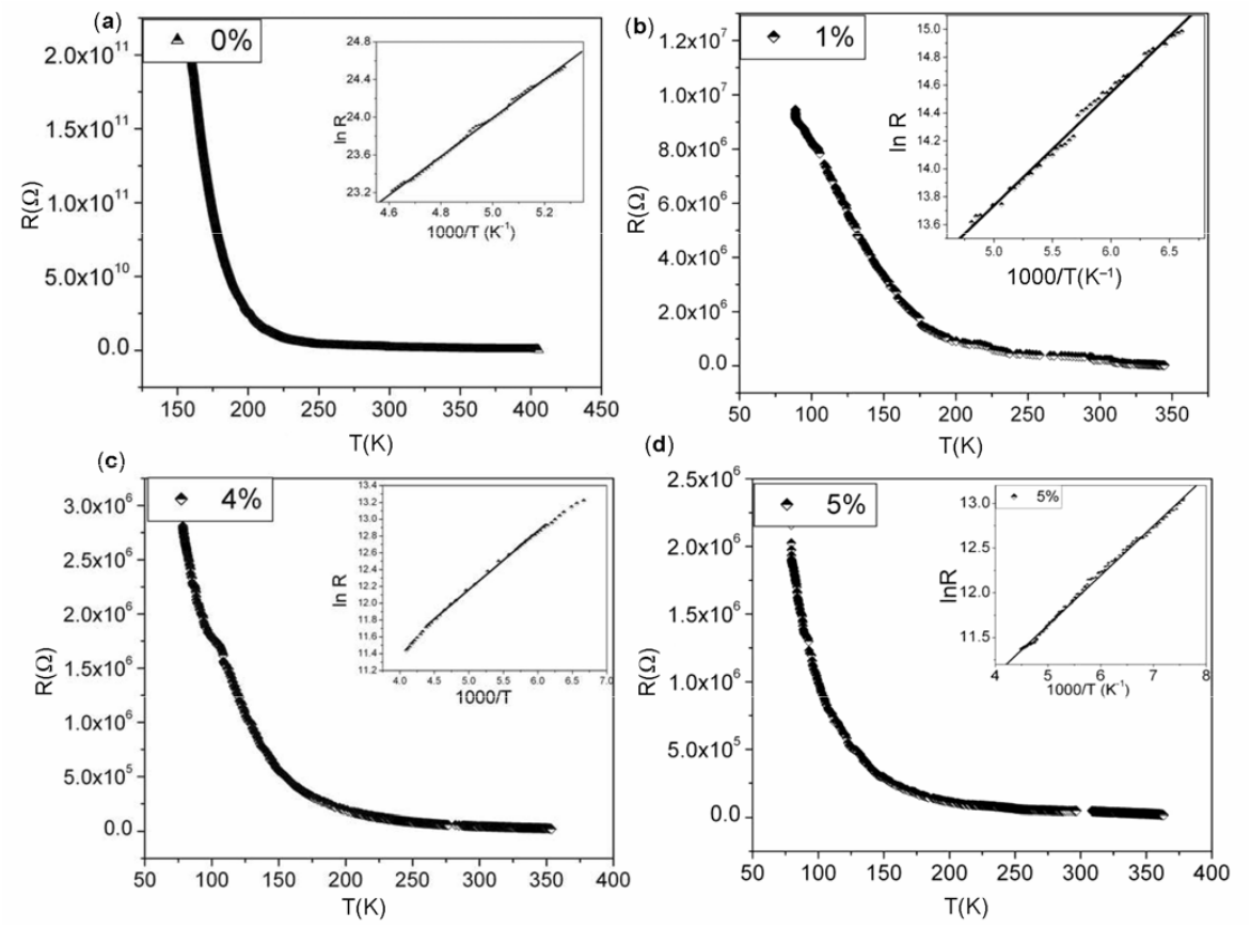

Fig.1.68: Temperature vs resistance curve for IZO films [67].

Electrical studies: The resistivity measurement of the above prepared films has been done by using conventional four probe resistivity method at various dopant concentrations. The results so obtained are shown in figure 1.68(a–d). From the figure it is clear that resistance decreases as the temperature increases showing the semiconducting behaviour of ZnO.

Ilican [137] deposited In-doped ZnO thin films onto glass substrates by the spray pyrolysis method at 350 ^{o}C substrate temperature. The crystal structure and orientation of the In-doped ZnO thin film (thickness = 337 nm) were investigated by the XRD pattern. The X-ray diffraction pattern of this film revealed its hexagonal wurtzite structure. The films exhibited high transparency (T≥ 91%) in the visible and infrared region.

Structural properties of the In-doped ZnO thin film: XRD spectrum of the In-doped ZnO thin film (t = 337 nm) is shown in Fig.1.69. The peaks of the XRD pattern correspond to those of the theoretical ZnO patterns from the JCPDS data file, with a hexagonal wurtzite structure of the bulk and lattice constants: a = 3.24982 Å, c = 5.20661 Å. The analytical method was used to calculate the lattice constants (a = 5.21580 Å, c = 3.26064 Å) for the film. The full width at half maximum (FWHM) of the (002) peak is 0.284°. Another major orientation present is (101), while other orientations like (102) and (100), are also seen with comparatively lower intensities. Therefore, the crystallites are highly oriented with their c-axes perpendicular to the plane of the substrate. 2θ and d values are given in Table 1.9.

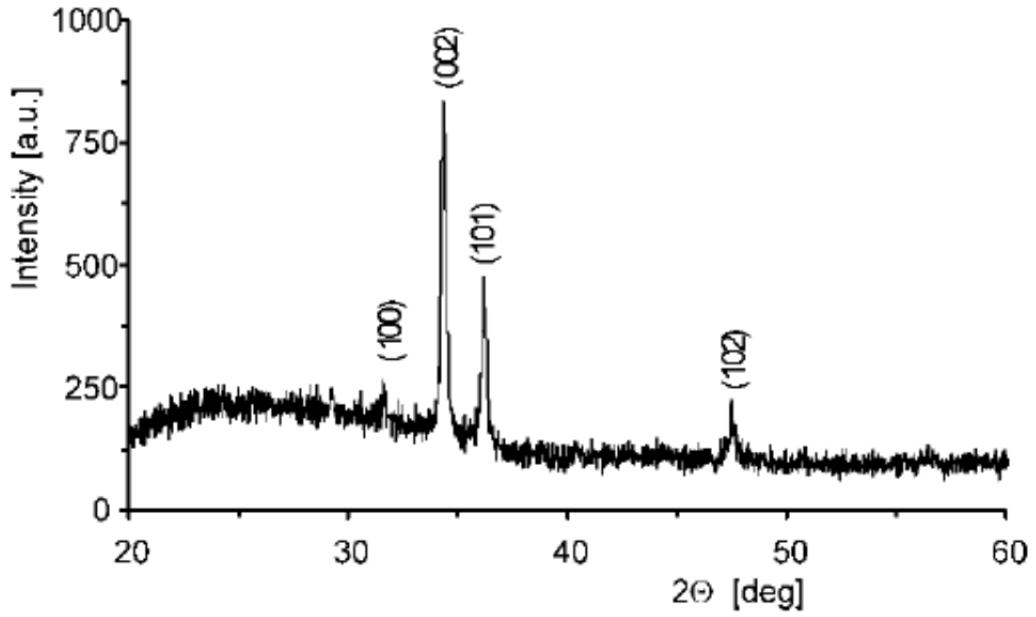

Fig. 1.69: XRD spectrum of the In-doped ZnO thin film [137].

Optical properties of indium doped ZnO thin film: Figure 1.70 shows transmittance curves for In-doped ZnO thin films at various thicknesses. These films exhibited good transparency (between 91% and 93%) in the visible and infrared region.

Table 1.9: The X-ray diffraction data results of the In-doped ZnO thin film [137].

(*hkl*)	2θ [deg]	*d* [Å]	I/I_0	*TC* [%]
(100)	31.660	2.8238	11.5	6.58
(002)	34.360	2.6079	100.0	57.21
(101)	36.200	2.4794	48.3	27.63
(102)	47.443	1.9148	15.0	8.58

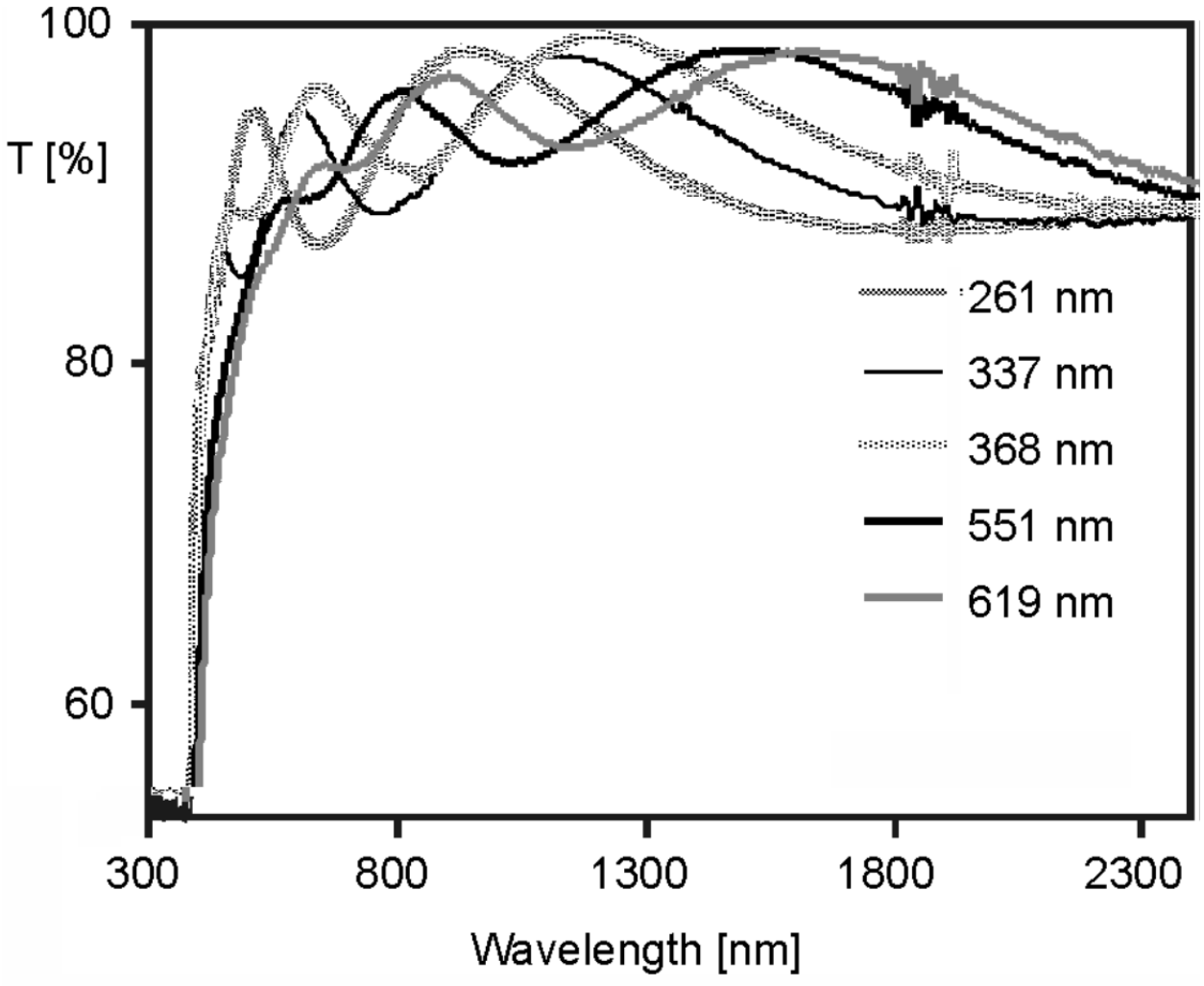

Fig.1.70. Transmittance spectra of the In-doped ZnO thin films [137].